Journal of Paleolithic Archaeology (2024) 7:6
https://doi.org/10.1007/s41982-024-00171-5

RESEARCH

Intriguing Occupations at Gran Dolina (Atapuerca, Spain): the Acheulean Subunits TD10.3 and TD10.4

Marina Mosquera[1,2] · Andreu Ollé[1,2] · Palmira Saladié[1,2,3] · Adrián Arroyo[1,2] · Lena Asryan[2,4] · Amèlia Bargalló[1,2] · Arturo de Lombera-Hermida[2,5,6] · Juan Luis Fernández-Marchena[2,7] · Paula García-Medrano[1,2,8,9] · Diego Lombao[2,10] · Antonio Rodríguez-Hidalgo[2,11] · María Soto[2,12] · Josep Vallverdú[1,2,3] · Andion Arteaga-Brieba[1,2] · Javier Villalobos[1,2] · Görkem-Cenk Yeşilova[1,2] · Eudald Carbonell[1,2]

Accepted: 13 January 2024

Abstract
This paper presents the zooarchaeological, technological, use-wear, and spatial analyses of the earliest sedimentary subunits of TD10 (TD10.3 and TD10.4) of the Gran Dolina site (Sierra de Atapuerca, Burgos, Spain), dated to c. 400 ka. Both units have yielded Acheulean technology, with occupational models characterized by the superimposition of multiple and independent events paired with short, sporadic occupations. Subunits TD10.3 and TD10.4 formed during a period in which the cave was largely reopened after a temporary closure. This period of reopening is evidenced by several blocks that fell from the ceiling and walls. Fifty-seven groups of refits and anthropic conjoins, of which 43 resulted from deliberate hominin activity, confirm the low disturbance of the deposits. Contrary to TD10.4, TD10.3 shows good preservation of faunal remains, although anthropogenic modifications are very scarce. Technologically, both deposits represent well-developed Acheulean assemblages, with high proportions of large-shaped tools and percussive material, which place this area among those that have yielded the most evidence of this type among all the excavated Atapuerca sites. The question of why these subunits contain so many hammerstones, manuports, and large tools associated with faunal remains that have been so scarcely modified is discussed based on data from spatial, technical, and use-wear analyses, which have identified butchery activities, and for the first time in the Pleistocene Atapuerca record, borer elements and possible thrusting stone spear tips. Furthermore, the occupational and technological characteristics of these subunits were compared with other western European archaeological sites, including the nearby site of Galería, with which a broad correlation can be made.

Keywords Acheulean occupations · Archaeostratigraphy · Technology · Zooarchaeology · Middle Pleistocene · Sierra de Atapuerca · Western Europe

Introduction

The cave site of Gran Dolina is located in the Sierra de Atapuerca (Burgos, Spain), and its evidence of occupations have been dated to between 0.9 Ma (Duval et al., 2012, 2022) and 200 ka (Berger et al., 2008a, 2008b). It contains 12 sedimentary units, of which neither the oldest three (TD1–TD3) nor the youngest one (TD11) have yielded an archaeopaleontological record. The former (TD1–TD3) contain hydric stages dated to 1.4 Ma (Parés et al., 2018), but the earliest fossil-bearing facies from outside the cave have been dated to 900 ka (TD4) (Álvarez de Posada et al., 2018). The latter (TD11) lacks an archaeological record, because at that time the entrance of the cave was already blocked by sediments.

Unit TD10 is the last archaeological bearing sedimentary deposit of Gran Dolina (Fig. 1). It is about 3 m thick and divided into four subunits: TD10.4 to TD10.1, from bottom to top. The chronostratigraphy of TD10.3–TD10.4 remains debatable due to the stratigraphic inconsistency of the dates established. The date for TD10.4 was obtained by means of ESR-OB at 390 ± 55 ka (Moreno et al., 2015), and the date of the overlying TD10.3 ESR-OB covers a temporal span of 458 ± 39 to 455 ± 47 ka. In sum, the age of TD10.4–TD10.3 can be estimated as being between 450 and 350 ka (MIS

Extended author information available on the last page of the article

Published online: 02 March 2024

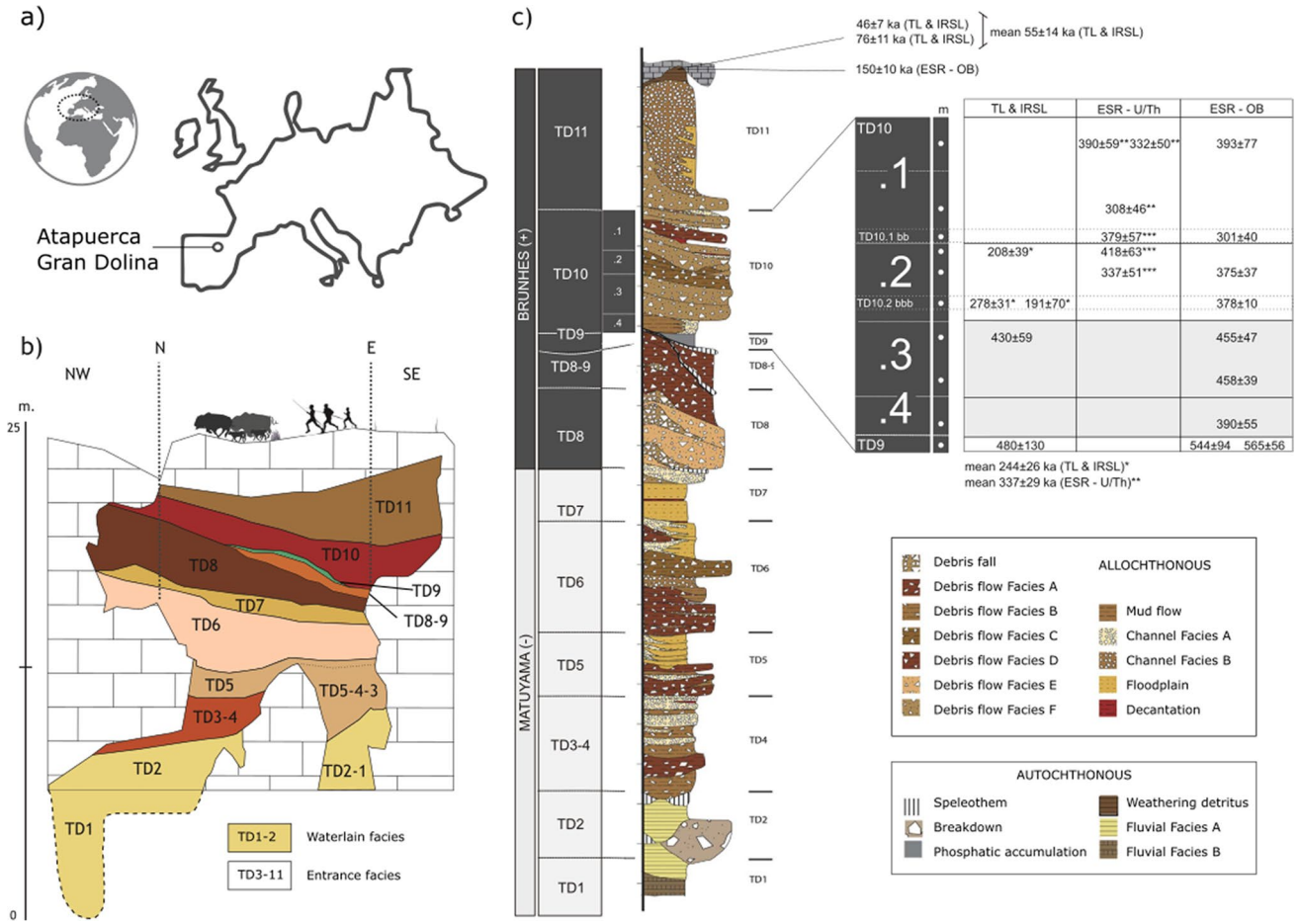

Fig. 1 **a** Location of Gran Dolina and Sierra de Atapuerca, in the north of the Iberian Peninsula. **b** Gran Dolina palaeomorphology from the railway trench (south archaeological section) and main lithostratigraphic units. **c** Synthetic sedimentary facies column of Gran Dolina site and location of available dates for TD10 (Berger et al., 2008a, 2008b; Falguères et al., 1999; Moreno et al., 2015). From Arteaga-Brieba et al. (2023)

10–11) (Berger et al., 2008a, 2008b; Falguères et al., 1999, 2013; Moreno et al., 2015). The underlying TD9 unit has been dated to 565 ± 56 ka and 544 ± 94 ka (Moreno et al., 2015) and 480 ± 130 ka (Berger et al., 2008a, 2008b), while the overlying TD10.2 subunit is dated to 378 ± 10 ka and 375 ± 37 ka (Moreno et al., 2015), 418 ± 63 ka and 337 ± 51 ka (Falguères et al., 1999), and 244 ± 26 ka (Berger et al., 2008a, 2008b).

Gran Dolina was used by Middle Pleistocene hominins as a butchery site in TD10.2 (Rodríguez-Hidalgo et al., 2016, 2017), a base-camp in Lower TD10.1 (de Lombera-Hermida, 2020; de Lombera-Hermida et al., 2020; Rodríguez-Hidalgo et al., 2015), and a succession of lower-intensity cumulative events in Upper TD10.1 (Ollé et al., 2013; Saladié et al., 2018).

Subunits TD10.3 and TD10.4 were excavated primarily during the 2014–2019 field seasons over an area of about 95 m^2. The completed excavation of TD10 offers the opportunity to delve more deeply into the following questions: (1) What diachronic changes or transitions in occupation, subsistence and technology were recorded in the last unit of Gran Dolina cave, a 3 m sequence of Middle Pleistocene hominin occupations? (2) How valuable are lithic assemblages in the interpretation of the function of occupations, particularly in karst complexes such as Atapuerca where different models of hominin occupations occurred in the same place and similar models of occupations occurred in different caves? (3) Related to that, to what extent and in what way might occupational patterns affect the features of the spatial distribution of the archaeological remains,

faunal representation, and technological variability? (4) To what extent might palimpsests provide paleo-ethnographic information? How should they be dealt with? (5) What correlations can be drawn with nearby Middle Pleistocene sites, such as the caves of Galería and Sima del Elefante, 50 m and 200 m away from Gran Dolina, respectively? And finally, (6) what other archaeological sites outside Atapuerca are similar to TD10.3 and TD10.4?

The fact that Gran Dolina contains a long sequence, which makes it a key site for the European Early and Middle Pleistocene, may contribute to the formulation of answers to most of these questions. Analyses of subunits TD10.3 and TD10.4 will complete the study of this sequence, particularly between TD6 (c. 900 ka) and TD10.2 (c. 400 ka) (Arteaga-Brieba et al., 2023). In addition, analyzing these two subunits will lead to an improved understanding of the way in which different patterns of occupation may affect archaeological assemblages, and will allow us to characterize the technological and spatial features for each of the strategies and models of occupation used by the hominins who visited the cave. Furthermore, this study will contribute to drawing occupational, subsistence and technological correlations between Gran Dolina and Galería, an issue that was first raised about 7 years ago (Ollé et al., 2016a, 2016b). Finally, taken together with the lithic assemblage of Galería, the results of this study will allow us to add to the current body of knowledge regarding Acheulean subsistence and technological strategies in the Sierra de Atapuerca.

An improved understanding of these strategies in Atapuerca, whose sites contain long sedimentary sequences that can be correlated in terms of chronological, occupational, environmental, and subsistence characteristics, will in turn allow us to better understand the subsistence strategies of the Middle Pleistocene in Europe. This is of particular interest with regard to the severe glacial MIS 12, which seems to have forced the hominin populations of central and northern Europe to retract to southern areas, and MIS 11, a long interglacial stage, which triggered a hominin demographic dispersal throughout Europe, as evidenced by the increase in the number of sites on the subcontinent and the behavioral diversity that they represent (Moncel et al., 2021).

Cave Apertures During the Formation of Subunits TD10.4 and TD10.3

In order to approach an understanding of subunits TD10.3 and TD10.4, it is important to first go back to the lower units: TD9 and TD8. At the top of TD8, the sediments sealed the main entrance of Gran Dolina, making the cave an enclosed space. TD8 is an extremely rich paleontological deposit, including some lithic tools (*c*. 30) that were only recovered during the most recent field seasons, refuting what was thought until the entire surface had been excavated (Mosquera et al., 2013; Ollé et al., 2013). During the last stages of TD8, stalagmites, stalactites, and stalagmitic breccias formed, which were subsequently partially covered and eroded (unit TD8-9). TD9 contains bedded mud of different colors (green, red, yellowish red) with very weathered limestone gravels and is rich in phosphates (Campaña et al., 2017; Pérez-González et al., 2001). TD10.4 sits directly on top of TD9 and contains markedly weathered faunal remains. During the formation of TD10.4, the cave opened again (Mallol and Carbonell, 2008; Campaña et al., 2017), allowing hominins and other animals to occupy it once again. It is not a massive opening, as evidenced by the fact that the sediment contains fewer blocks than the next subunit. Specifically, 3000 blocks exceeding 10 cm in size have been recorded in TD10.4, while 16,600 blocks similar in size were documented in TD10.3 over the same excavation surface area (c. 95 m^2).

The cave apertures during the formation of units TD10.4 and TD10.3 are evident in the east and southwest archaeological profiles. The east profile entrance point is an *aven* or shaft, similar to other cave entrance spots in the Trinchera del Ferrocarril sites (Galería and Sima del Elefante). The southwest entrance is more unusual because it consists of a deep fissure (gull), likely related to Cretaceous anticlinal fractures.

We estimate at least three sediment entry points for levels TD10.4 and TD10.3. The size of the shaft (or *aven*) in the southern section of the excavated surface would have made it the most accessible entry point for prehistoric hominin groups. We cannot rule out that entry was gained from other points in the conduit, given the well-known continuity between the cavities of the Trinchera del Ferrocarril (Ortega, 2009).

The Lithostratigraphy of TD10.3 and TD10.4

The stratigraphy of unit TD10 of Gran Dolina has primarily been described in detail in two publications: Hoyos and Aguirre (1995) and Campaña et al. (2017). These studies use two different reference systems to describe the deposits of TD10. Hoyos and Aguirre's reference framework for sedimentary petrography is based on the weathering processes of the source area for the paleoclimatic interpretation of the Gran Dolina sediments. Campaña et al. (2017) used fluvial sedimentary models in

an attempt to identify the sedimentary processes and facies of Gran Dolina.

Sedimentary successions from TD10.3 and TD10.4 lithostratigraphy are relatively in agreement with archaeostratigraphic units. TD10.4 lithofacies is made up of sorted very fine boulders and mud has erosional contacts with TD9 and TD10.3. Microlamined mud on sorted pavement of very fine boulders suggest transport in suspension. Generalized boulder black patina and other sedimentary structures (desiccation cracks, black cryptocrystalline coatings in mud aggregates) point out no deposition episodes according to basal scour surfaces with TD9 and TD10.3. Weathering and erosional episodes during TD10.4 represent a zonal hiatus and truncation (hiatus with lacunae)/paraconformity. Hiatus suggested by generalized black patina and weathering patterns in TD10.4 sediments are reported in cave sedimentology research (Campy et al., 1994).

Diamicton from TD10.3 contain a bedded lenticular bedsets of different provenance (entrance points). Rhythmic stratification of very fine graded beds point to grain flow. Another type of current flow identified in TD10.3 is solifluction using soil micromorphology (unpublished). Fine to coarse (millimeter to centimeter size) platy microstructure on thin section observations point to a slow rate of solifluction perturbation. Debris creep is largely reported in cave entrance sedimentology from temperate settings (Bertran et al., 2010).

Grain Size and Textural Description of TD10.4 and TD10.3

Angular gravels constitute the main grain sediment size and form the breccias of TD10 unit of Gran Dolina. The following lithological descriptions of units TD10.4 and TD10.3 are based on the conceptual framework proposed by Blair and McPherson (1999) for coarse sediments.

TD10 has two different bedsets due to the stratification and the size of the gravels in the matrix. They are separated by a paraconformity. The upper bedset contains discontinuous, homogenously fine, bedded granular sandy mud of one to two granular gravels thick. The lower bedset is made up of poorly bedded bimodal granular and fine pebbly sandy mud. The gravel fabric is variably clast-to-matrix-supported and weakly organized to unorganized. The gravels are poorly sorted with outsized cobbles and boulders, ungraded and unimbricated. The upper bedset contains the archaeological levels of subunit TD10.1. The lower bedset comprises archaeological levels included in subunits TD10.2, TD10.3, and TD10.4.

In terms of sedimentary composition, the lower subunits are described as follows:

TD10.3 is made up of matrix supported bimodal granular to fine pebbly sandy mud with outsized coarse boulders and fine blocks. Prismatic-blocky sandy mud contains dark mottling and variable calcium carbonate cementation.

TD10.4 is formed by variable clast to matrix supported muddy fine to coarse cobble gravels. Facies of prismatic-blocky mud and cortex of subangular to rounded cobble gravels have dark coatings.

Materials and Methods

To determine the function of the hominin occupations of TD10.3 and TD10.4, we looked at the archaeostratigraphy, the characteristics of the lithic and faunal remains and their spatial distribution, and the lithic refits and technical conjoins and their distribution. Therefore, the study involved several disciplines and techniques, each with its own methodology.

All the materials studied here are deposited at the Centro Nacional de Investigación sobre la Evolución Humana (CENIEH, Burgos, Spain) and at the Institut Català de Paleoecologia Humana i Evolució Social (IPHES-CERCA, Tarragona, Spain).

Archaeostratigraphy and Spatial Analyses

Archaeostratigraphy and spatial analyses were performed with ArcGis 10.2 (Esri Spain) in order to individualize the archaeological deposits, determine the role of the topography of the paleosurfaces and visualize the materials. For this purpose, all spatially recorded archaeological items were included, comprising all lithic pieces, regardless of size, bone remains equal to or greater than 20 mm in length, and natural limestone blocks equal to or greater than 100 mm. Isolating occupational or temporal packages in TD10.3 during the excavation was very complicated due to a lack of clear sedimentary changes all over the surface, the high number of blocks that disturbed the surface readability, and the relatively low density of archaeopaleontological remains. We started dividing the archaeological remains into longitudinal, transversal, and diagonal sections with thicknesses of 10, 15, and 25 cm across the entire excavation surface. However, the great number of limestone blocks in this area consistently resulted in projections showing significant scattering of remains, making it very difficult to visualize any possible clustering. Eventually, it was possible to observe some clustering in the block falls by isolating sections with thicknesses of 50 cm, which

were systematically followed in all the longitudinal, transversal, and diagonal sections. This revealed that, although continuous, the block fall episodes slowed down towards the second half of the TD10.3 sequence. Density maps were generated through Kernel density classified analysis using the mass of the lithics and the dimensions of the faunal remains as population fields, with 5 natural breaks (Jenks). The mass of the lithics was considered instead of their dimensions as a more reliable method of approaching the possible influence of the slope of the deposit on the distribution of the remains.

For spatial statistics, Besag's L(r) function allowed us to characterize the spatial structure of the three groups (lithic and faunal remains/lithic remains/faunal remains) and specified whether the points had a uniform, aleatory or aggregated distribution (Besag, 1977). Acceptance intervals were obtained through a Monte Carlo simulation process involving 50 random samplings of the original data (Baddeley et al., 2000). The curve of the observed data was interpreted to show an object aggregation process (above the CSR line), a regular object scattering process (below the theoretical CSR line), or complete spatial randomness (if within the CSR line confidence intervals). A cross-type approach was applied to study point distribution patterns by material type in order to detect spatial co-dependency between lithic remains and fauna. We used an inhomogeneous cross-type L-function (Ripley, 1979) to determine whether the two material types were spatially dependent, which would be indicated if the results on the data line fell outside the acceptable confidence interval. This can be expressed as either clustered (the probability that i points are within the distance of any specific radius of j points is greater than the reference value) or regularly spaced (the probability that i points are within the distance of any specific radius of j points is less than the reference value). This analysis is shown on a bivariate quadruple chart. Diagonal graphs (top left and bottom right) indicate the inhomogeneous Lii distribution. Graphs outside the diagonal (upper right and lower left) indicate the type of inhomogeneous association of Lij. An overall confidence interval of 95% was used (Baddeley et al., 2015).

Mass of the Lithic Assemblage

For the first time in Atapuerca, we have assessed the total mass of the raw materials that the hominins carried or handled into the cave. To do this, each archaeological piece of all raw materials except Neogene chert was weighed in order to assess the amount of raw material recovered from the site. This variety of evaporithic chert was excluded because it undergoes marked postdiagenetic alteration that causes a considerable decrease in density and, as a result, a considerable loss of mass (Zornoza-Indart et al., 2017, 2021). Given that this alteration may vary from piece to piece, we calculated the mass of the pieces of this raw material by calculating their volume.

To do this, we used the maximum technical dimensions (technical length in mm × technical width in mm × technical thickness in mm) according to the Laplace method (Laplace, 1968). Then, we divided each result by 1000 to transform the result into cm^3. Subsequently, using the formula mass = volume × density, we multiplied each volume by 2.4, which is the average density of undisturbed Neogene chert recovered from the environment of the archaeological sites. To test the statistical reliability of these mass estimates, we performed these calculations on 50 experimental pieces made from undisturbed Neogene chert, whose mass was known. We then calculated the differences between the actual mass and the estimated mass, which amounted to a total of 1.92 times the actual mass. Therefore, to correct for this overestimation we applied a correction factor to the mass estimates by dividing each result by 1.92.

Raw Material Groups

Raw material groups (RMGs) (Machado et al., 2011) were macroscopically determined based on the following characteristics: (1) texture; (2) grain size; (3) color of the cortical and non-cortical surfaces; (4) inner inclusions such as veins of other raw materials and/or minerals; and (5) other characteristics, such as incipient fractures, microfossils, alterations, etc. The method used here has previously been applied to the quartzite (López-Ortega et al., 2017) and quartz (de Lombera-Hermida, 2009; de Lombera-Hermida et al., 2020) of TD10.1. To determine the type of neocortex of the blanks, the dorsal or central surfaces (fresh fractures that allow us to see the interior texture of the artifacts) and the cortical surfaces were photographed at low magnification (40×, 20×, and 10×, Dino-Lite Digital USB Microscope) (Prieto et al., 2020). The quartz and quartzite from the site are optimally preserved, but other materials such as sandstone and, particularly, Neogene chert exhibit intense postdiagenetic degradation. Ascribing RMG requires good preservation and a size large enough to observe the characteristics of the piece. Therefore, we excluded the following from this analysis: (1) pieces smaller than 10 mm; (2) pieces with a concretion cover that was difficult to extract without endangering the piece; (3) totally cortical pieces; and (4) pieces with degraded surfaces.

Percussive Material

The cobble assemblage was analyzed and classified into three technological groups:

1) Unmodified material: complete cobbles without any trace of use and/or modification. This group also includes cobbles with poorly preserved surfaces and/or carbonate crust. These have been called *manuports*, because they entered into the occupations from outside. The only exception are the limestone cobbles, some of which may have formed inside the karst.
2) Hammerstones: complete and broken cobbles with traces of percussion on their surfaces, vertices and/or their fracture plains.
3) Percussive by-products: fragments of cobbles.

We performed a series of statistical tests to assess the correlation between the dimensions of the hammerstones and the manuports. We first performed a normality test of the general measurements. Only the length was normally distributed in both groups (Shapiro–Wilk test, $p > 0.05$). Consequently, to test the length, we ran a parametric test, while non-parametric (Mann–Whitney *U*) tests were run to test the width and thickness. Finally, chi-square tests were run in SPSS at a significance level of $\alpha = 0.05$, in order to check if some raw materials were selected for use as hammerstones.

Large Tools

In this study, shaped pieces measuring ≥ 10 cm are defined as *large tools*. They include heavy-duty tools and large cutting tools (sensu Isaac, 1977), as well as retouched flakes bigger than 10 cm. In addition, tools slightly smaller than 10 cm but shaped as handaxes, cleavers, and choppers/chopping tools were also included. For these tools, we studied the raw materials, blanks, faciality and percentage of the surfaces and perimeter modified by shaping.

Geometric morphometrics analyses were applied to 3D models to analyze tool shape variation. All the tools were scanned using the Artec Space Spider 3DScan (ArtecStudio v15 software) and the Breuckmann SmartSCAN3D-HE Scanner with a 250-mm field of view (Breuckmann Optocat 2012 R2-2206 software). The 3D models were processed using the AGMT3-D software v.3.1 (Herzlinger & Goren-Inbar, 2020; Herzlinger & Grosman, 2018; Herzlinger et al., 2017). This consists of a data-acquisition procedure for automatically positioning 3D models in space and fitting them with grids of 3D semi-landmarks. Each point on the grid consists of two semi-landmarks, one placed on each face of the artifact, so that a 50×50 grid provides 5000 landmarks. The dimensionality of the multivariate outline data was reduced using PCA, and the individual principal components were visualized in two dimensions so that the underlying shape variables could be qualitatively examined and compared. In order to interpret the PCA results from a morphological perspective, Procrustes superimposed shape data were examined using thin-plate splines to facilitate the visualization of shape changes from the group mean along relative warp (i.e., PC) axes.

By examining the morphological deformations and XY plots of specimens from the PCA scatters, it is possible to interpret shape variation by itself and compare the different tools within a site or between different sites. In addition, the derived principal component scores also allow for the application of other quantitative tests of multivariate equality of means between the groups (Costa, 2010; Herzlinger & Goren-Inbar, 2020; Herzlinger & Grosman, 2018).

Cores, Small Tools, and Flakes

The analysis of the cores consisted first of identifying the raw material and the type of blank used for each core (block, cobble, flake, etc.). The next step of the core analysis was carried out after a technical reading (sensu Inizan et al., 1999) in order to understand and reconstruct the knapping sequences, especially considering the dynamic nature of the knapping sequences (Andrefsky, 1998; Dibble, 1995; Guilbaud, 1995; Inizan et al., 1999).

The technological analysis of the core was inspired by the logical-analytical system (LAS) (Carbonell et al., 1983, 1992) (Carbonell et al., 1983, 1992) and structured in two levels of analysis: at a general level to analyze the core as a whole (i.e., its general characteristics) and an elementary level to analyze each surface individually (Lombao, 2021; Lombao et al., 2023; Vaquero, 1999, 2011).

Therefore, in order to define the different knapping methods and techniques applied in the cores and how they relate to each other, we used three basic attributes: (a) the number of percussion surfaces, which can be unipolar (one percussion surface), bipolar (two percussion surfaces), or multipolar (three or more percussion surfaces); b) the number of flaking surfaces, which can be unifacial (one flaking surface), bifacial (two flaking surfaces), trifacial (three flaking surfaces) or multifacial (four or more flaking surfaces); and (c) the orientation of scar removals. Regardless of the number of flaking surfaces, the most common knapping methods found were as follows:

- Unipolar longitudinal: removals were performed from the same percussion platform following the same flaking axis.
- Bipolar opposed: removals were performed from two opposing percussion platforms and the direction of the negatives was also opposing.

- Bipolar orthogonal: extractions were performed from two adjacent percussion platforms following perpendicular flaking axes.
- Multipolar centripetal: extractions followed directional axes oriented towards the center of the flaking surface.

In addition to these freehand knapping techniques, we also included the bipolar on anvil technique: the core was supported on an anvil so that each impact resulted in the detached flake or core having two opposing impact points not always visible.

Core fragments and cores with partially or completely altered surfaces were excluded from this analysis of knapping strategies, although they were included in the analysis of frequencies by raw material.

The technical characteristics of the simple flakes and flake-blanks of small tools were also analyzed using the LAS (Carbonell et al., 1983, 1992; Rodríguez-Álvarez, 2004), complemented by some additional attributes, such as knapping accidents, the presence of a lip, and types of ends. Shaped pieces smaller than 10 cm were classified as small tools, with the exception of those slightly smaller, but shaped as large cutting tools (see the "Large Tools" section). Small tools were classified by type according to Laplace (1974).

Use-Wear Analyses

Due to the poor preservation of the main raw material (Neogene chert), preliminary use-wear studies focused especially on Cretaceous chert, quartzite, and quartz, although some Neogene chert pieces were also considered. Firstly, we selected the pieces based on macroscopic observation, prioritizing well-preserved objects without clear alterations and fresh edges and ridges. Before proceeding with the microwear study, some hammerstones, small and large tools and some flakes were put aside in order to analyze possible residues on their edges and surfaces. The bulk of the selection was cleaned and prepared following the protocols established in previous works (Fernández-Marchena et al., 2020; Ollé & Vergès, 2014; Pedergnana et al., 2016; Vergès & Ollé, 2011).

Use-wear and residues were documented with the combined use of optical microscopy, scanning electron microscopy (SEM), and 3D digital microscopy (3D DM). Firstly, a systematic screening at different magnifications was conducted with an optical microscope (Zeiss Axioscope A.1, with differential interference contrast (DIC) prisms and a Nomarski interference contrast filter, with 10× oculars and EC Epiplan objectives ranging from 5×/0.13 to 50×/0.5 HD DIC, resulting in nominal magnifications of 50 to 500 times) and a 3D digital microscope (Hirox KH8700, with a MXG-5000REZ dual illumination revolver zoom lens allowing for magnifications ranging from 35 to 5000×). The pieces with well-preserved use-wear traces and those with possible residues were also observed with the environmental SEM (FEI Quanta 600 ESEM, with an EDX-EXL System Analytical Oxford energy dispersive X-ray spectrometer, combined with large field detectors (LFD) and back-scattered electron detectors (dual BSD)). Observations were performed entirely in low-vacuum mode, which does not require sample conductive coating.

To interpret the use-wear traces, we used the experimental collection of the Laboratory of Technology at IPHES-CERCA. The collection includes a wide variety of samples resulting from experiments (i.e., butchery, hide work, woodwork, vegetal tissues, ochre, projectiles, hafting, etc.), in which the main varieties of raw materials found in the Sierra de Atapuerca are well represented (e.g., Asryan & Ollé, 2021; Byrne et al., 2006; Fernández-Marchena & Ollé, 2016; Fernández-Marchena et al., 2020; Martín-Viveros & Ollé, 2020; Ollé, 2003; Ollé et al., 2016a, 2016b; Pedergnana & Ollé, 2017, 2018; Pedergnana et al., 2017).

Lithic Connections

Lithic connections were sought for all the raw materials present in TD10.3 and TD10.4, excluding pieces smaller than 10 mm ($n = 188$) and/or undetermined (altered) items ($n = 179$) and/or pieces that could not be recovered from the excavation ($n = 35$). However, 131 lithic items were not included in this section because they came from the 1993–2004 field seasons, when certain areas of Gran Dolina were excavated in order to regularize entire sections of the deposit. These pieces are stored at the Centro Nacional de Investigación sobre la Evolución Humana (CENIEH, Burgos, Spain). In total, we looked for lithic connections among 949 pieces.

We employ the terminology proposed by Sisk and Shea (2008) in this work, which has also been applied to other subunits of TD10 (López-Ortega et al., 2011, 2017 and 2019):

- Refit: intentional connection produced by knapping/shaping.
- Conjoin: fractures that may have been produced by natural, postdepositional processes (natural fractures) and accidental hominin actions during knapping and use (technological fractures).

Distinguishing between postdepositional and technological conjoins is often very difficult. In these cases, we considered the technical characteristics, the distance between fragments and the spatial context in which they appeared in order to classify them.

Zooarchaeology and Taphonomy

To determine taxonomic distribution and human impact, anatomical and taxonomic identification was performed with the support of the comparative anatomy collection at IPHES-CERCA and the atlas published by Pales and Lambert (1971). Unidentifiable remains were classified into mass-size groups, in which we considered large (animals > 300 kg), medium (between 100 and 300 kg), small (between 10 and 100 kg), and very small (animals < 10 kg) sizes. In order to determine taxonomic diversity in the three assemblages, we used the Shannon diversity index, which expresses how uniform the distribution of species in an assemblage is compared to their abundance. We also used the Simpson dominance index, which considers the dominant species within an assemblage and indicates the probability that two specimens belong to the same species.

The faunal remains were observed under a binocular microscope (OPTECH HZ) with a maximum of 60 × magnification and an intense and oblique light source, following the recommendations of Blumenschine et al. (1996). We identified cut-marks (Shipman & Rose, 1983), percussion marks (Blumenshine & Selvaggio, 1988) and carnivore tooth marks (Binford, 1981; Brain, 1981). The presence and absence of each mark were described, as well as the bone type and area on the bone the alteration was located.

Results

Subunit TD10.3 yielded a total of 24,076 faunal remains and 1,236 lithic artifacts, while 742 faunal remains and 247 lithic artifacts were recovered from subunit TD10.4 (Fig. 2).

Disentangling Phases in TD10.3 and TD10.4

Given the number of archaeological remains in TD10.3 ($n = 25{,}312$) and the thickness of this deposit due to block falls, we endeavored to differentiate hominin occupational stages. 50-cm-thick sections isolated across the entire surface (Fig. 3) allowed us to individualize two major stages within subunit TD10.3: Upper-TD10.3 (TD10.3-Sup) and Lower TD10.3 (TD10.3-Inf), each of which contained evidence of different events resulting from hominin and animal occupations. A polymodal vertical density plot of faunal and lithic remains supports the existence of two sublevels in TD10.3 (Sup and Inf) superimposed on TD10 (SI Fig. S1).

In view of the remarkably irregular surface of the deposits due to the large number of blocks, we used the lithic artifact connections to further refine the distinction between them (Fig. 3g–h). This analysis revealed that no connections crossed the two sub-units (TD10.3 and TD10.4), and only in a few cases was there extreme proximity between the base of one sublevel and the top of the underlying one (e.g., between TD10.3-Sup and TD10.3-Inf).

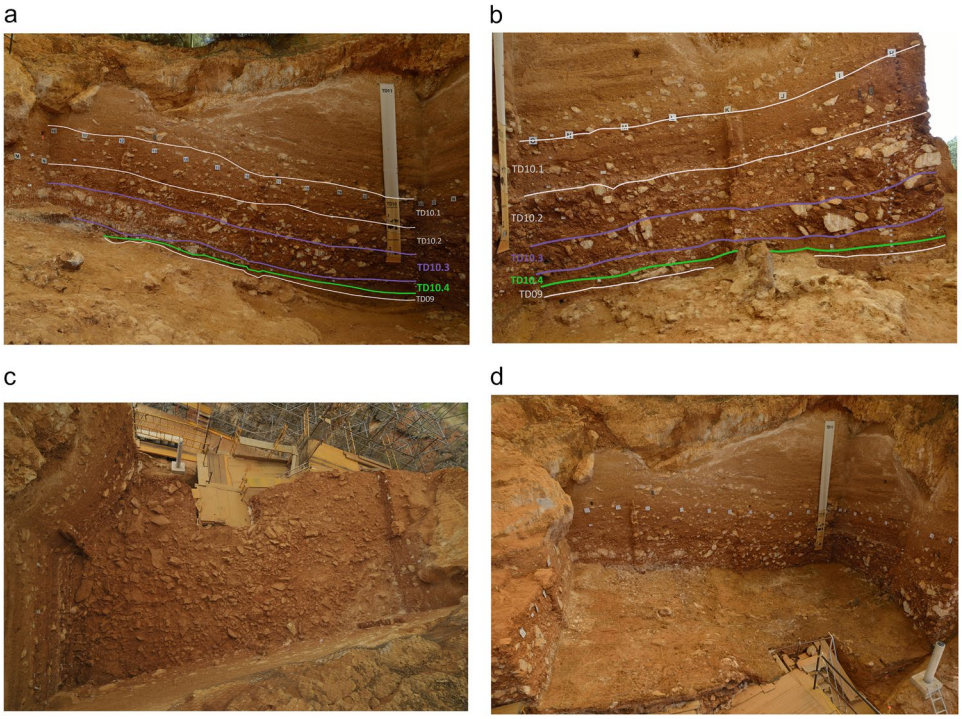

Fig. 2 **a** Stratigraphic subunits TD10.3 and TD10.4 projected in a georeferenced transversal profile picture of unit TD10. **b** Stratigraphic subunits TD10.3 and TD10.4 projected in a georeferenced longitudinal profile picture of unit TD10. **c** Excavation area of Gran Dolina TD10.3, field season 2013. **d** Excavation area of Gran Dolina TD10.4, field season 2018

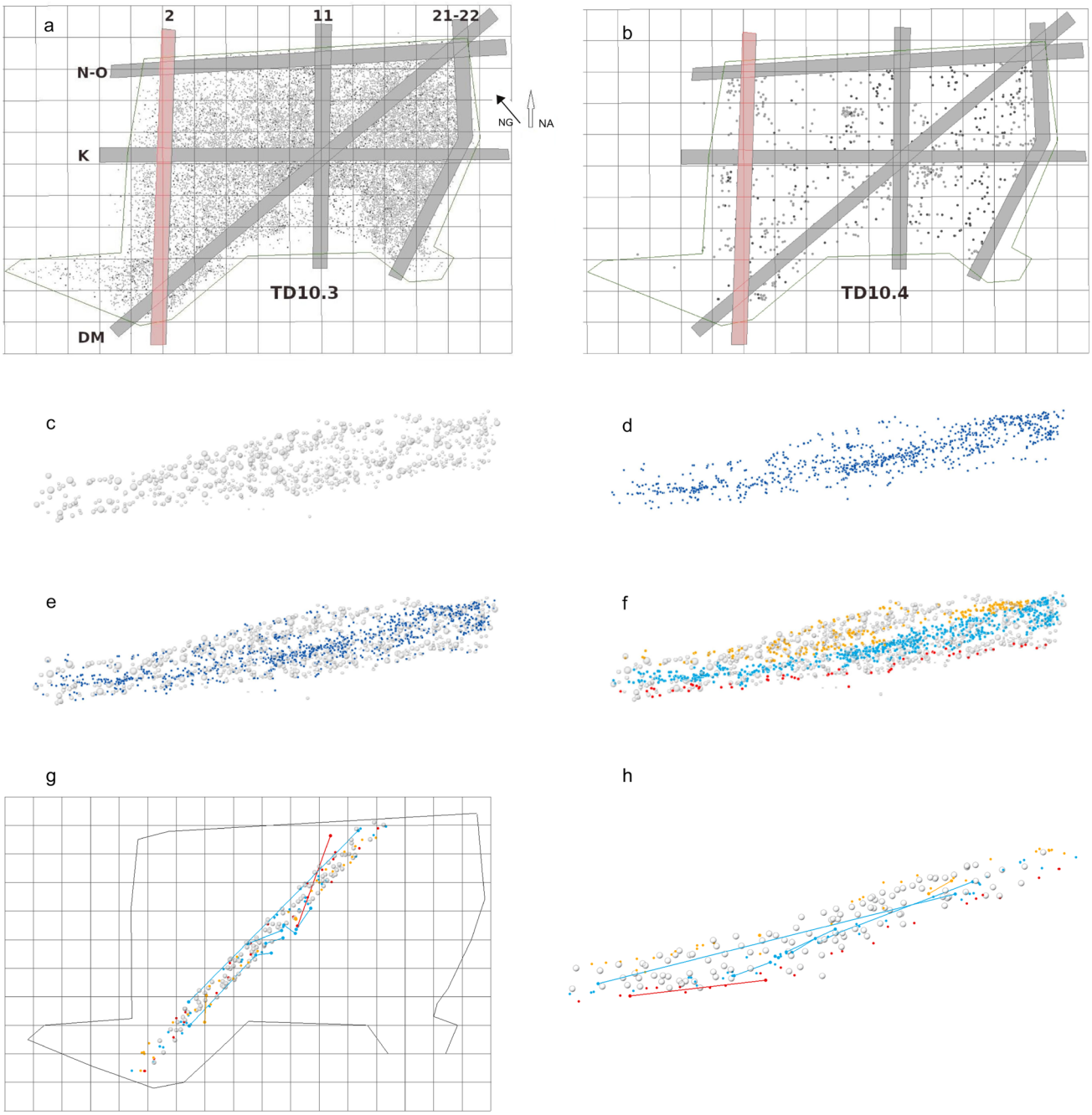

Fig. 3 Archaeological materials (artifacts and faunal remains) of TD10.3 (**a**) and TD10.4 (**b**), with some of the sections used to individualize archaeostratigraphic deposits (each square = 1 m^2). Section 2: **c** natural blocks of TD10.3 and TD10.4. **d** Faunal and lithic remains of TD10.3 and TD10.4, without distinction of levels and subunits. **e** Natural blocks, faunal and lithic remains (**c** + **d**) of TD10.3 and TD10.4. **f** Faunal and lithic remains individualizing TD10.3-Sup (yellow), TD10.3-Inf (blue) and TD10.4 (red). **g** Diagonal section selected as it contains connections of the three levels/subunits. It includes natural blocks larger than 30 cm and lithic artifacts from TD10.3-Sup (yellow), TD10.3-Inf (blue) and TD10.4 (red), as well as the connections between pieces. **h** Vertical projection of **g**. Note that connections are always shown as straight lines, regardless of the topography of the deposits

The archaeological deposit of TD10.3 is thinner towards both the back (conventional northeast) and the entrance (conventional southwest) of the cave. The average thickness of TD10.3 in both areas is about 60 cm. Occupational and depositional events of TD10.3-Sup and TD10.3-Inf have an average thickness of 25 cm and 35 cm, respectively. Archaeological subunit TD10.4 has an average thickness of 15 cm.

Finally, the count of archaeological materials is as follows: TD10.3-Sup contains 11,395 faunal remains and 666 lithic artifacts, and TD10.3-Inf contains 12,681 faunal remains and 570 lithic artifacts. TD10.4, meanwhile, contains 742 faunal remains and 247 lithic artifacts.

The Lithic Assemblages of TD10.3 and TD10.4

Composition and Mass

A total of 1,483 lithics form the assemblage of TD10.3 ($n = 1236$; 666 for TD10.3-Sup; 570 for TD10.3-Inf) and TD10.4 ($n = 247$). All raw materials traditionally used at the Sierra de Atapuerca sites are represented in both subunits: Neogene chert, Cretaceous chert, quartzite, quartzarenite, sandstone, limestone, and quartz.

All the raw materials are available in the immediate surroundings, within 4 km of the site (García-Antón et al., 2007; Ollé et al., 2013; García-Antón, 2016; de Lombera et al., 2020). Only the limestone cobbles may have formed inside the karst. Neogene chert appears as large blocks in Astaracian gypsiferous and marly limestone formations. Cretaceous chert is available at Alto de San Vicente and Valdecuende, at the top of the hill. Cobbles of sandstone, quartzite, quartz and quartzarenite can be found in the Middle Pleistocene fluvial terraces of the river Arlanzón (T8AZN + 26–35 m and T7AZN + 38–42; Moreno et al., 2012), between 2 and 4 km southwest of the site. Finally, some quartz and quartzite from both the Utrillas Formation and the River Vena terraces complete these resources. Except for the chert and limestone, the rest of the cobbles are considered fluvial materials.

Each piece was weighed, except for the Neogene chert items, whose mass were approached as described above (see the "Materials and Methods" section). We found a total mass of about 72 kg of raw materials left by hominins between the two subunits (Table 1).

A total of c. 17 kg came from TD10.3-Sup; 37.3 kg from TD10.3-Inf; and 17.6 kg from TD10.4. Both the numbers and the mass of the fluvial materials (quartzite, sandstone, quartz, and quartzarenite) slightly dominate in TD10.3-Inf (51%) due to the abundance of quartzite pebbles/cobbles and hammerstones and the great density of this raw material.

Raw Materials and Lithic Categories

In each deposit, more flakes (complete or fractured) were found than any other category in most raw materials because knapping processes result in the extraction of flakes. In addition, disregarding the nonintentional elements (i.e., the knapping fragments, because some raw materials are better given to producing them) and the indeterminate elements (most of which are of Neogene chert and poorly preserved sandstone) results in an inventory of intentionally selected and used lithotypes and categories (Table 2).

In all three deposits, both varieties of chert were mainly invested in producing flakes and small tools, although Cretaceous chert stands out in the latter. All fluvial materials and limestone were selected for manuports (unmodified cobbles) and hammerstones. Most of the hammerstones were selectively chosen from quartzite. Large tools were equally made of quartzite, Neogene chert and sandstone. There are two particular features: (1) no limestone items were recovered from TD10.4 and (2) the lower deposits (TD10.3-Inf and TD10.4) presented (a) a higher production of flakes in fluvial materials than in the upper deposit (TD10.3-Sup) and (b) three pieces with double functions (two core-and-hammerstones and one core recycled into a small tool).

The assemblage composition of TD10.3-Sup, TD10.3-Inf, and TD10.4 is shown in Fig. 4.

Statistical analyses confirmed significant differences among the three deposits, both in type of artifacts ($x^2 = 81.37$; $df = 16$; $p < 0.05$) and raw materials ($x^2 = 183.35$; $df = 16$; $p < 0.05$). Furthermore, significant differences

Table 1 Number of items, percentage and mass of lithic pieces of TD10.3-Sup, TD10.3-Inf, and TD10.4

Raw materials		TD10.3-Sup			TD10.3-Inf			TD10.4			Total		
		n	%	M	*n*	%	M	*n*	%	M	*n*	%	M
Chert	Neogene	401	60.2	4.7	224	39.3	6.1	151	61.1	5.5	776	5.5	16.3
	Cretaceous	81	12.1	0.3	18	3.1	-	20	8.1	0.1	119	8	0.5
	Indet.*	13	1.9	0.0	4	0.7	-	3	1.2	0.0	20	1.3	0.0
Limestone		17	2.5	5.0	35	6.1	7.8	-	-	-	52	3.5	12.8
Quartzarenite		2	0.3	0.5	4	0.7	0.0	3	1.2	0.4	9	0.6	1
Quartzite		79	11.8	5.2	210	36.8	19.2	47	19	8.5	336	22.6	33
Quartz		13	1.8	0.0	24	4.2	0.1	7	2.8	0.0	44	3	0.2
Sandstone		60	9	1.2	51	9	4.1	16	6.5	3.1	127	8.5	8.5
Total		666	100	17	570	100	37.3	247	100	17.6	1483	100	72.3

% = percentage of items in each deposit; M = mass in kg of each raw material and deposit. Indet.* = indeterminate, possibly Neogene chert

Table 2 Raw materials and lithic categories at TD10.3-Sup, TD10.3-Inf and -TD10.4

	CHERT								
	NCh	CCh	Ch	LM	QRT	QT	QZ	SD	Total[ç]
TD10.3-Sup (%)									
Unmodified cobbles (*Manuports*)	-	-	-	9 (42.8)	-	6 (28.5)	1 (4.8)	4 (19)	20 (3.8)
Hammerst. and frags*	-	-	-	5 (25)	1 (5)	14 (70)	-	-	20 (3.8)
Large tools	3 (27.3)	-	-	1 (9.1)	-	4 (36.3)	-	3 (27.3)	11 (2.1)
Cores	5 (50)	5 (50)	-	-	-	-	-	-	10 (1.9)
Small tool	26 (67)	10 (25.6)	-	-	-	2 (5.1)	1 (2.5)	-	39 (7.4)
Flakes	259 (61.4)	64 (15.1)	6 (1.4)	2 (0.5)	1 (0.2)	50 (12)	9 (2.1)	31 (7.3)	422 (80.5)
Intentional items	293 (55.8)	79 (15)	6 (1.1)	17 (3.2)	2 (0.4)	76 (14.5)	11 (2.1)	40 (7.7)	524 (78.7)
Knapping fragments	14 (54)	2 (7.7)	-	-	-	3 (11.5)	2 (7.7)	5 (19.2)	26
Indetermined	94 (81)	-	7 (6)	-	-	-	-	15 (13)	116
Total	401 (60.1)	81 (12.1)	13 (1.9)	17 (2.5)	2 (0.3)	79 (11.8)	13 (1.9)	60 (9)	666
TD10.3-Inf (%)									
Manuports	-	-	-	11 (64.7)	-	5 (29.4)	-	1 (5.9)	17 (3.4)
Hammerst. and frags*	-	-	-	9 (16.7)	-	41 (76)	-	4 (7.4)	54 (10.7)
Large tools	7 (30.4)	-	-	1 (4.3)	-	12 (52.2)	-	3 (13)	23 (4.6)
Cores[$]	10 (43.5)	2 (8.7)	-	-	-	8 (34.8)	3 (13)	-	23 (4.6)
Small tool	18 (36)	5 (10)	-	-	1 (2)	18 (36)	2 (4)	6 (12)	50 (9.9)
Flakes**	145 (43.1)	11 (3.3)	-	10 (3)	3 (0.9)	125 (37.2)	15 (4.4)	27 (8)	336 (67)
Intentional items	180 (36)	18 (3.6)	-	31 (6.2)	4 (0.8)	208 (41.4)	20 (4)	41 (8.2)	503 (88.2)
Knapping fragments	7	-	-	3	-	1	4	4	19
Indetermined	37	-	4	1	-	1	-	6	49
Total	224 (39.3)	18 (3.1)	4 (0.7)	35 (6.1)	4 (0.7)	210 (36.8)	24 (4.2)	51 (8.9)	570
TD10.4 (%)									
Manuports	-	-	-	-	-	2 (66.7)	1 (33.3)	-	3 (1.3)
Hammerst. and frags*	-	-	-	-	2 (9.5)	16 (76.2)	-	3 (14.3)	21 (10.8)
Large tools	4 (40)	-	-	-	-	4 (40)	-	2 (20)	10 (4.5)
Cores[$]	5 (41.7)	1 (8.3)	-	-	1 (8.3)	1 (8.3)	1 (8.3)	3 (25)	12 (5.4)
Small tool	12 (54.5)	3 (13.6)	-	-	-	5 (22.7)	1 (4.5)	1 (4.5)	22 (9.9)
Flakes**	108 (70.6)	13 (8.5)	2 (1.3)	-	-	19 (11.7)	4 (2.6)	8 (5.2)	154 (69.3)
Intentional items	129 (57.6)	17 (8.5)	2 (0.9)	-	3 (1.3)	47 (21)	7 (3.1)	17 (7.6)	222 (90.7)
Knapping fragments	9	1	-	-	-	-	-	-	10
Indetermined	14	-	1	-	-	-	-	-	15
Total	152 (61.5)	18 (7.3)	3 (1.2)	-	3 (1.2)	47 (19)	7 (8.5)	17 (6.9)	247

NCh Neogene chert, *CCh* Cretaceous chert, *Ch* indetermined chert, *LM* limestone, *QRT* quartzarenite, *QT* quartzite, *QZ* quartz, *SD* sandstone

Italics: percentages of raw materials invested in each lithic category (without fragments and indetermined pieces)

*Hammerstones and fragments of hammerstones

**Include complete flakes, broken flakes and flake fragments

[$]Some elements have played two roles (i.e., core + hammerstone) and have counted for both categories, so the totals may not match the number of pieces

[ç]Percentages of each category of pieces regarding the total of intentional items

regarding the types of artifacts were found between TD10.3-Sup and the other two underlying deposits, while significant differences in raw materials were found between all three deposits.

Raw material groups (RMG). Subunits TD10.3-Sup, TD10.3-Inf, and TD10-4 yielded 1483 lithic artifacts, made on seven different lithotypes: Neogene chert, Cretaceous chert, quartzite, quartzarenite, sandstone, limestone, and quartz. We analyzed a total of c. 900 pieces (60.6%, see the "Raw Material Groups" section), of which we were able to classify 467 (52%) into 136 RMG (Table 3): 90 quartzite groups, 19 sandstone groups, seven quartz groups, six Neogene chert groups, five quartzarenite groups, five limestone groups, and four Cretaceous chert groups (SI Fig. S2).

The high ratio of RMG attribution for sandstone, quartzite, and especially Cretaceous chert is directly linked to the

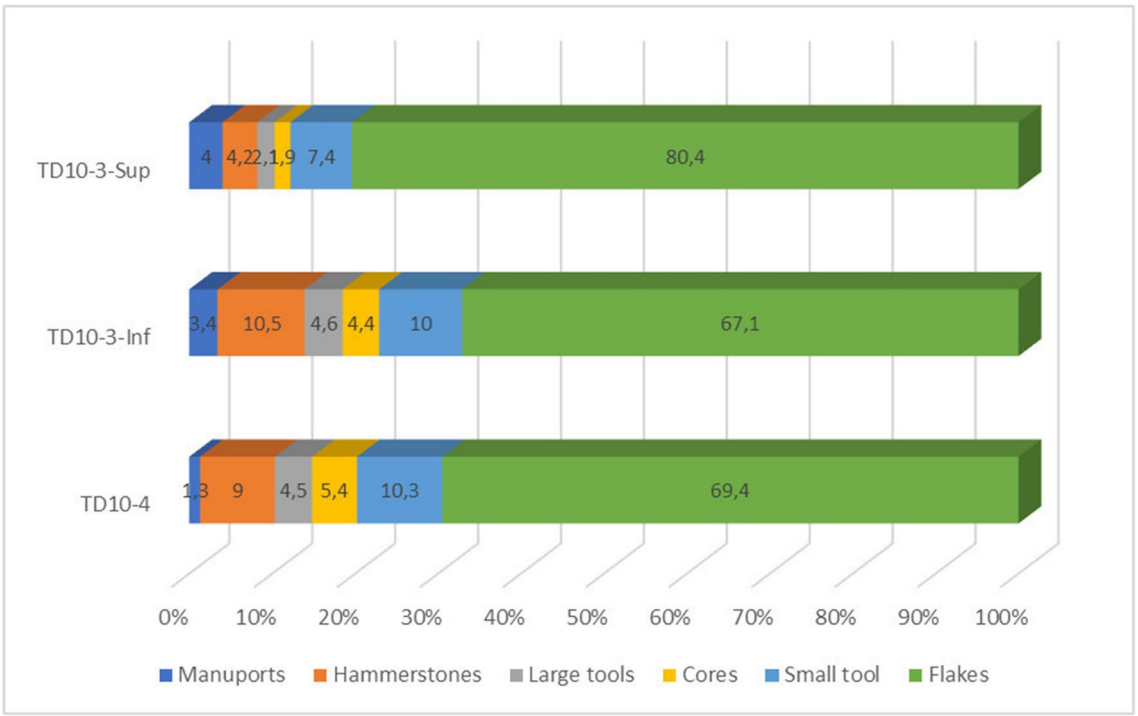

Fig. 4 Investment of each type of artifact at TD10.3-Sup, TD10.3-Inf, and TD10.4

better preservation of these materials, which allowed us to identify more taphonomic conditions such as type of neocortex, alterations, etc. Although some pieces of Cretaceous chert also present a white patina across their surfaces, the attributes of the only two varieties that exist in the Sierra facilitate attribution. On average, 67.55% of the quartzite pieces were ascribed to an RMG, and only 5.86% of the Neogene chert was possible to identify due to the poor preservation of both the surface and the interior.

We should mention that, although the diversity of quartzite is high (RMG = 90), only four specific RMGs appear in the three deposits. They are CTb1, CTg, CTh, and CTj2 (SI Fig. S2).

Percussive Tools

The complete cobble assemblage retrieved from TD10.3 and TD10.4 includes a total of 128 objects (8.6% of the whole assemblage), of which 103 were analyzed (Fig. 5). The 25 pieces from the excavations conducted in the 1990s and deposited in the Museo de la Evolución Humana (MEH, Burgos) were not revised. The distribution by levels of the cobble assemblage is summarized in the following table (Table 4).

A predominance of quartzite, followed by limestone and sandstone elements, with a minor representation of other raw materials (quartz, quartzarenite, and others), was documented across TD10.3 and TD10.4. In general, the main difference in raw materials is that limestone elements are present in TD10.3 while in TD10.4, they are completely absent (Table 5).

The main alterations identified were weathering dissolution ($n = 8$) and fissures ($n = 9$). In terms of sizes (SI Table S1), the manuports and the hammerstones are of similar dimensions.

Percussive Assemblage from TD10.3-Sup The assemblage from TD10.3-Sup comprises a total of 41 objects. The most abundant tools are manuports ($n = 19$, 45.2%), followed by hammerstones ($n = 14$, 33.3%). Quartzite was the main raw material used for hammerstones ($n = 7$), followed by limestone ($n = 4$). In contrast, most of the manuports are limestone ($n = 9$), followed by quartzite ($n = 6$) and sandstone ($n = 3$) cobbles.

Statistical comparisons of the manuports and the hammerstones found no significant differences in length ($t_{31} = -0.415$, $p = 0.681$) (SI Table S2). The Mann–Whitney U test found no significant differences in width ($U = 114.500$, $p = 0.50$), thickness ($U = 115.500$, $p = 0.52$), or mass ($U = 83.000$, $p = 0.73$) between clusters. These results confirm the homogeneity of the size of the cobbles that were collected and transported into the cave during the time TD10.3-Sup was in use.

Table 3 Lithic pieces according to raw material, pieces ascribed to RMG, percentage regarding the total number of pieces of each raw material, and number of RMG identified at each deposit

Raw material	TD10.3-Sup				TD10.3-Inf				TD10.4			
	No. of pieces	Pieces RMG	%	Num RMG	No. of pieces	Pieces RMG	%	Num RMG	No. of pieces	Pieces RMG	%	Num RMG
Ch	81	65	80.2	4	18	13	72.2	3	20	13	65	2
NCh	401	23	5.7	5	224	10	4.4	4	151	14	9.3	5
LM	17	4	23.5	3	35	18	51.4	4	-	-	-	-
QRT	2	1	50	1	4	4	100	3	3	3	100	1
QT	79	43	54.4	33	210	151	72	59	47	33	70.2	24
Qz	13	6	46	4	24	9	37.5	5	7	1	14.3	1
SD	60	11	18.3	8	51	34	66.6	17	16	11	68.7	7
Total	653	153	23.4	58	566	239	42.2	95	244	75	30.7	40

None RMG has been found into the Ch (indetermined chert) group ($n=20$)

CCh Cretaceous chert, *NCh* Neogene chert, *LM* limestone, *QRT* quartzarenite, *QT* quartzite, *QZ* quartz, *SD* sandstone

Percussive Wear Patterns of TD10.3-Sup We analyzed 10 of the 14 hammerstones identified in TD10.3-Sup. Overall, we determined that the hammerstones were not intensively used based on the macroscopic traces recognized on their surfaces, as their surfaces exhibited few percussive traces. Nearly all of them had only one area of use, while one hammerstone showed two areas with percussive marks. Two hammerstones bore small battered areas on the surfaces located on convex and distal areas, while clusters of impact points were more frequent ($n=9$), mostly located on convex surfaces. Fractures were documented on eight hammerstones. Most of the fractures identified were caused by a direct impact; only in one case was it evident that the hammerstone fractured due to a fatigue process (the repetitive use of the same area of the tool).

Percussive Assemblage from TD10.3-Inf It comprises 66 pieces. Most of them are hammerstones (54.5%), followed by manuports (30.3%). Fifty-eight pieces of this assemblage were analyzed, and a clear dominance of quartzite (60.6%), followed by limestone (27.3%) and sandstone (12.1%) was documented in this subunit. The distribution of the raw materials is clearly biased in terms of technological categories. The great majority of the hammerstones are on quartzite ($n=27$), while the manuports are mainly limestone cobbles ($n=12$). The low number of quartzite manuports selected ($n=6$) indicates that practically any quartzite cobble that was transported to the cave was, to some extent, used.

The general mean values for tool size (SI Table S3) were very similar between the hammerstones and the manuports. A normality test showed that their dimensions (length, width, and thickness) were normally distributed (Shapiro–Wilk test $p>0.05$ in all parameters). A *t*-test comparison of both groups (manuports and hammerstones) revealed no significant differences in length ($t_{23.042}=0.810$, $p=0.42$), width ($t_{23.231}=0.024$, $p=0.98$), or thickness ($t_{54}=0.042$, $p=0.96$). Additionally, when comparing their mass, the Mann–Whitney test showed no significant differences between the hammerstones and the manuports ($U=256.000$, $p=0.33$). Therefore, the similarity in the sizes of the hammerstones and manuports is statistically supported.

Percussive Wear Patterns of TD10.3-Inf Of the 36 hammerstones, 33 were analyzed. In the case of TD10.3-Inf, a high number of tools bore superficial percussive traces ($n=18$), while the rest exhibited deeper percussive marks, with at least four tools presenting a high degree of surface modification. The great majority of tools ($n=21$) had only one active area. However, interestingly, nine hammerstones showed two active zones, and two additional hammerstones had three and four active zones. This indicates that 11 tools were reoriented (flipped) during their use or they were used in different events.

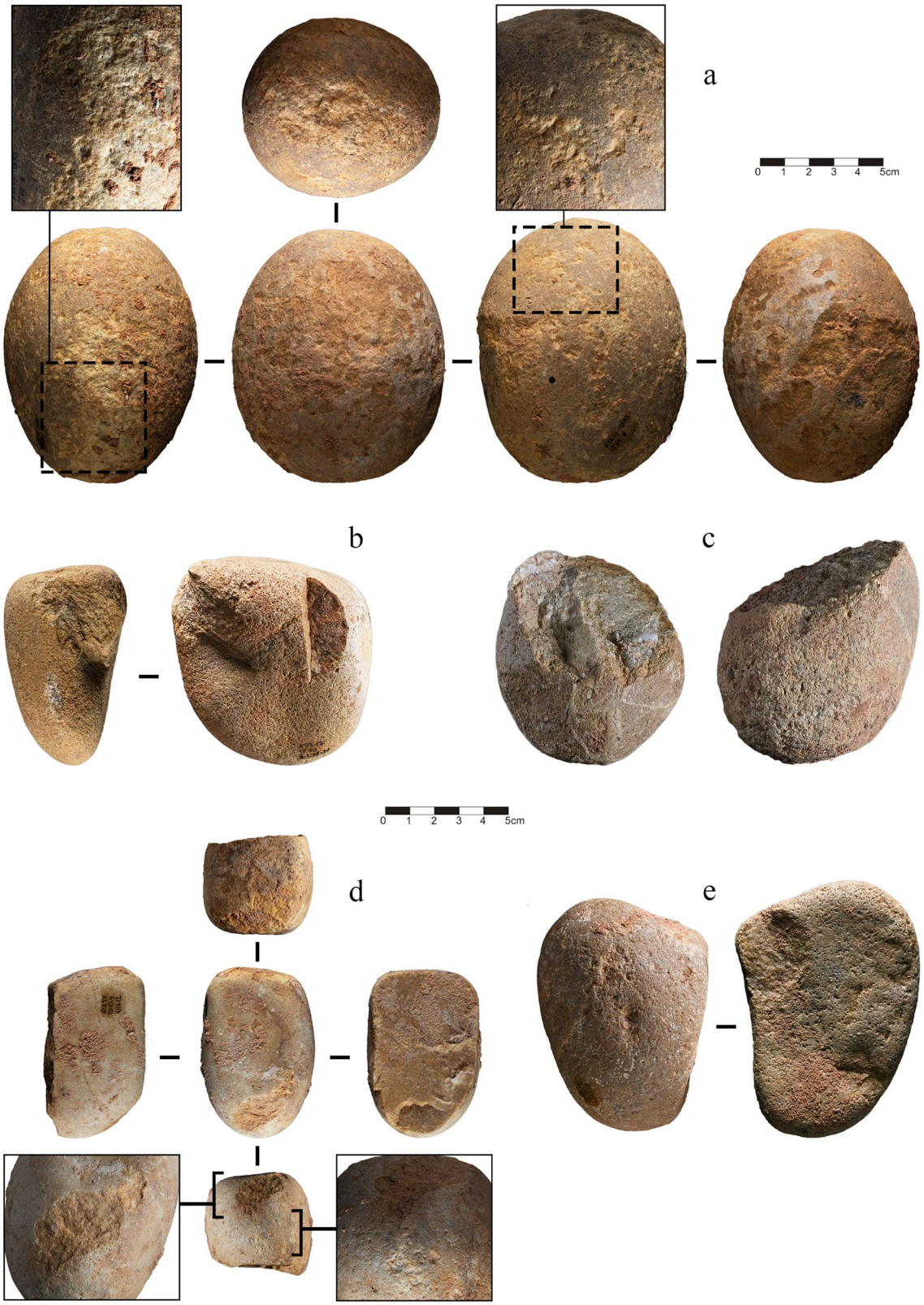

Fig. 5 Percussive tools from TD10.3 bearing deep percussive marks (**a**, **b**) and large fractures (**c**), and TD10.4 (**d, e**) showing a less degree of modification

Table 4 Technological categories of the percussive material from TD10.3 and TD10.4

Category	TD10.3-Sup	TD10.3-Inf	TD10.4	Total *n* (%)	
Unmodified material (*manuports*)	18	20	1	39	30.4
Hammerstones	14	36	18	68	53.1
Percussive by-products	9	10	2	21	16.4
Total	41	66	21	128	100

Table 5 Percussive elements and raw materials from TD10.3-Sup, TD10.3-Inf, and TD10.4

	Limestone (%)	Quartzite (%)	Quartz (%)	Quartzarenite (%)	Sandstone (%)	Total
TD10.3-Sup						
Manuports	9	6	-	-	3	18
Hammerstones	4	7	1	1	1	14
Percussive by-products	1	5	-	1	2	9
Total	14 (33.3)	18 (43)	1 (2.4)	2 (4.8)	6 (14.3)	41
TD10.3-Inf						
Manuports	12	6	-	-	2	20
Hammerstones	3	27	-	-	6	36
Percussive by-products	3	7	-	-	-	10
Total	18 (27.3)	40 (60.6)	-	-	8 (12.1)	66
TD10.4						
Manuports	-	1	-	-	-	1
Hammerstones	-	14	1	1	2	18
Percussive by-products	-	1	-	1	-	2
Total	-	16 (76.2)	1 (4.8)	2 (9.5)	2 (9.5)	21
Total	32	74	2	4	16	128

The high degree of use is also reflected in the percussive marks identified. Battered areas were documented on 18 hammerstones, and 27 of the hammerstones bore surface impacts. The distribution of the marks is quite consistent, with the convex areas of the blanks being preferentially selected. We identified fractures on 19 hammerstones.

Percussive Assemblage from TD10.4 It is made up of 21 pieces. In total, we identified 18 hammerstones (85.6%). The assemblage from TD10.4 is predominantly made of quartzite, with isolated representation of other raw materials.

In terms of size, the mean dimensions of the hammerstones were [L × W × T] 70.9 × 54.3 × 39.3 mm, and their mean mass was 298.5 g (SI Table S4), a similar value to that recorded for the manuport cobbles. In this case, given the extremely low number of pieces, no statistical tests were applied.

Percussive Wear Patterns of TD10.4 Fourteen of the 18 hammerstones included in the assemblage were analyzed. The hammerstones from TD10.4 are characterized by the presence of impact points, mainly with a clustered distribution (on eight tools), with five artifacts bearing scattered impact marks. Within the entire hammerstone assemblage, battered areas located on convex zones of the cobbles were identified on seven tools, while seven of them also presented fractures. Overall, the wear traces were generally superficial on the blanks, with only four tools bearing traces pointing to more intensive use.

When comparing the percussive assemblage diachronically, there are two points to consider:

a) No significant differences were found in the length ($U = 200.500$, $p = 0.26$), width ($U = 201.000$, $p = 0.27$), thickness ($U = 195.500$, $p = 0.22$) or mass ($U = 180.000$, $p = 0.54$) of the tools when comparing the hammerstones from TD10.3-Sup and TD10.3-Inf. This indicates that the percussive tools from these two deposits are morphologically similar. Nonetheless, TD10.3-Sup yielded a higher percentage of manuports than TD10.3-Inf.
b) Statistically significant differences were found in the length ($U = 205.500$, $p = 0.030$) and the width ($U = 202.500$, $p = 0.02$) of the hammerstones of TD10.3-Inf (larger) and TD10.4 (shorter). In contrast, no significant differences were found in the mass of the two groups ($U = 196.000$, $p = 0.11$). A common characteristic in both levels is that the majority of the transported cobbles were used to some extent (or at least have percussive marks and/or fracture on their surfaces).

When comparing the hammerstones and the manuports regarding the raw material:

a) In TD10.3-Sup, there is no clear association between the raw materials in the type of tool (χ^2 (5, $N=33$) = 5.37, $p=0.373$).
b) On the contrary, in TD10.3-Inf, there is an association between raw material and type of tools (hammerstone and manuports) (χ^2 (2, $N=56$) = 17.63, $p<0.001$). This correlation is most likely related to the overrepresentation of manuports of limestone (60%, $N=12$) and hammerstones of quartzite (75%, $N=27$).
c) Finally, in TD10.4, we did not find a statistical association between the raw material and the type of tools (percussive tools and manuports) (χ^2 (3, $N=19$) = 0.28, $p=0.963$). This means that there is an even representation of raw materials, with no preference in their selection for a specific type of tool.

In sum, we can argue that based on these results, hominins seemed to select preferentially quartzites to be used as hammerstones, while limestone cobbles were transported to the cave but not used.

Large Tools

TD10.3 and TD10.4 together yielded 44 large tools (LT), most of which are large cutting tools (LCT; $n=30$) (Fig. 6) (Table 6). Out of the 44 LT, three of them exhibited a high degree of alteration, making technological analyses difficult. Large tools represent 3% of the whole lithic assemblage of TD10.3 and TD10.4. However, there are quantitative differences between the deposits. The frequency of LTs is reduced to less than half at the top of the sequence: from c. 4% in TD10.4 and TD10.3-Inf to 1.6% in TD10.3-Sup.

By far, the most represented LT type was the handaxe (sensu Isaac, 1977) (54.5% of large tools), followed by cleavers (sensu Isaac, 1977) (11.3%), unifacial tools (6.8%) and large sidescrapers (4.5%). The predominance of handaxes over any other large shaped tool did not occur in TD10.3-Sup, from which two handaxes and three cleavers were recovered. In addition, TD10.3-Sup did not yield any choppers or chopping tools, which were only present in the lower deposits.

Omitting the choppers and chopping tools, which are made on cobbles, the majority of large tools were made on flakes in all three deposits (Table 7). In addition, in all three deposits, the LTs made on blocks/cobbles, although found in fewer numbers than those made on flakes, were more intensely shaped in terms of the percentage of the perimeter that was knapped. In contrast, the LTs on flakes, although more abundant, include several pieces that were shaped on 25% of their perimeter or less (SI Fig. S3). Diachronically, there is a slight increase of LTs on flakes moving up the sequence (TD10.4 = 66.7%; TD10.3-Inf = 75%; and TD10.3-Sup = 77.7%), and a clear decrease in the intensity of LT shaping. All of this is regardless of the raw materials used.

To assess the intra-group variability in the shape of the LCTs, we applied geometric morphometric techniques on 26 LCT 3D models, excluding fragmented tools which had lost their final shape. The principal component analysis confirmed the great heterogeneity of this assemblage. More than 84% of the variability is explained by the first 10 principal components (SI Table S5). The best characterization of this assemblage resulted from the combination of PC1 (23.88%) and PC3 (11.42%) (Fig. 7), although we also explored the combination of PC1-PC2 and PC2-PC3.

PC1 accounted for 23.88% of the variability and relates to the profile shape, from thicker pieces on negative values to thinner tools on positive values. PC2 accounted for 11.62% of the variability and represents the variation mainly concentrated on the proximal parts only, with wider shapes on negative values and convex proximal parts on positive ones. PC3 accounted for 11.42% of the variability and described an axis of variation from pointed and wider-butt bases in positive values to oval tools with wider distal parts. PC2 and PC3 therefore represent a similar percentage of variability. Nevertheless, PC3 gathers more information according to our assemblage. Therefore, although we also examined the combination of PC1-PC2 (SI Fig. S4), the best characterization of this assemblage resulted from the combination of PC1 and PC3 (Fig. 7).

In general, the intra-group variability was found to be high and slightly increased along the sequence (Table 8). However, the LTs of TD10.4 and TD10.3-Inf present very similar intra-group variability, which seems to reinforce the differences between TD10.4 and TD10.3-Inf and between TD10.4 and TD10.3-Sup.

TD10.4 and TD10.3-Inf share the majority of the scatter distribution for this type of tool, with a clear tendency toward wider butts and thicker implements, together with classical oval distal ends (tear-drop shape). The Wilcoxon Rank-sum test on the interpoint distance between group means found no statistically significant differences between TD10.4 and TD10.3-Inf (rank sum = 345; n1 = 8; n2 = 12; $p=0.08$). In both cases, tool shape variability was mainly caused by thickness (see Table 8). In contrast, the mean shapes between TD10.3-Inf and TD10.3-Sup were found to be significantly different (rank sum = 267; n1 = 12; n2 = 7; $p \leq 0.01$). TD10.3-Sup presented the highest intra-site variability. Most of this variation was due to the width of the tools, which affects also the mid-distal parts. Those tools present the widest measures in the mid-distal ends. In addition, a progressive reduction in LT volume was identified from TD10.4 to TD10.3-Sup.

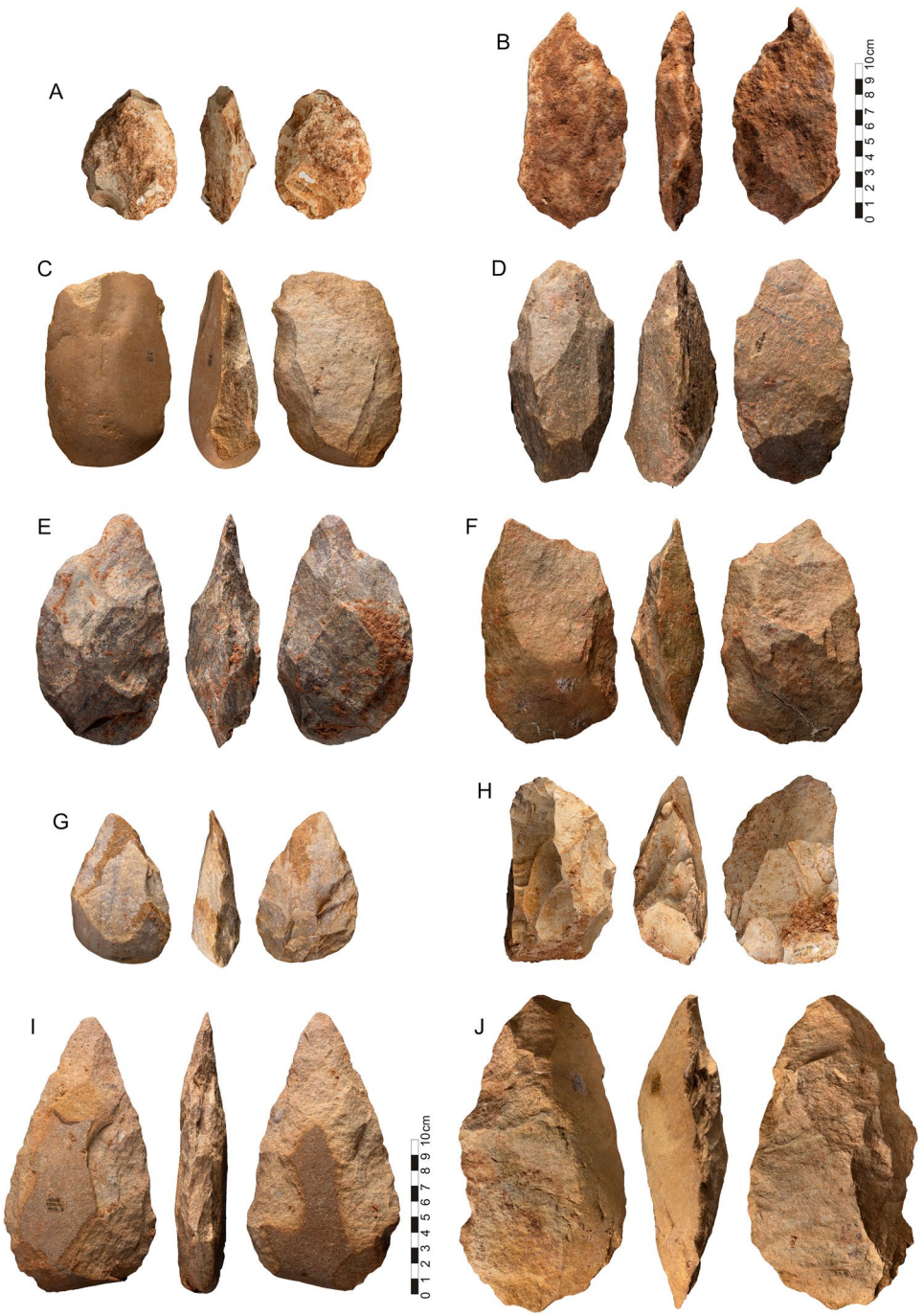

Fig. 6 Large cutting tools from TD10.3-Sup: **A** Neogene chert handaxe ATA14-M20-1, **B** limestone handaxe ATA13-I14-20, **C** quartzite cleaver on flake ATA14-N13-14; TD10.3-Inf: **D** quartzite handaxe ATA15-N17-109, **E** quartzite handaxe ATA16-J11-50, **F** quartzite cleaver on flake ATA17-J19-92); TD10.4: **G** quartzite handaxe ATA16-N19-199, **H** Neogene chert handaxe ATA17-H19-4, **I** quartzite handaxe ATA17-N21-3, **J** sandstone handaxe ATA17-K18-103

To sum up, the large tools from TD10.4 and TD10.3 presented high intra-group variability. Also, the dimensions of the tools from TD10.4 and TD10.3-Inf together differentiate them from those of TD10.3-Sup. A slight transition was detected from the classical "tear-drop" shapes in TD10.4 and TD10.3-Inf, to wider shapes increasing their variability in TD10.3-Sup (Fig. 8).

Cores

In total, 45 cores were recovered from TD10.3 and TD10.4, distributed as follows (Fig. 9) (Table 9): 10 cores at TD10.3-Sup (1.34% of the whole assemblage), 22 at TD10.3-Inf (c. 4%) and 12 at TD10.4 (c. 5%). One core from TD10.3-Inf was extremely damaged and could not be analyzed.

Table 6 Types of large tools at each archaeological deposit

Large tools		TD10.3-Sup	TD10.3-Inf	TD10.4	Total	Type
Handaxe	Neogene chert	2	6	2	10	24
	Quartzite	-	5	2	**7**	
	Sandstone	-	1	2	3	
	Limestone	-	1	-	1	
Handaxe fragment	Quartzite	-	1	-	1	
Handaxe tip	Quartzite	-	2	-	2	
Cleaver	Neogene chert	-	-	1	1	5
	Quartzite	2	-	-	2	
	Sandstone	1	1	-	2	
Pick	Quartzite	1	-	-	1	1
Chopper	Quartzite	-	1	-	1	1
Chopping-tool	Quartzite	-	1	1	2	2
Denticulate	Limestone	1	-	-	1	1
Distal fragment of LT	Quartzite	1	-	-	1	1
Rabot	Quartzite	-	1	-	1	1
Sidescraper	Neogene chert	1	-	-	1	2
	Sandstone	1	-	-	1	
Unifacial LT	Quartzite	-	1	1	2	3
	Sandstone	-	1	-	1	
Indetermined LT	Neogene chert		1	1	2	3
	Sandstone	1	-	-	1	
Total		11	23	10	44	44

Table 7 Large tools per blank type and raw material (choppers and chopping tools are excluded)

LT blank	TD10-3-Sup	TD10-3-Inf	TD10-4	Total
Cobble/block	2	4	3	9
Limestone		1		1
Neogene chert	1		1	2
Quartzite	1	2	2	5
Sandstone		1		1
Flake	7 (77.7%)	12 (75%)	6 (66.7%)	25
Neogene chert	2	5	3	10
Quartzite	2	5	1	8
Sandstone	3	2	2	7
Total	9	16	9	34

All three archaeological deposits share a type of knapping pattern based on the raw materials (SI Fig. S5a) and/or type of blank (SI Fig. S5b): (1) cores in fluvial materials were usually flaked through unipolar longitudinal knapping, using cortical surfaces as striking platforms and hitting at 80° to 90° angles (Fig. 9a, b, f). This strategy is present in TD10.3-Inf and TD10.4, but it is absent in TD10.3-Sup, where no cores have been recovered in these raw materials; (2) cores in Cretaceous chert were usually reduced by orthogonal and centripetal knapping (Fig. 9j, k); (3) when the blanks were flakes, the knapping strategy tends to be centripetal (although poorly standardized) (Fig. 9e, g, h), while when the blanks are nodules or fragments (especially in Neogene chert), the knapping strategy tends to be unipolar longitudinal and orthogonal (Fig. 9d, i). The bipolar technique on an anvil was also possibly present (Fig. 9c).

Although the flakes are the best represented category in these assemblages, the reduction sequences tend to be relatively short based on the number of scars present on the cores and the cortical reserves of the cores, which would indicate partial volume management.

Diachronically, no qualitative changes in knapping strategies were found through the progression of the sequence, but qualitative changes were detected in raw material selection: the variation in knapping strategies from TD10.4 to TD10.3-Sup (SI Fig. S5a) is more related to the decrease in the varieties of raw materials used through the progression of the sequence: in TD10.4 cores were made on six lithotypes; in TD10.3-Inf, they were made on four lithotypes; and in TD10.3-Sup on two lithotypes (SI Fig. S5a and c). Actually, this would also explain why no testing cores were recovered from TD10.3-Sup, because these hominins only used Cretaceous and Neogene chert (SI Fig. S5a). Cretaceous chert is always good quality, and Neogene chert comes from the mega-blocks in the gypsiferous and marly limestone facies on the slopes of the hill that need to be broken in order to bring fragments into the cave, so testing had already occurred at the supply area.

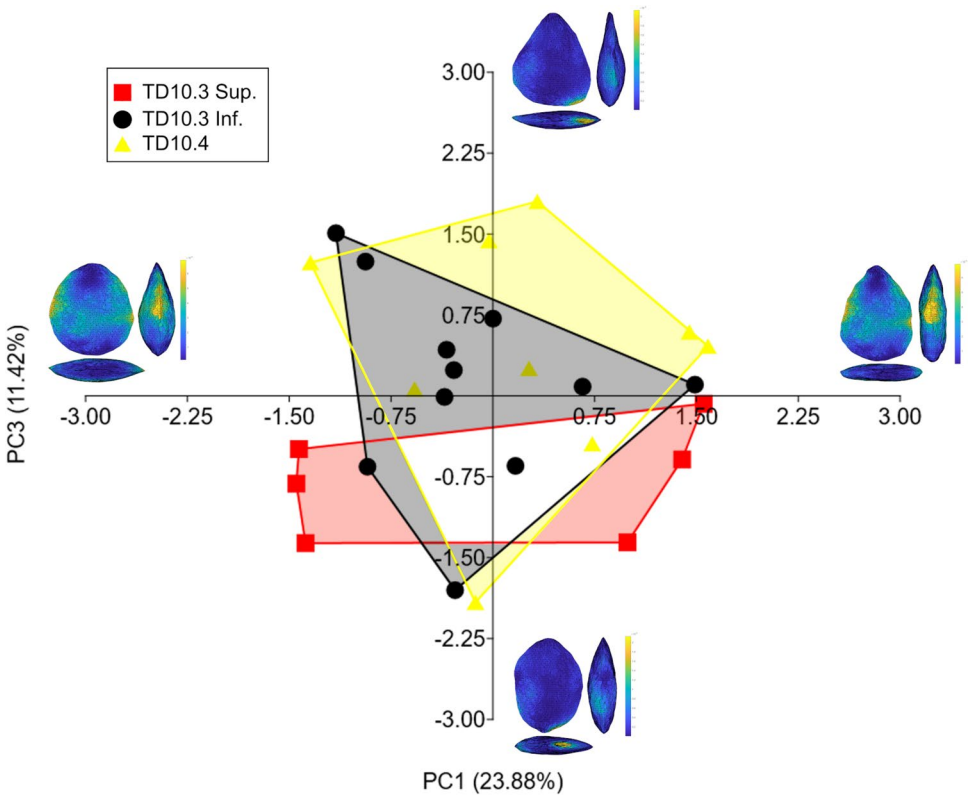

Fig. 7 PCA on handaxes 3D models by sites. Illustrations show hypothetical objects situated at the extremities of each principal component, reflecting the shape trend it represents. Convex hulls represent the scatter plot limits on each group (TD10.3-Sup; TD10.3-Inf; TD10.4). White area is the shared space between three groups

Table 8 Intra-assemblage shape variability analysis (mean multidimensional Euclidean distance of all artifacts from its centroid) and distribution of relative shape variability across dimensions of Fig. 7

				% of variability caused by		
	(n)	Volume	Shape variability	*x* (Width)	*y* (Length)	*z* (Thickness)
TD10.3-Sup	6	126,408.09	8.27	55.95	2.28	41.77
TD10.3-Inf	11	143,298.33	7.86	38.96	1.62	59.42
TD10.4	9	190,662.06	7.72	44.91	1.44	53.65

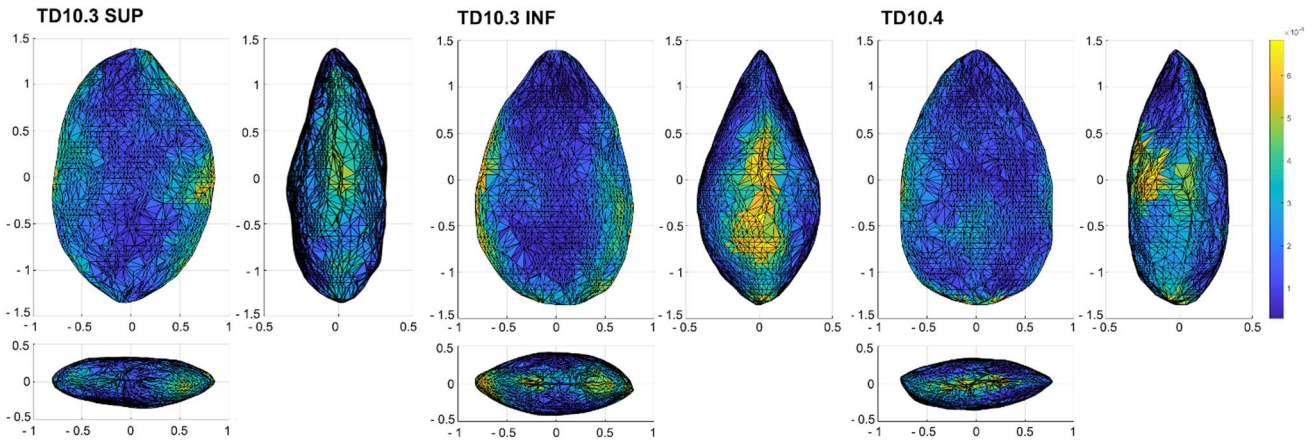

Fig. 8 Mean shapes of Large Tools by subunits. Color coding represents the relative degree of variability of each individual landmark reflecting the spatial distribution of variability across the tools

Fig. 9 Cores from TD10.3 and TD10.4. TD10.3-Sup: **a** Neogene chert, unipolar longitudinal ATA15-I14-35; **b** Cretaceous chert, unipolar longitudinal ATA13-J19-32; **c** Cretaceous chert, bipolar on an anvil ATA14-K15-24; TD10.3-Inf: **d** Neogene chert, unipolar longitudinal ATA16-M19-523; **e** quartzite, centripetal ATA17-L15-99; **f** quartzite, unipolar longitudinal ATA17-M20-1; **g** quartz, centripetal ATA17-J13-192; **h** Neogene chert, centripetal ATA17-H20-42; TD10.4: **i** quartzite, unipolar longitudinal ATA17-H12-1; **j** sandstone, centripetal ATA18-L21-29; **k** Neogene chert, orthogonal ATA18-H19-10

Small Tools

A total of 111 small tools were recovered from TD10.3 and TD10.4 (see Table 2, Fig. 10a–c, e–g, i–j, m, n). The proportions in the three archaeological deposits, excluding indeterminable pieces and fragments, were similar: 7.4% for TD10.3-Sup, 9.9% for TD10.3-Inf and 9.9% for TD10.4. The following types were identified (Table 10).

Denticulates and side/transverse scrapers were the most common small tools in all three deposits. However, a turn occurred over the course of the sequence in which denticulates were more numerous than scrapers in TD10.4, an equal number of both types were present in TD10.3-Inf, and scrapers became dominant at TD10.3-Sup.

Although only a few specimens were recovered, there were two points, four endscrapers distributed among the three deposits, as well as four double tools, including one borer (see Fig. 11), and one triple tool. Also interesting is the almost exclusive use of Neogene and Cretaceous chert for small tools in TD10.3-Sup (see Table 2)—a bias already observed among the cores—and the abundance of small tools in fluvial materials in TD10.3-Inf. This demonstrates that the presence of these raw materials in TD10.3-Inf was not only related to percussive material.

Flakes

A total of 912 pieces belong to the simple flake category (Table 11) (Fig. 10d, h, k, l, o). In all three deposits, the majority of these pieces are complete flakes (56.5%). Technically, they share several technical attributes: the dorsal surfaces are mainly non-cortical (c. 68%); they have two or three (c. 28%) dorsal removals; and they were knapped using unipolar (58%) or centripetal (27%) directions. The striking platforms (88%) are mainly non-cortical (80.5%) and flat (62%), the ventral surfaces present diffuse bulbs (69%), and the morphology of the flakes is trapezoidal (29%), triangular (18%) or rectangular (15%).

Only complete flakes were considered in the dimension analysis. Given the small number of items classified into different RMGs, we did not perform any comparative analyses of the dimensions.

The values of the technical (not morphological) length, width and thickness of the different assemblages did not present a normal distribution ($p < 0.05$) (SI Table S6), so non-parametric tests were applied for the statistical analysis. The Kruskal–Wallis test (K-W) revealed significant differences among the lengths (K-W: 12.422; p value: $p < 0.01$), widths (K-W: 15.779; p value: $p < 0.01$), and thicknesses (K-W: 95.185; p value: $p < 0.01$) of the complete flakes from the three assemblages. The flakes from TD10.3-Inf were slightly larger and those from TD10.3-Sup were the smallest.

Nevertheless, examining each lithic assemblage separately, it becomes clear that the main differences in the flake dimensions are not related to raw material types and their representation within the assemblage. Sandstone and quartzite flakes are slightly longer and wider than their counterparts on Neogene and Cretaceous chert, but no statistically significant differences were found among them, even though Cretaceous chert is usually available in small nodules (SI Tables S7 to S9). Only in the TD10.4 assemblage were slight differences between the width (K-W: 10.843; $p = 0.01$) and thickness (K-W: 8.1664; $p = 0.04$) of the flakes observed. Therefore, the statistically significant differences concerning the length, width and thickness of the assemblages may be related to diachronic changes, with a focus on the production of smaller flaking products in TD10.3-Sup.

Table 9 Cores: blank type, knapping strategy, and raw materials in TD10.3-Sup, TD10.3-Inf, and TD10.4

Raw material	Blank type	Knapping strategy																	
		Unipolar unifacial longitudinal			Bip./multip. bif./trif. orthogonal			Multipolar unifacial centripetal			Multipolar bifacial centripetal								
		3S	3I	4	3S	3I	4	3S	3I	4	3S	3I	4						
Cretaceous chert	Flake										1		1						
	Fragment																		
	Nodule	1			1		2												
Neogene chert	Flake	1					1												
	Fragment						1				1								
	Nodule		2	1	1		1												
Quartzarenite	Cobble			1															
Quartzite	Flake		1							1									
	Cobble		4	1						1									
Quartz	Flake									1									
	Fragment																		
	Cobble																		
Sandstone	Cobble						1						1						
Total		**2**	**7**	**3**	**2**		**5**	**1**	**-**		**3**	**1**	**2**			**2**		**4**	

Raw material	Blank type	Knapping strategy															Total		
		Bipolar unifacial opposed			Bipolar bifacial opposed			Bipolar on anvil			Test			Indet					
		3S	3I	4	3S	3I	4	3S	3I	4	3S	3I	4	3S	3I	4	3S	3I	4
Cretaceous chert	Flake																**1**	**-**	**1**
	Fragment													1			**1**	**-**	**-**
	Nodule													1			**3**	**2**	**-**
Neogene chert	Flake								1				1	2	1		**3**	**5**	**4**
	Fragment																**1**	**1**	**-**
	Nodule											1					**1**	**4**	**1**
Quartzarenite	Cobble																**-**	**-**	**1**
Quartzite	Flake														1		**-**	**3**	**-**
	Cobble																**-**	**5**	**1**
Quartz	Flake																**-**	**1**	**-**
	Fragment															1	**-**	**1**	**1**
	Cobble		1														**-**	**1**	**-**
Sandstone	Cobble						1										**-**	**-**	**3**
Total			**1**				**1**		**1**			**1**	**1**	**4**	**2**	**1**	**10**	**22**	**12**

3S TD10.3-Sup, *3I* TD10.3-Inf, *4* TD10.4

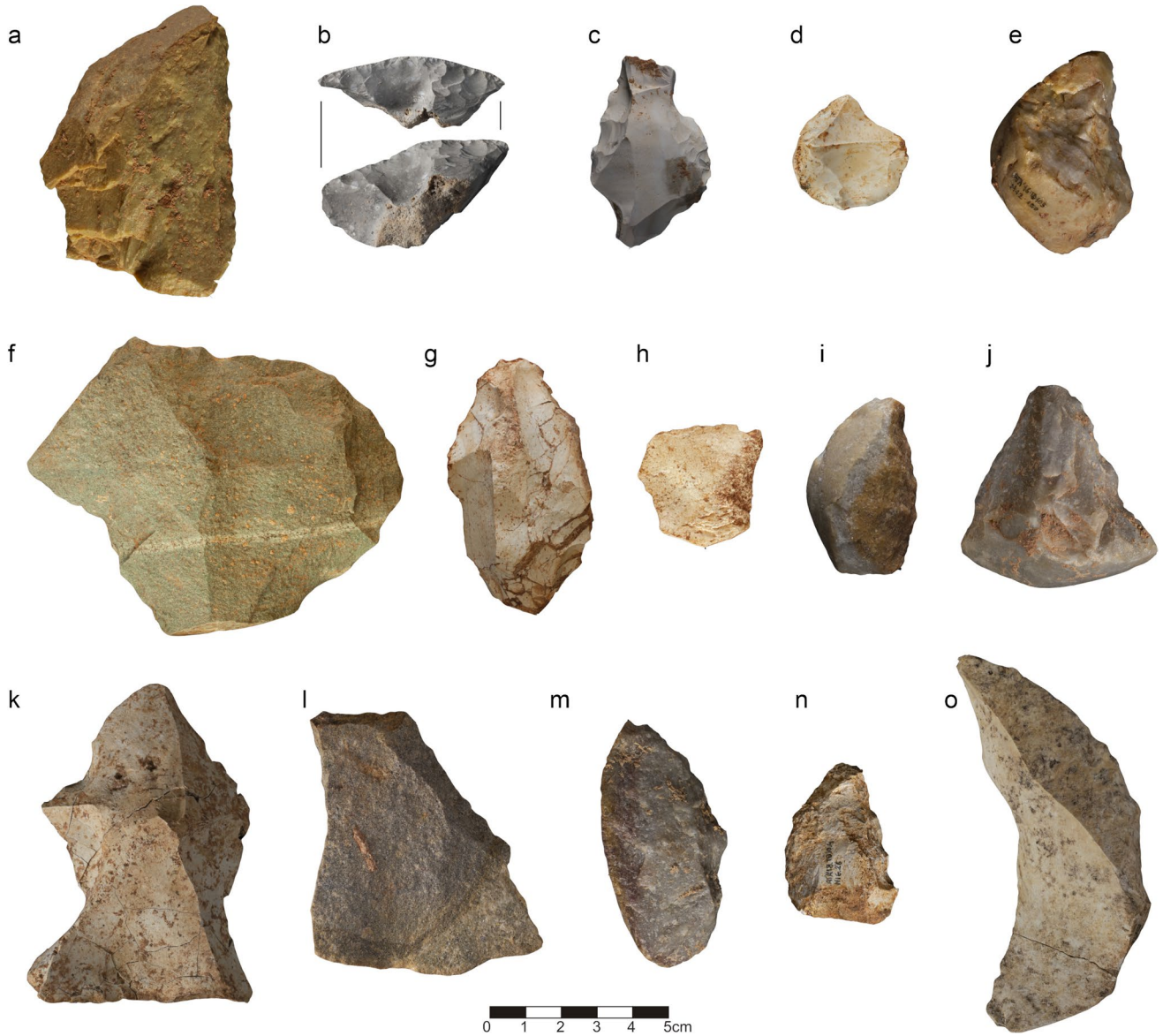

Fig. 10 Flakes and small tools from TD10.3-Sup: **a** quartzite sidescraper ATA13-TD10.2.2-I20-114, **b** Cretaceous chert transverse carinated scraper ATA15-TD10.3-L20-29, **c** Cretaceous chert multiple tool (denticulate + notch + endscraper) ATA14-TD10.3-K15-70, **d** Cretaceous chert flake ATA16-TD10.3-I12-20; TD10.3-Inf: **e** quartz denticulate ATA16-TD10.3-H12-150, **f** sandstone denticulated scraper ATA16-TD10.3-L17-71, **g** Neogene chert denticulate + sidescraper ATA16-TD10.3-H13-77, **h** Neogene chert flake ATA16-TD10.3-N17-30, **i**) quartzite sidescraper ATA17-TD10.3-L19-169, **j** quartzite denticulated point ATA17-TD10.3-J19-23; and TD10.4: **k** Neogene chert flake ATA18-TD10.4-I12-20, **l** quartzite flake ATA18-TD10.4-J13-1, **m** quartzite sidescraper ATA18-TD10.4-L20-46, **n** Neogene chert denticulate ATA18-TD10.4-N16-26, **o** Neogene chert flake ATA18-TD10.4-M18-9

Within the flakes and small tools ($n = 1025$), 4.4% of them ($n = 45$) exhibit a lip, frequently indicative of soft hammering during flaking (Inizan et al., 1999). Overhang regularization was performed in 66 pieces (6.4%) in all raw materials. Most of the flakes and the small tool-blanks had feathered ends (c. 75%), followed by hinged ends (13%), in all three deposits. Finally, the most common knapping accidents and mistakes consist of transversal and distal fractures (17%) and stepped ends (11%). Siret fractures account for 4% of the total of knapping accidents and mistakes.

Diachronically, from the bottom to the top of the sequence, increases were observed in (1) noncortical dorsal surfaces; (2) centripetal dorsal removals; (3) bifaceted butts; and (4) stepped ends, while, interestingly, overhang preparation decreased along the stratigraphy.

Table 10 Small tools categories for each deposit

Types (%)	TD10.3-Sup	TD10.3-Inf	TD10.4	Total
Abrupt	-	1	-	1
Denticulate + notch + endscraper	1	-	-	1
Denticulate	10 (25.6%)	21 (42%)	11 (50%)	42
Other	-	3	1	4
Borer + sidescraper	-	1	-	1
Points	1	-	1	2
Sidescraper + trihedral	1	-	-	1
Sidescraper + denticulate	2	1	-	2
Side/transverse scraper	20 (51.3%)	20 (40%)	8 (36.4%)	49
Endscraper	2	1	1	4
Indeterminable	2	2	2	6
Total	39	50	22	111

Functional Studies on the Knapped Material

Although functional studies on TD10.3 are still in their initial stages, some preliminary results can be presented. To date, only 19 pieces among those initially screened have been analyzed: five from TD10.3-Sup and 14 from TD10.3-Inf. They are of quartzite ($n=11$), quartz ($n=1$), Cretaceous chert ($n=4$), and Neogene chert ($n=3$). The sample includes three sets of quartzite connections, as well as flakes, small tools, and some large tools (Table 12), thus covering the main tool groups present in the assemblage, although with limited representativity. A detailed use-wear analysis of the TD10.4 materials has not been conducted to date.

Surface preservation of quartz and quartzite pieces was notably good, with minimal postdepositional surface modifications (PDSM) observed. Occasional chaotic striations, slight crystal erosion, and rare edge damage were identified, as outlined elsewhere (Pedergnana & Ollé, 2020). But the chert elements presented characteristic chemical weathering that especially affected the Neogene variety (Font et al., 2010). This weathering greatly constrains the feasibility of a detailed microscopic analysis. However, neither the screened material nor the ones that underwent a thorough microscopic investigation exhibited any aggressive postdepositional surface modifications.

In the analyzed sample, there is a high proportion of pieces with use-wear traces. However, we must consider that a certain overrepresentation of them can be due to selection criteria quite steered towards potentially used/usable tools. There were 12 tools with use-wear identified with different degrees of precision, 4 pieces with fresh surfaces, of which 3 were resharpened elements and 1 is a core, and finally 3 cases (1 quartzite, 1 Cretaceous chert, and 1 Neogene chert) were described as indeterminate mainly because of the weathering or slight PDSM. This weathering includes patina and desilicification for chert, as well as some chaotic striations and a slight crystal edge rounding for quartzite.

Table 11 Simple flakes and their fragments at the three deposits

Flakes	TD10.3-Sup	TD10.3-Inf	TD10.4	Total
Complete flake	247	178	91	516
≥ 20 mm	*105 (42.5%)*	*112 (62.9%)*	*42(46.1%)*	*259 (50%)*
Broken flake	51	54	16	121
Flake fragment	124	104	47	275
Total	422	336	154	912

Different knapping activities were identified among the three groups of quartzite elements that were parts of refits and conjoins. In the first case (CT-07-TD10.3-Inf), we identified a triangular blank with alternate and bifacial retouch along the lateral edges, which converge in a notched point. After its initial use for a boring action on a hard material, this tool was resharpened and used again for the same activity. Both the resharpening small flake and the final tool show clear transversal traces, with intensive micro-scars, abrasion of the border of the crystals, striations, and initial polish formation (Fig. 11(1), SI Fig. S6). The second set (CT-10-TD10.3-Inf) is made up of a fractured sidescraper and its distal fragment. Both elements present very fresh surfaces and edges, with the only noticeable modifications being a few transversal percussion marks close to the fracture. Consequently, this set is interpreted as discarded pieces after a sharpening accident (SI Fig. S7). The third set (CT-02-TD10-3-Inf) involves a long-distance connection (8.4 m), a complex knapping and use sequence on an extraordinarily elongated and thin bifacial point made on a flake that was apparently detached using a soft hammer. First, the point was fractured likely because of thrusting action, as suggested by a marked transverse bending fracture, associated with minor lateral crushing (SI Fig. S8). Then the proximal part was retaken, slightly retouched on the distal portion of its left edge, and intensively used in a grooving-sawing action on a hard material, likely bone (Fig. 11 (2)).

The remaining quartzite pieces with use-wear traces include a large retouched flake (rabot) with macroscopic

Table 12 Summary of the use-wear results. Technical dimensions (L, W, T) in mm

Ref	Sub-unit	Material	Tool type	Connection code	L	W	T	Wear features	Interpretation	Observations
2016-J14-85	TD10-3-Inf	Quartzite	Shaped tool—borer	CT-07-TD10-3-Inf	57	56	30	Isolated transversal striations, edge rounding and micro-scarring	Boring action, hard material	Resharpened piece
2016-K15-130	TD10-3-Inf	Quartzite	Resharpening flake	CT-07-TD10-3-Inf	15	26	8	Intensive crystal abrasion, edge rounding, transversal striations, and initial polish formation	Boring action, hard material	Resharpening flake after edge dulling
2016-H12-133	TD10-3-Inf	Quartzite	*Rabot*/hammerstone		98	79	42	Transversal step terminated macro scars/ battering marks	Possible forcefully chopping action / Percussion activity	Percussion marks on the dorsal face, apparently previous to the shaping of the final end
2016-L13-21	TD10-3-Inf	Quartzite	Shaped tool—transverse scraper		27	51	13	Fine striations parallel to the edge, occasional retouch traces	Butchery	Slight use after (re) sharpening
2017-L19-169	TD10-3-Inf	Quartzite	Shaped tool—sides-craper		49	30	15	Isolated retouch traces	Fresh surface	Probably resharpened edge
2016-J16-342	TD10-3-Inf	Quartzite	Shaped tool—sides-craper distal fragment	CT-10-TD10-3-Inf	22	14	4	Retouch traces	Fresh surface	Fracture during retouch (probably with soft hammer)
2016-K16-180	TD10-3-Inf	Quartzite	Shaped tool—sides-craper	CT-10-TD10-3-Inf	52	48	10		Fresh surface	Fracture during retouch (probably with soft hammer)
2015-N17-138	TD10-3-Inf	Quartzite	Shaped tool—end-scraper		68	61	24	Possible postdepositional surface modifications; retouch traces	Indeterminate	
2017-H12-2	TD10-3-Inf	Quartzite	Shaped tool—distal point fragment	CT-02-TD10-3-Inf	30	38	4	Distal feather terminating transverse bending fracture associated with minor lateral crushing, retouch traces on the left side	Possible thrusting action, fresh laterals	Transversal fracture, likely produced after the thrusting action
2015-N18-134	TD10-3-Inf	Quartzite	Shaped tool—proximal point fragment	CT-02-TD10-3-Inf	70	51	9	Very marked striations (furrows and sleeks), edge rounding, crystal abrasion and polish	Linear action on hard material (bone), probably grooving (sawing?)	Slight retouch after the transversal fracture and use of only a short portion of the right lateral

Table 12 (continued)

Ref	Sub-unit	Material	Tool type	Connection code	L	W	T	Wear features	Interpretation	Observations
2016-N16-64	TD10-3-Inf	Quartzite	Shaped tool—sides-craper		67	55	19	Proximal and distal edges with marked crashing, scarring, and transverse short striations	Fresh lateral retouched edge/crashing pointing to and use as a wedge on a medium to hard material	
2017-I18-3	TD10-3-Inf	Quartz	Core		25	31	18	Knapping traces (percussion platform)	Core (not tool)	
2015-J20-54	TD10-3-Inf	Cretaceous chert	Flake		40	39	8	Continuous micro-scarring, soft animal matter polish, sporadic linear features	Butchery; cutting soft animal matter	
2014-J20-139	TD10-3-Sup	Cretaceous chert	Flake		44	43	8	Macro and micro-scarring on the distal and right lateral edges; locally well-developed polish with incipient linear features	Distal: transversal positive scraping action on a medium-hard material; Right lat.: possible cutting action on a soft material	Possible hafting macro-scars on the right lateral with intense spot of polish
2016-K15-70	TD10-3-Sup	Cretaceous chert	Side and end scraper + denticulate		56	35	14	Dispersed spots of polish along the retouched lateral and proximal convex edges, affected by a strong weathering of the chert	Indeterminate. Possible transversal use—soft material?	
2015-L20-29	TD10-3-Sup	Cretaceous chert	Transverse scraper		24	54	19	Continuous edge rounding and polish all along the retouched edge	Transversal action (negative scraping with high working angle) on a soft animal matter (fresh hide)	Use before and after resharpening
2016-L13-15	TD10-3-Inf	Neogene chert	Handaxe		139	86	50	Macro-scarring on the tip, with large step-terminated scars. Highly weathered chert	Use of the tip in a forcefully action by striking	
2016-L17-106/K16-267	TD10-3-Inf	Neogene chert	Broken small bifacial point	SN-04-TD10-3-Inf	80	57	17	Distal hinge terminating bending fracture. Highly weathered chert	Possible thrusting action	Proximal thinning for possible handle arrangement
2013-J15-4	TD10-3-Sup	Neogene chert	Large scraper		73	99	23	Highly weathered chert	Indeterminate	

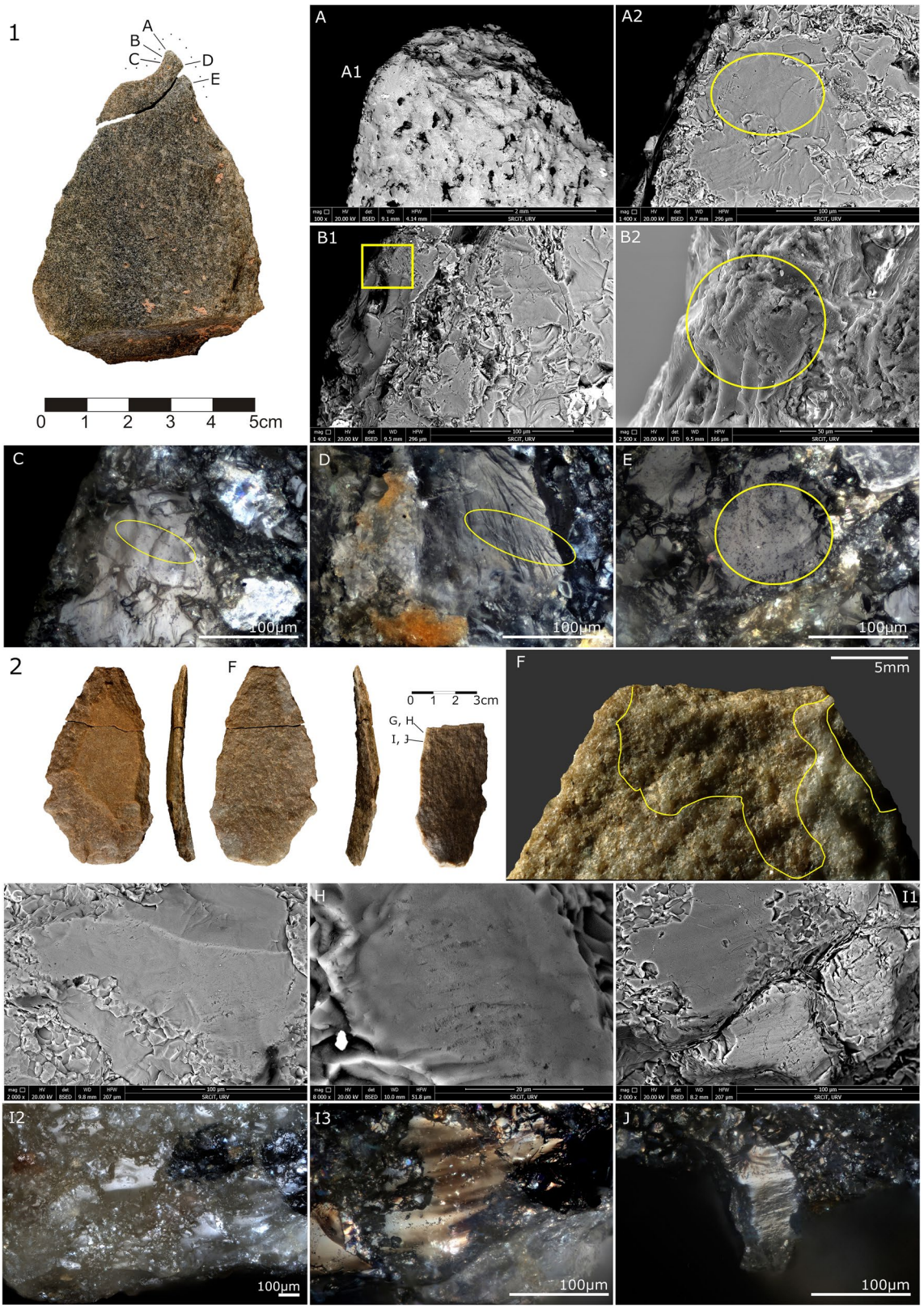

step-terminated scars on the distal edge likely produced by a chopping action, also bearing clear battering marks on its cortical dorsal face attesting to previous percussion activity as a hammerstone (SI Fig. S9); a convex transverse scraper used on soft animal matter in a cutting action related to butchery activities (SI Fig. S10); and finally, a well-shaped

◂**Fig. 11** Refitted quartzite tools with use-wear. (1) Refit CT-07-TD10.3-Inf; A to D, use-wear traces on the resharpening flake, with intensive crystal abrasion, edge rounding, transversal striations and initial polish formation; and E. similar pattern on the tip of the borer, produced by a rotatory action on a hard matter. (2) Refit CT-02. TD10-3-Inf; F: distal feather terminated bending transverse fracture on the ventral face, associated with minor lateral crushing, likely produced by a thrusting action; G, H, parallel striations (furrows) on the crystal surfaces, with some edge abrasion and initial polish formation; I and J: strong striations, edge rounding, and polish at the rim of the slightly retouched edge producing by a grooving/sawing action on a hard material. A, B, G, H, I1 (low vacuum SEM), C, D, E, I2, I3, J (OM), F (3D DM)

side scraper with fresh lateral edges but abundant impact traces—crushing, scarring, and striations—on the proximal and distal sides that point to its use as a wedge on a medium to hard material.

The Cretaceous chert group includes a small flake with clear butchery traces on its lateral edge, which shows continuous micro-scarring as well as polish development on the rim of the edge and ridges of the micro-scars, together with some parallel striations (Fig. 12(1)). A similar action was identified in the second analyzed flake made of this material. This piece, however, shows more intensive use on its distal portion, with micro-scarring, transverse polish and striations likely produced by a positive scraping action on a medium-hard material. A compound piece (denticulate + end scraper) shows dispersed spots of polish along the retouched lateral and proximal convex edges that could indicate a transversal action on a soft material, although the weathering of the raw material prevents a precise assessment. Lastly, a transverse scraper bears marked macro and micro-scarring all along the edge, interrupted by resharpening processes, and accompanied by developed edge rounding and some polish, pointing to a high-angle scraping action on the hide (Fig. 12(2)).

Despite the bad preservation of the Neogene chert artifacts, we identified low-magnification use-wear on two of the three selected pieces. The first was a handaxe, which shows macro-scarring on both sides of its tip with step-terminated removals produced by a forceful impact on an undefined hard material (Fig. 13(1)). The second was the distal part of a small handaxe, which should actually be considered a bifacial point. Its tip exhibits a large hinge terminated bending fracture. A thinning feature, possibly associated with handle insertion, becomes evident when the distal and proximal parts are refitted. These combined features lead us to interpret the artifact as a thrusting spear point, as illustrated in Fig. 13(2). Furthermore, its metrics would fit within those published for some spear points (e.g., Rots et al., 2011). In both cases, the fracture patterning is consistent with the proposed forceful activities, although the limited preservation of the material prevented further findings through microscopic analysis.

Lithic Connections

Together, the TD10.3 and TD10.4 deposits contain a total of 57 connection groups made up of 143 pieces.

The TD10.3-Sup Connections

The TD10.3-Sup connections consist of 44 pieces belonging to 17 connection groups (Table 13, Fig. 14).

These 44 pieces represent 7.8% of the TD10.3-Sup assemblage analyzed for connections ($n = 560$). At least 66% of these connections are of anthropic origin, and 32% of which belong to knapping sequences. At least 29 pieces are parts of technical conjoins and refits, which include two hammerstone and fragment groups, four broken flake and flake fragment groups, and four knapping sequence groups (SI Table S10).

The following groups are of particular interest:

- SN-06-TD10.3-Sup (Fig. 14a, Fig. 15): knapping sequence made up of seven flakes (without the core). From the former flake (location 0), extracted flakes were found (in order) at 71 cm, 66 cm, 181 cm, 18 cm, and 16 cm. The last flake was broken into two pieces.
- SN-07-TD10.3-Sup (Fig. 14b): made up of a fractured sidescraper on Neogene chert and the fragment. The group was considered a postdepositional fracture. However, the two pieces were separated by a distance of 2.21 m, too great a distance to have occurred naturally after deposition, so it is conceivable that one of the fragments was moved and used in a location away from the other after a previous postdepositional fracture.

The TD10.3-Inf Connections

The TD10.3-Inf connections are made up of 79 pieces belonging to 33 connection groups (Table 14, Fig. 16).

These 79 pieces represent 15% of the whole assemblage of TD10.3-Inf analyzed for connections ($n = 522$). At least 67% of the connections are of anthropic origin, among which 14% come from knapping sequences. At least 53 pieces were part of technical conjoins and refits, including four large tool and flake groups, seven hammerstone and fragment groups, five broken flake and flake fragment groups, one sidescraper group and a knapping accident, and four knapping sequences (SI Table S11).

The following groups are of particular interest:

- CT-02-TD10.3-Inf (Fig. 16a, Fig. 17): transversal fracture of a large quartzite flake, whose distal fragment is a well-made point. The entire size of the piece is $96 \times 52 \times 8$ mm. When complete, the piece was finely shaped with soft-hammer percussion. The two fragments

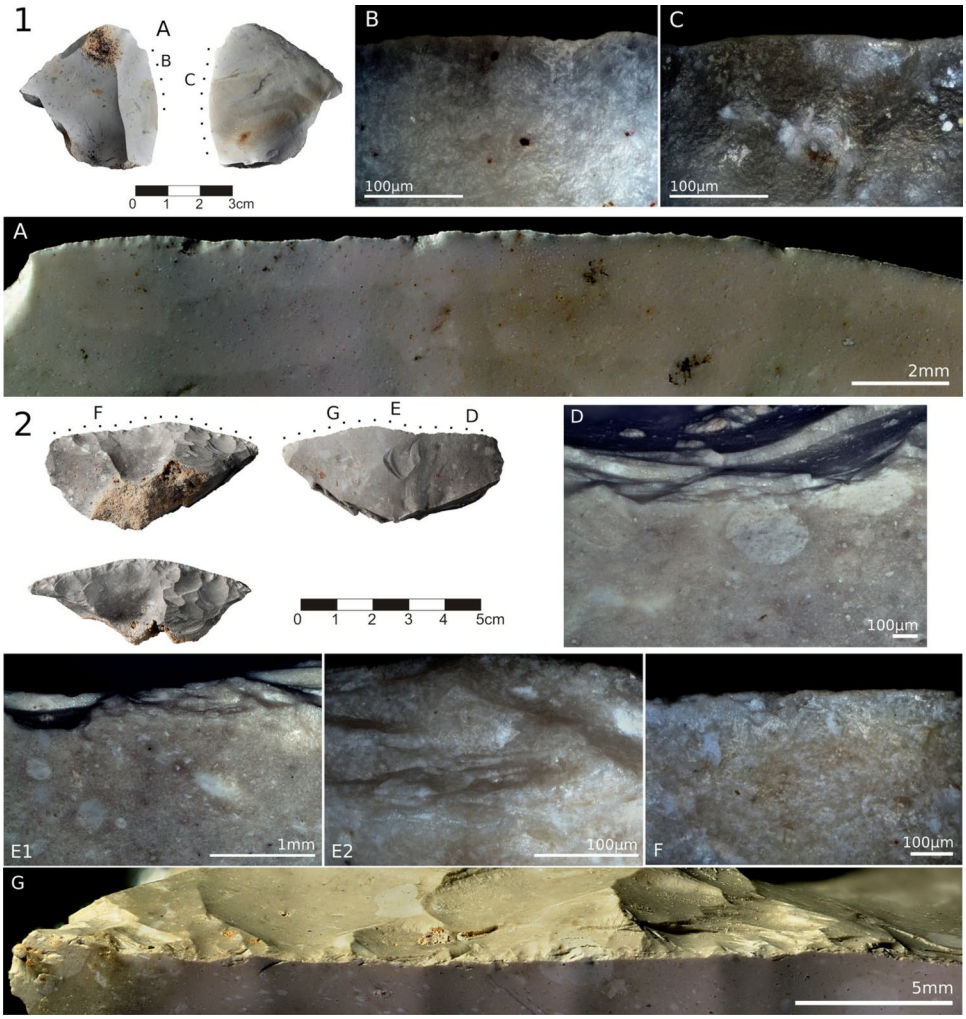

Fig. 12 (1) ATA15-TD10.3-Inf-J20, 54. Cretaceous chert flake with continuous micro-scarring on its right lateral (A), with a soft animal matter polish (B and C) and sporadic linear features produced by a butchery activity. (2) ATA15-TD10.3-Sup-L20, 29. Cretaceous chert transverse scraper with resharpening evidence and continuous edge rounding (G) and polish all along the retouched edge (E1-E2 and F), resulting from a high-angle scraping on hide. A, G (3D DM), B to F (OM)

were found at a distance of about 8 m from one another, which likely means that, once broken, the larger piece was moved, used (see Fig. 11(2)) and discarded on the other side of the occupation.

- CT-07-TD10.3-Inf: a quartzite borer and a flake from resharpening it. They were recovered at a distance of 125 cm from one another. Both the borer and the resharpening flake show traces of boring (Fig. 16b; see Fig. 11 (1)).
- CT-17-TD10.3-Inf (Fig. 16c, Fig. 18): three quartzite pieces, likely produced at recycling a handaxe into a core. The set is formed by a handaxe-core, one fragment, and the pointed tip of the handaxe. First, the tip of the handaxe is removed by knapping. Then, the handaxe-core is moved about 3 m to the northwest, where another flake is extracted. The core was again moved 2.9 m to the southwest, where it was discarded.
- SN-05-TD10.3-Inf (Fig. 16d): knapping sequence consisting of two flakes, one small tool and one core on Neogene chert. The first flake was detached from the core at location 0. The core was moved 478 cm to the northeast, where the second and third flakes were consecutively detached. They were recovered at a distance of 60 cm from one another. Again, the core was moved 311 cm to the northeast and abandoned.

The TD10.4 Connections

The TD10.4 connections are made up of seven groups of 20 pieces, mainly of chert (Table 15, Fig. 19).

These 20 pieces represent 9.4% of the whole TD10.4 assemblage analyzed for connections ($n = 213$). Connections of anthropic origin account for 80% of these, of which 62.5% belong to knapping sequences. There are 16 pieces belonging to technical conjoins and refits, which include one large tool and flake group, three hammerstone and fragment

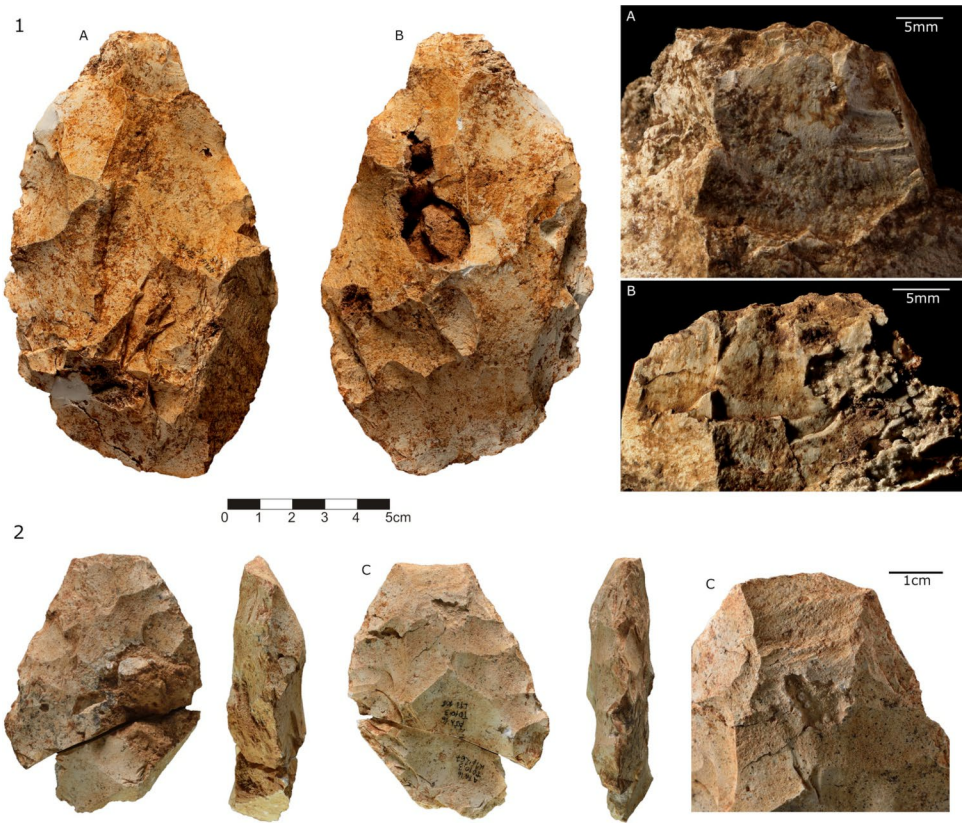

Fig. 13 (1) ATA16-TD10.3-Inf-L13, 15. Macroscopic scarring on the tip of the handaxe, likely produced by its use in a forcefully impact action. Note (B) the highly weathered surface of the chert. (2) Refit SN-04-TD10.3-Inf. Fractured small Neogene chert bifacial point with a large hinge terminated bending fracture on the ventral face (C), likely produced by a thrusting action; after refitting, a proximal thinning for handle arrangement is noted

Table 13 Groups of conjoins and refits for each raw material at TD10.3-Sup

TD10.3-Sup ($n=560$ of 666)			Conjoins			Refits	Total anthropic
Raw material	Groups	Num. pieces	Postdepositional	Technical	Indet		
Sandstone	1	2	2	-	-	-	-
Limestone	1	2	2	-	-	-	-
Quartzite	5	10	2	8	-	-	8
Cretaceous chert	4	13	1	1	2	9	10
Neogene chert	6	17	2	6	4	5	11
Total	17	44	9 (20%)	15 (34%)	6 (13.6%)	14 (32%)	29 (66%)

Indet. = some pieces were not categorically ascribed to postdepositional or to technical fractures

groups, one fractured small tool and fragment group, and one group associated with reshaping a handaxe into a core (SI Table S12).

Group CRT-30-TD10.4 (Fig. 19a) is of particular interest. It is made up of a fractured quartzarenite hammerstone and a fragment. Judging by the hammerstone percussion marks, it broke due to use. The fragment was recovered at a distance of 3.36 m from the main piece. Therefore, the hammerstone was likely used and broke in the northern area of the occupation (where the fragment was found) and was thrown or moved 3.36 m southward.

Zooarchaeology and Taphonomy of TD10.3 and TD10.4

Taxonomic Distribution and Human Impact (Fig. 20)

In TD10.3-Sup, 15 taxonomic groups were identified. The Simpson index of dominance ($D=0.71$) and the Shannon index of uniformity ($H'=0.33$) indicate that, although the assemblage is heterogeneous, some species stand out above the others. Ungulates, and equids among them, play a dominant role, together making up about 40% of the NISP

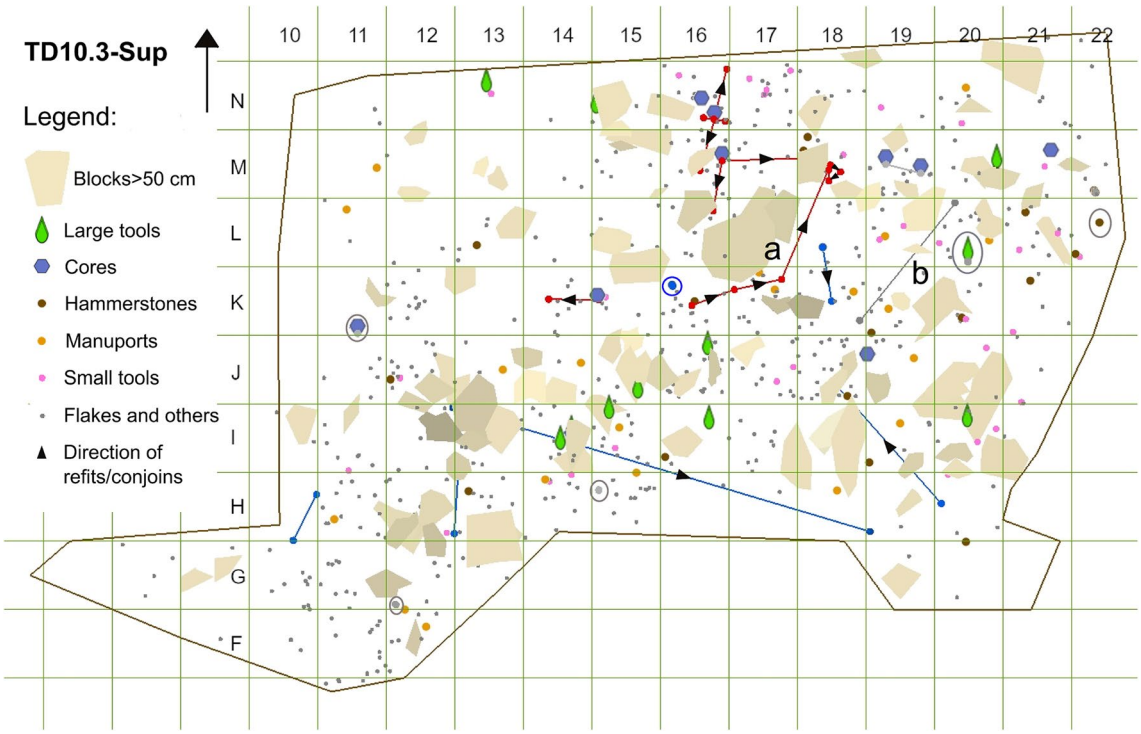

Fig. 14 TD10.3-Sup lithic remains, refits, conjoins, and blocks bigger than 50 cm. Red lines/circles: refits; blue lines/circles: technical conjoins; grey lines/circles: postdepositional conjoins. Each square = 1 m.^{2}

(number of identified specimens). They are followed by cervids and bison (Table 16). Carnivores are not abundant (NISP = 152; 8.4%), but they are highly diverse and include canids and *Panthera leo fossilis*.

Isolated teeth dominate the assemblage, although remains of whole skeletons of the three main taxa based on their NISP were also recovered (Table 17). Anthropogenic modifications are scarce and they are all in the form of cut-marks (3.6%, $n = 344$) and percussions (0.03%, $n = 3$). Cut-marks were identified on the trunk bones (ribs and vertebrae) and on the diaphyses of the limb long bones. Large animals were the most affected (NISP = 9), although cut-marks were also present on the remains of medium-sized animals (NISP = 3). Carnivore tooth marks were observed on the 12% of the assemblage ($n = 1144$) (SI Table 13).

The TD10.3-Inf assemblage is very similar to TD10.3-Sup in taxonomic representation. However, TD10.3-Inf presents greater diversity ($D = 0.70$, $H' = 0.24$), as it contains up to 18 taxonomic groups. Despite this diversity, *Equus ferus* (NISP = 1134; 35%), *Bison* sp. (NISP = 933, 28.8%), and cervids (NISP = 640; 19.8%) dominate. Several rhinoceros teeth complete the assemblage, as do a hippopotamus tooth and four cf. *Hemitragus bonalis* specimens. Among the carnivores, the coexistence of two large felids in the same deposit stands out: *Panthera leo fossilis* and *Homotherium latidens* (García, 2003).

Remains of the complete skeleton were identified among the most abundant species. The number of isolated teeth is notable, as is the quantity of distal limb bones. Just like in TD10.3-Sup, cut-marks are scarce (0.4%, $n = 52$), as are percussion marks (0.3%, $n = 9$). When they were documented, they were on the ribs and long bones of equids (NISP = 2), bovids (NISP = 4), cervids (NISP = 1), and unidentifiable remains of large (NISP = 24), medium-sized (NISP = 13), and small (NISP = 4) animals, as well as on indeterminate remains (NISP = 4).

In contrast, carnivore modifications were more abundant, accounting for 10% (NISP = 1283) of the TD10.3-Inf assemblage. Equids (NISP = 75, 6.6%), bovids (NISP = 45, 4.8%), and cervids (NISP = 7.3%) were the most affected taxa. They are followed by unidentifiable large (NISP = 353, 15.6%), medium-sized (NISP = 323, 16.1%), and small (108; 13.5%) animals. Although not as abundant, other taxa also show evidence of chewing marks on the bone surfaces: cf. *Hemitragus bonalis* (NISP = 1, 25%); *Canis/Cuon* (NISP = 4, 5.9%); *Vulpes vulpes* (NISP = 1; 2.7%); *Panthera leo fossilis* (NISP = 4, 9.3%); *Oryctolagus* sp. (NISP = 4; 8); Aves (NISP = 5; 3.8%), and unidentifiable very small animals (NISP = 2, 2.8%). Another 306 (6.7%) remains could not be taxonomically identified.

The TD10.4 assemblage is made up of 716 faunal remains. Taxonomic diversity is high, with up to 12 taxonomic groups

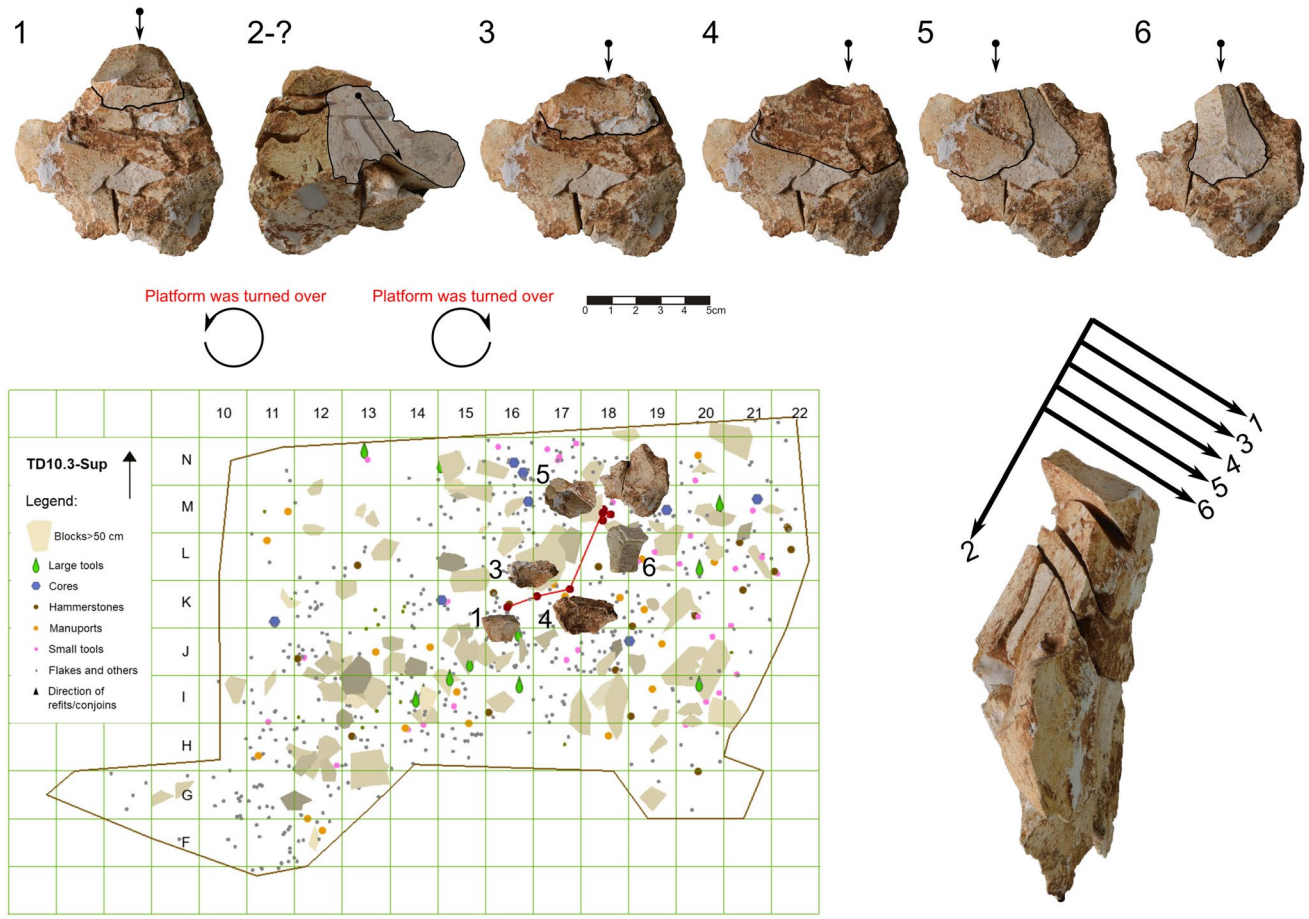

Fig. 15 Spatial distribution of refit code SN06-TD10.3-Sup of Neogene chert, formed by seven flakes from a knapping sequence

identified. However, this diversity is slightly lower than in the previous deposits. Some species dominate over the others, such as cervids and bison (Table 16), and the assemblage is moderately uniform in the distribution of remains by taxonomic groups ($D = 0.70$, $H' = 0.24$). Among the carnivores, again two large felids stand out: *Panthera leo fossilis* and *Homotherium latidens*, suggesting a certain continuity in landscape mosaics between the two subunits (TD10.4 and TD10.3). Isolated teeth were the most common identified remains, although the presence of limb and trunk elements was not negligible (Table 17).

No elements with anthropogenic modifications were identified in this subunit, although carnivore modifications were observed on 8% of the assemblage. The affected taxa comprised cervids (NISP = 7), bison (NISP = 6), and equids (NISP = 1). An additional 27 unidentifiable elements of small, medium, and large-sized animals also presented these modifications.

Subunit TD10.4 is characterized by the influence of the weathering observed in its sediments and those of underlying unit TD9. Therefore, no bones have been preserved in TD9, and its influence on the overlying TD10.4 has resulted in poorly bone surfaces preserved, with an influence of chemical corrosion. In addition, a continuous layer of roots grew on a package of sediments in the eastern half of the site, which prevented that sediment from preserving any faunal remains. Therefore, the absence of anthropogenic modifications in TD10.4 may be related to the poorer preservation of bone surfaces in this subunit, although carnivore modifications, usually deeper and more intense, were identified here.

Spatial Statistics

For TD10.3-Sup, Besag's inhomogeneous L-function indicated a regular distribution of faunal remains at distances of less than 50 cm and the distribution of clusters at longer distances (SI Fig. S11). Slight clustering of the lithic remains was identified at distances of less than 20 cm, regular distribution from 20 to 75 cm, and random distribution from 75 cm onwards, because the data line matches that of the Poisson distribution. However, the inhomogeneous multitype L-function showed a clustering trend of fauna and

Table 14 Groups of conjoins and refits for each raw material at TD10.3-Inf

TD10.3-Inf ($n=522$ of 570)			Conjoin			Refits	Total anthropic
Raw material	Groups	Num. pieces	Postdepositional	Technical	Indet		
Sandstone	1	2	-	-	2	-	-
Limestone	4	9	-	7	-	2	9
Quartzarenite	1	2	-	2	-	-	2
Quartzite	24	58	19	34	-	5	39
Neogene chert	3	8	2	-	2	4	4
Total	33	79	21 (26.5%)	43 (54.4%)	4 (5%)	11 (14%)	54 (68.3%)

Indet. = some pieces were not possible to ascribe for sure to postdepositional or to technical fractures

lithics beyond a distance of 70 cm. This suggests a co-dependency of stone tools and bones clustering at distances of 70 cm from any aleatory point.

In TD10.3-Inf, the L-Besag test result for inhomogeneous distributions indicated the existence of groups of bones found at a distance of 120 cm and an aleatory distribution for lithic remains (SI Fig. S12). The relation of the inhomogeneous multitype L-function suggests a clustering trend between bones and lithics at distances of around 70 cm.

In TD10.4, the inhomogeneous L-function indicated a regular distribution of faunal remains on the surface of TD10.4. Lithic remains showed regular distribution at distances of up to 100 cm. At greater distances, these objects appeared in clusters (SI Fig. S13). The inhomogeneous multitype L-function relation showed that fauna and lithics were co-dependent in terms of the clustering of stone tools and bones at distances of 175 cm from any aleatory point.

Archaeological Materials and Topography of Gran Dolina

The area excavated at the Gran Dolina site corresponds to the entrance ramp of the cave and part of the outer flat area. More than half of its surface is markedly inclined toward the conventional NE, and then stabilizes horizontally in the eastern area of the surface (see Fig. 1).

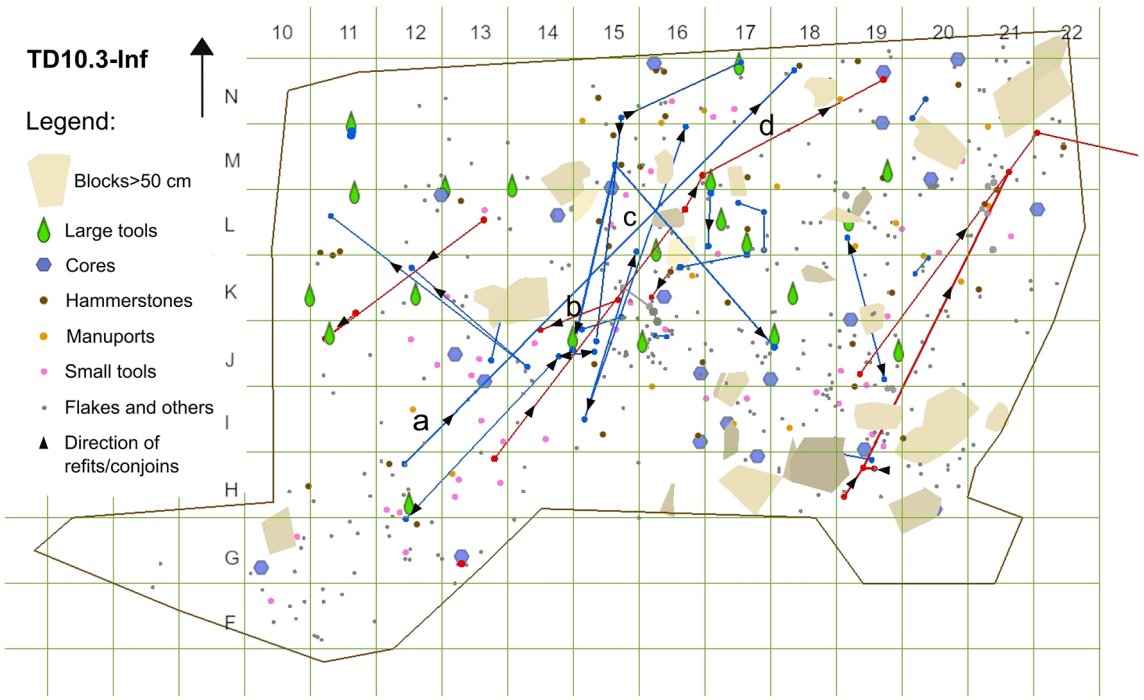

Fig. 16 TD10.3-Inf lithic remains, refits, conjoins, and blocks bigger than 50 cm. Red lines/circles: refits; blue lines/circles: technical conjoins; grey lines/circles: postdepositional conjoins. Each square = 1 m.^{2}

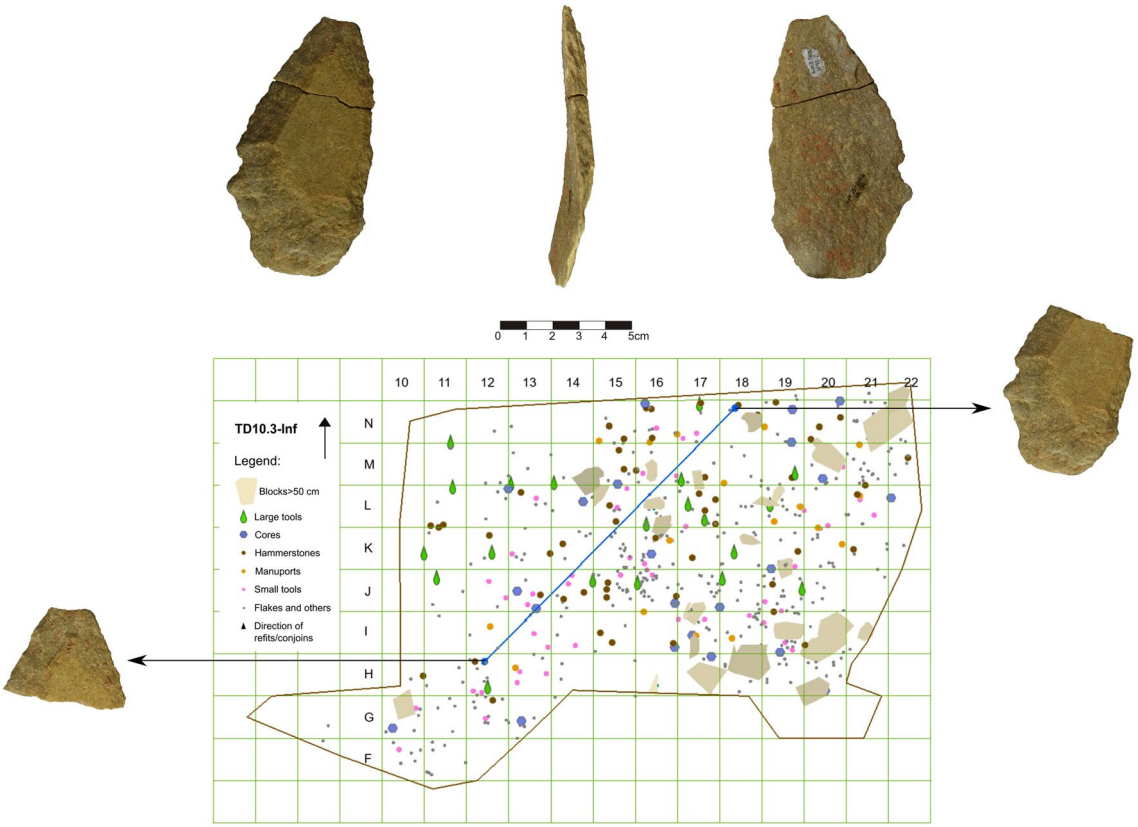

Fig. 17 Spatial distribution of technical conjoin code CT-02-TD10.3-Inf on quartzite

The possible role of the topography of Gran Dolina in the archaeopaleontological scattering as well as the influence of the high number of blocks that pave the paleo-surfaces of TD10.3 were spatially visualized for each deposit. We grouped the archaeopaleontological material by mass (lithics) and dimension (faunal remains) ranges (Figs. 21, 22, and 23).

TD10.3-Sup (Fig. 21)

This deposit contains 103 natural blocks measuring 50 cm or larger, although they do not seem to have affected the distribution of the archaeological remains: the lithics were homogeneously distributed across the surface of the excavation, independently of their mass. There was not a gradient toward the slope. However, heavier pieces were more abundant in the eastern, flatter half of the excavation, simply because higher concentrations of lithics were documented in this area in general. In addition, higher densities of lithic remains were found in the NW area, which is flat, but their density by mass does not show any particular distribution conditioned by the slope. We did not find a gradient of faunal remains by size in favor of the slope, as the higher densities were documented in the south of the major diagonal (NE-SW), with a particular cluster of sizes < 20 mm and > 100 mm at the entrance (SW) of the cave.

TD10.3-Inf (Fig. 22)

All sizes of faunal remains were concentrated in the eastern half of the cave, with higher clusters of pieces larger than 50 mm in the last third of the whole area. The case of lithics is similar, although we did not find a gradient by mass in favor of the slope. Higher mass elements were concentrated in the eastern half, but, again, more pieces were documented in that area in general. Here again large natural blocks (≥ 50 cm, $n = 26$) do not seem to have played any special role, as lithics are spread all over the surface, regardless of the presence of large blocks.

TD10.4 (Fig. 23)

Bones and lithics were documented in higher densities in the major diagonal (NE-SW), represented by the large natural blocks (≥ 50 cm, $n = 11$). No gradient was found by sizes or mass, as in the upper deposits. Interestingly, several faunal remains of different sizes were recovered

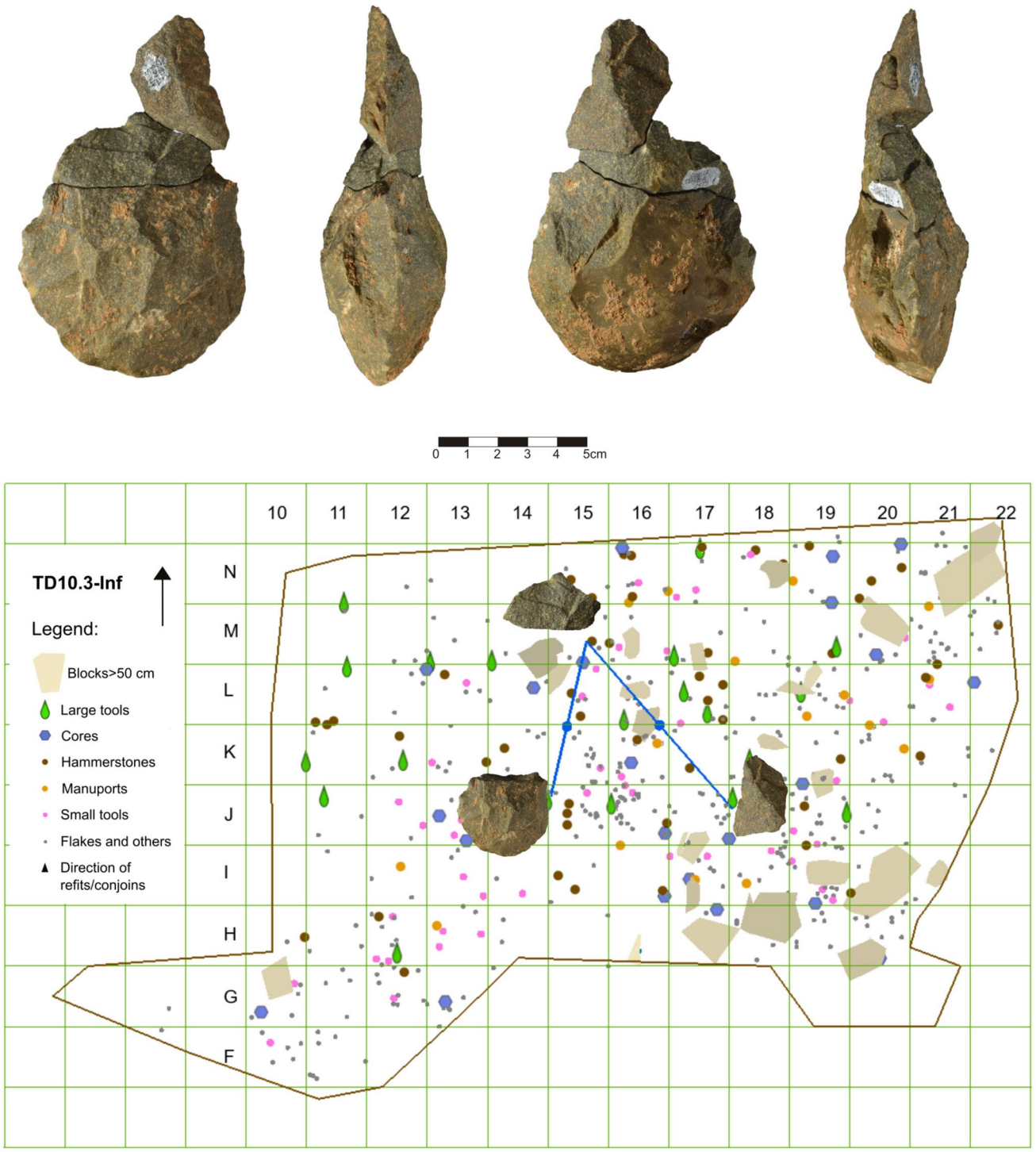

Fig. 18 Spatial distribution of technical conjoin code CT-17-TD10.3-Inf on quartzite

in the northwest "corner" of the cave, where the ceiling is lower and the space narrows. This may mean that the modern mouth to the cave of Gran Dolina was not yet as open as during the second half of the Middle Pleistocene. As such, it may have served as a better shelter for carnivores than in later times, when the enormous block fall during the formation of TD10.3 enlarged the entrance and rendered that corner exposed. No differential concentrations, gradients of lithics mass or bones sizes in favor of the slope were found in this subunit.

To sum up, no gradients of faunal remains by size, nor lithics by mass in favor of the slope of Gran Dolina were

Table 15 Groups of conjoins and refits for each raw material at TD10.4

TD10.4 ($n=213$ of 247)			Conjoin		Refits	Total anthropic
Raw material	Groups	Num. pieces	Postdepositional	Technical		
Sandstone	1	4	4	-	-	-
Quartzarenite	1	2	-	2	-	2
Quartzite	2	4	-	4	-	4
Neogene chert	3	10	-	2	8	10
Total	7	20	4 (20%)	8 (40%)	8 (40%)	16 (80%)

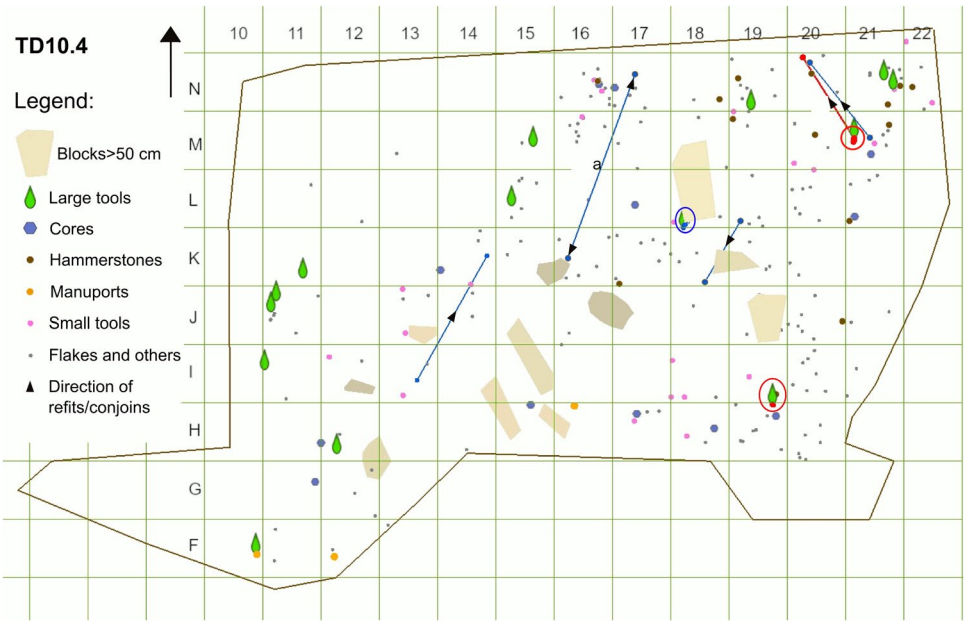

Fig. 19 TD10.4 lithic remains, refits, conjoins and blocks bigger than 50 cm. Red lines/circles: refits; blue lines/circles: technical conjoins; grey lines/circles: postdepositional conjoins. Each square = 1 m.^{2}

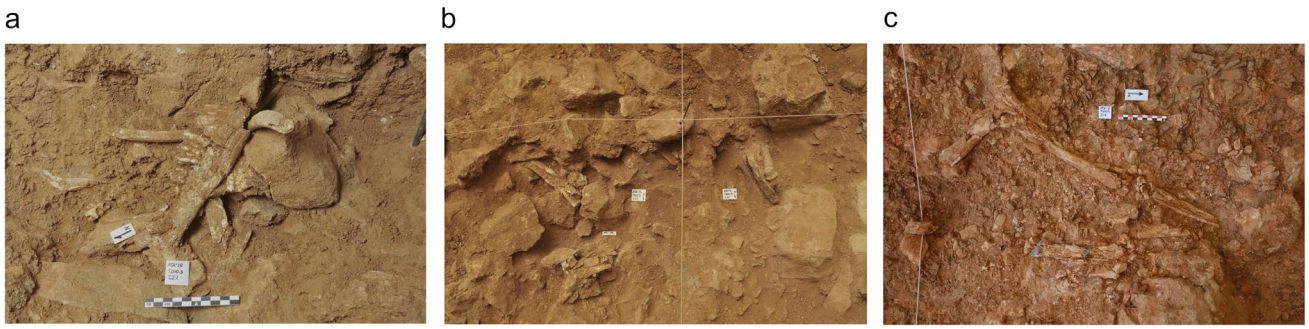

Fig. 20 Bone remains from TD10.3-Sup (**a**), TD10.3-Inf (**b**), and TD10.4 (**c**)

found in any of the three deposits. Although most of the lithic connections were down-slope, some of them were counter-slope. Therefore, the archaeological materials of TD10.3 and TD10.4 seem to have remained mostly in place, preserving most of the spatial relations of when they were abandoned, although slight postdepositional movement of some pieces cannot be ruled out.

Discussion

The Occupational Characteristics of TD10.3 and TD10.4

TD10.3 and TD10.4 are the lowermost subunits of unit TD10, the last archaeological deposit of Gran Dolina, and they are dated at about 400 ka. TD10.4 represents the

Table 16 Taxonomic distribution according to NISP (number of identified specimens) in TD10.3-Sup, TD10.3-Inf and TD10.4

Taxa	TD10.3-Sup		TD10.3-Inf		TD10.4	
	NISP	%NISP	NISP	%NISP	NISP	%NISP
Cervus elaphus/Dama dama	318	17.6	640	19.8	77	29.6
Bison sp.	369	20.4	933	28.8	74	28.5
cf. *Hemitragus bonali*	7	0.4	4	0.1	-	
Artiodactyla	5	0.3	70	2.2	6	2.3
Equus ferus	725	40.1	1134	35.0	42	16.2
Stephanorhinus hemitoechus	8	0.4	10	0.3	8	3.1
Ungulata	2	0.1	9	0.3	8	3.1
Hippopotamus sp.	-	-	1	0.01	-	
Canis/Cuon	54	3.0	68	2.1	9	3.5
Vulpes vulpes	25	1.4	37	1.1	2	0.8
Ursus sp.	4	0.2	1	0.01	4	1.5
Homotherium latidens	-	-	2	0.1	2	0.8
Panthera leo fossilis	34	1.9	43	1.3	7	2.7
Felidae (large) gen. sp. indet	-	-	33	1.0	-	
Lynx pardinus spelaeus	5	0.3	4	0.1	-	
Mustelidae indet	5	0.3	3	0.1	-	
Carnivora indet	25	1.4	56	1.7	3	1.2
Meles meles	-	-	-	-	1	0.4
Mustela cf. *putorius*	-	-	-	-	1	0.4
Marmota cf. *marmota*	18	1.0	1	0.0	-	
Castor fiber	2	0.1	3	0.1	-	
Hystrix sp.	-	-	3	0.1	-	
Rodentia	4	0.2	2	0.1	2	0.8
Oryctolagus sp.	64	3.5	49	1.5	10	3.8
Aves	132	7.3	130	4.0	3	1.2
Testudinae	-	-	-	-	1	0.4
Total	1806	18.9	3236	25.3	260	40.4

reopening of Gran Dolina, after a period during which the cave was semi-closed (TD9). It is an archaeological deposit with a thickness of 15 cm and an assemblage consisting of 749 faunal remains and 247 lithic objects. The cortical surfaces of bones of TD10.4 are highly altered, a feature closely related to the weathering observed in the deposit. This characteristic suggests a long period of subaerial exposure. The degradation of bones and other organic material (roots) contributed to the increase in phosphates. The lithic remains are generally well preserved, even for the Neogene chert, which tends to exhibit higher degrees of alteration in other deposits of Atapuerca.

Subunit TD10.3 overlies TD10.4, and it represents a period of massive reopening of the cave. This period is documented by several blocks which fell from the ceiling and walls, a process that continued to happen throughout the sedimentation of TD10.3 and TD10.2 (Arteaga-Brieba et al., 2023).

Even though archaeostratigraphic analyses suggest that TD10.3 evidences at least four main stages of hominin occupations, they were extremely difficult to individualize over most of the excavation surface. However, they could be grouped into two phases, as there is a certain archaeological gap towards the halfway point in the sequence. This gap coincides with a period in which the blocks fell less frequently, which allowed us to distinguish between an upper and a lower deposit: TD10.3-Sup and TD10.3-Inf, respectively.

Although the faunal remains in TD10.3-Sup and TD10.3-Inf are well preserved, in the former the percentage of anthropogenic modifications is very low. In TD10.3-Inf, some cases of anthropogenic breakage by percussion were identified, and cut-marks were documented on a few remains, among which bovids and cervids stand out.

TD10.4, TD10.3-Inf and TD10.3-Sup are characterized by great taxonomic diversity in which large and medium-sized ungulates dominate. The closest similarities are between TD10.3-Sup and TD10.3-Inf, in which equids are dominant in both, in contrast to the underlying

Table 17 Anatomical distribution according to NISP (Number of identified specimens) of the main taxa of TD10.3-Sup, TD10.3-Inf, and TD10.4

	TD10.4						TD10.3-Inf						TD10.3-Sup					
	Bison sp.	*Cervus elaphus/Dama dama*	*Equus ferus*	Felidae (large)	*Stephanorhinus hemitoechus*	*Ursus* sp.	*Bison* sp.	*Cervus elaphus/Dama dama*	*Equus ferus*	Felidae (large)	*Stephanorhinus hemitoechus*	*Ursus* sp.	*Bison* sp.	*Cervus elaphus/Dama dama*	*Equus ferus*	Felidae (large	*Stephanorhinus hemitoechus*	*Ursus* sp.
Antler/Horn		9					2	16					1	17				
Skull	2		1				15	1	13	1		1	9	5	5			
Mandible	4	3				1	21	18	19	4			20	5	17			
Isolated teeth	47	12	24	2		2	658	397	627	32	3		212	158	306	13	3	3
Vertebra		1	2				3	3	5	1			2	5	7			
Rib	2				1		5		14		1		12		34			
Scapula			1				4	6	3	1			3	2	1			
Humerus		1					11	26	19				13	15	41	1		
Radius	2	5	4				13	9	21	1			9	7	29			
Ulna		3					4	5	2	1			4	6	6			
Radius/Ulna		1						6	5					4	3			
Femur	1	2	1				9	13	10				6	8	13	1		
Patella		1			1		11	14	20				8	6	43			
Tibia		3	1							2						1		
Fibula						1		1						1				
Tarsal	1	2					2	3	21	1			2	2	13	1		
Calcaneum	1				1		9	6	16	1	1		1	3	6	1		
Astragalus	2						15	7	60	2	1		11	5	40	2		
Carpal/Tarsal	1	13	3	1	1		50	60	107	8	2		26	35	60	1	3	
Metapodial	9	17	6	1	2		14	5	60	1	1		11	5	42	1		
Phalange	7	3	1	5	2	1	85	44	112	21	1		19	28	57	12	2	1

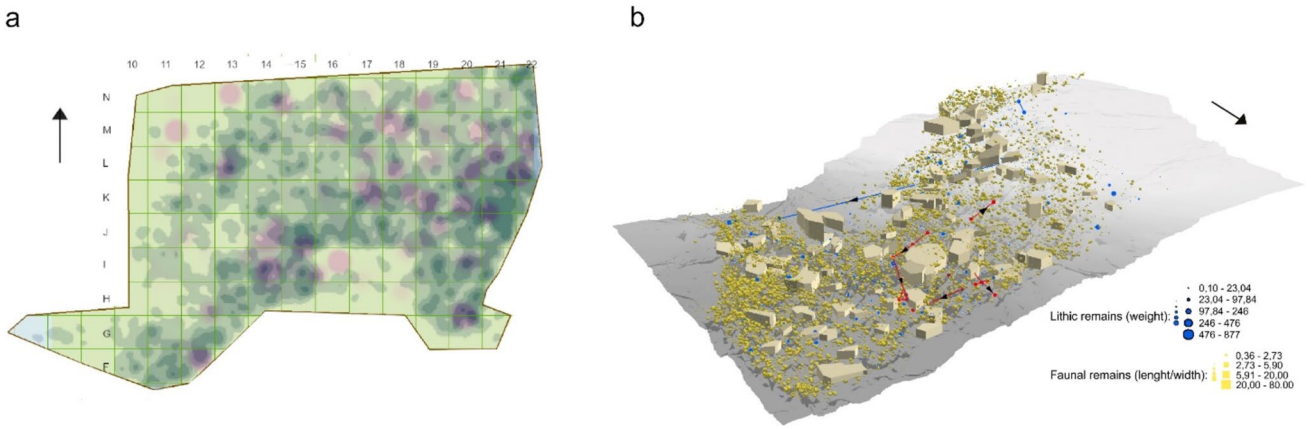

Fig. 21 **a** TD10.3-Sup. kernel densities of all lithic pieces by mass (pink) and faunal remains by size (dark green). Purple: coincidence of high mass of lithics and big sizes of faunal remains. **b** TD10.3-Sup topographic reconstruction from the conventional NE, showing blocks bigger than 50 cm, lithics by mass (blue), faunal remains by length/width (yellow). Refits (red lines) and anthropic conjoins (blue lines)

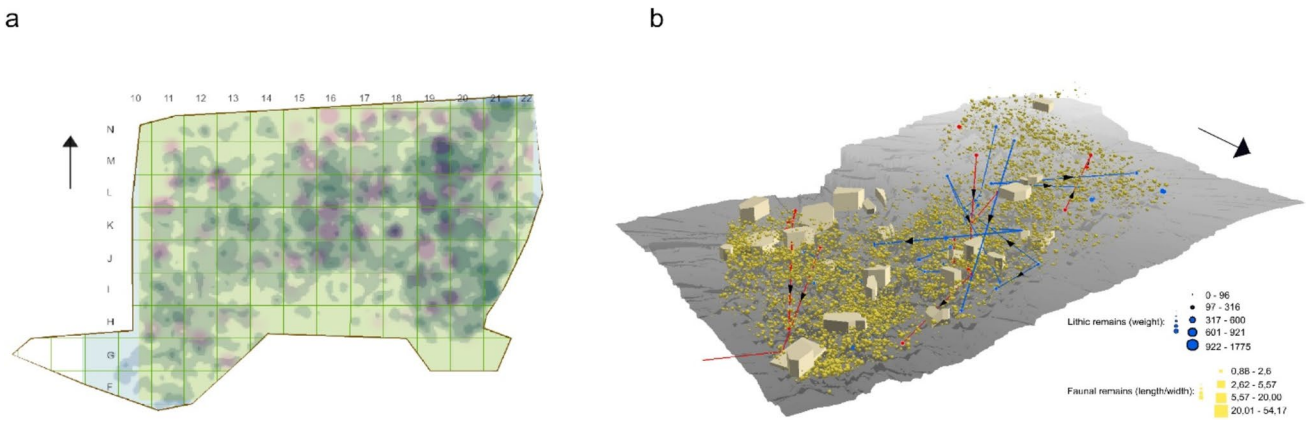

Fig. 22 **a** TD10.3-Inf. kernel densities of all lithic pieces by mass (pink) and faunal remains by size (dark green). Purple: coincidence of high mass of lithics and big sizes of faunal remains. **b** TD10.3-Inf topographic reconstruction from the conventional NE, showing blocks bigger than 50 cm, lithics by mass (blue), faunal remains by length/width (yellow). Refits (red lines) and anthropic conjoins (blue lines)

TD10.4. However, TD10.3-Inf is characterized by the last appearance of *Homotherium latidens* in Gran Dolina, also present in TD10.4. In both cases, *H. latidens* coexisted with another large felid, *Panthera leo fossilis*. Both taxa focused on the same size of prey, usually large ungulates. The presence of both taxa at the same site suggests the existence of a landscape that combines open and woodland environments (Antón et al., 2005). Other taxa like *Castor fiber* in all three deposits and hippos in TD10.3-Inf indicate aquatic areas. This palaeolandscape is in agreement with the combined results of the studies of micromammals, reptiles, birds, and pollen. Micromammals and pollen suggest open and wet habitats. The presence of mesic trees in TD10.3 does not point to an extreme environment. Amphibians and reptiles suggest diverse landscapes, since forest taxa are well represented (Blain et al., 2008, 2011; Cuenca-Bescós, 2011; Rodríguez et al., 2011).

Technologically, both TD10.3 and TD10.4 represent a well-developed Acheulean, with relatively high proportions of large tools (an average of 3.7%, excluding fragments and unidentifiable pieces), most of which were introduced into the cave already made, although a sort of slight reshaping was later performed on some of them. Technically and morphometrically, the handaxes are highly heterogeneous, while those from TD10.4 and TD10.3-Inf present similar intra-site variability, which increases along the stratigraphic sequence: a slight transition was detected from the classical "tear-drop" shapes in TD10.4 and TD10.3-Inf, to wider shapes increasing their variability in TD10.3-Sup.

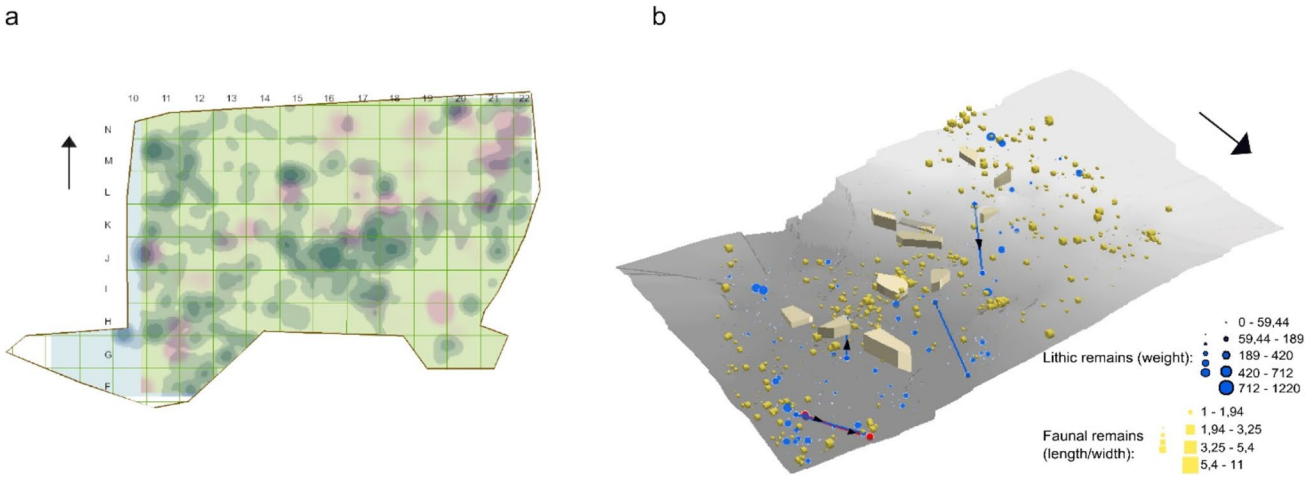

Fig. 23 **a** TD10.4 kernel densities of all lithic pieces by mass (pink) and faunal remains by size (dark green). Purple: coincidence of high mass of lithics and big sizes of faunal remains. **b** TD10.4 topographic reconstruction from the conventional NE, showing blocks bigger than 50 cm, lithics by mass (blue), faunal remains by length/width (yellow). Refits (red lines) and anthropic conjoins (blue lines)

Contrary to the large tools, there were flakes produced, and small tools retouched in situ in all of the main raw materials, except for in TD10.3-Sup, where cores were only recovered in Cretaceous and Neogene chert. The existence of these production and shaping processes is supported by the number of simple flakes in each assemblage, the refits and the evidence of shaping found. Sizes tend to be smaller in both varieties of chert and larger in fluvial materials, although the dimensions are generally homogeneous within each assemblage. In all three deposits, hammerstones and manuports were selected from the same varieties and sizes of cobbles, especially quartzite cobbles.

It should be noted that the percentage of large tools and percussive material (altogether an average of 13.8%, excluding fragments and unidentifiable pieces) is one of the highest in all the Atapuerca sites excavated to date, comparable only to Units GII and GIIIb of Galería (García-Medrano et al., 2014, 2015). As in the case of the large tools, the percussive material in TD10.3-Sup is also clearly different from that in TD10.3-Inf. In TD10.3-Sup, percussive material has a lower percentage (6%), hammerstones exhibit a lower degree of use, and there is a higher percentage of unmodified material (manuports). Therefore, the percussive activities in this deposit seem to have been more sporadic than in TD10.3-Inf, where a higher proportion of hammerstones were recovered with deeper percussive traces. This pattern is also present in TD10.4.

Much of this material with deeper percussive marks might be related to knapping activities. The proportion of cores decreases along the sequence, so the knapping events carried out inside the cave were more numerous in TD10.4 and TD10.3-Inf than in TD10.3-Sup. However, in some cases, the hammerstones were recovered smashed, a condition too intense to have resulted from flake production or tool shaping. Indeed, scarce evidence of the knapping of large tools has been documented. In addition, flake production increases along the sequence, but that does not explain the smashed hammerstones or the high number of manuports transported into the cave with no observable macroscopic marks. The faunal assemblage does not contain traces of fresh breakage, therefore precluding the possibility that the hominins who occupied TD10.3 and TD10.4 were systematically breaking the bones to access the marrow. However, we cannot rule out the possibility that these smashed hammerstones were repeatedly used in knapping in different occupational events, therefore being subject of repeated stress.

So, the question must be raised as to why so many previously knapped large tools ($n = 44$) were brought into the occupations, as well as manuports and hammerstones ($n = 128$), some of which ended up broken and smashed ($n = 35$). Also, why were 111 small tools knapped on flakes and over 900 flakes removed (256 of which are 20 mm or larger) in a faunal assemblage comprising about 25,000 remains, of which only about 0.5% bear cut-marks and 0.04% percussion marks?

In the future, it will be necessary to confirm whether the manuports and hammerstones might reflect up-to-now unknown activities that generate minimal modifications on the tools for the scattered impacts or intense modifications for the broken and smashed hammerstones. Some of the large tools show chips and scarring on their distal edges, which surely means that they were actually used. Perhaps some of these tools were also used with perishable materials in activities not yet documented.

Preliminary use-wear analyses on the tools confirm the generally good preservation of the materials, with virtually no postdepositional surface modifications besides the

characteristic chemical weathering of the chert, especially the Neogene variety. The use-wear results pointed to a variety of activities, some of them compatible with butchery activities and other actions related to the treatment of animal carcasses, like hide processing. This is consistent with that reported in previous studies of Gran Dolina TD10.1 (Pedergnana & Ollé, 2020) and the Galería site in broad-surface assemblages (Ollé et al., 2005).

Despite the low representativeness of our functional results due to the reduced sample analyzed so far, several technological and functional aspects should be highlighted. The combination of technological, refitting, and use-wear analyses showed, for the first time, that resharpening and retooling processes were undertaken during the occupations in Atapuerca. In the case of the borer (see Fig. 11(1)), it was used to bore a hard material (not sure where), then resharpened inside the cave, used in a subsequent similar action, and discarded. In the case of the broken point (see Fig. 11(2)), the piece was involved in a thrusting action, after which it broke (again, in an unknown place), then the proximal part was slightly transformed by retouch, used to groove a bone, and finally discarded. Finally, several pieces with stepped retouch showed retouch traces and very fresh edges, apparently ready to be used.

Indeed, this is the first time a boring action on a hard material has been documented in the Sierra de Atapuerca record and points to a certainly complex activity for such an apparently "expeditious" context. And, finally, two pieces with visible impact fractures point to a thrusting action.

Experimental studies have demonstrated the diagnostic nature of such distal fractures and that it is possible to distinguish between different types of points (Fischer et al., 1984). Distinguishing between different possibilities, such as thrust of throwing spears and stone arrow tips, is not so easy in archaeological artifacts (e.g., Rots & Plisson, 2014, Iovita & Sano, 2016, Coppe et al., 2022). In archaeological material, it is agreed that the secure identification of a spear point should ideally combine different types of evidence, including diagnostic impact traces, step-terminating tip fractures, microscopic linear impact traces and hafting wear (Rots, 2013; Sano, 2009). Thrusting spear stone tips are rarely reported in archaeological assemblages, but are relatively common at Middle Palaeolithic sites such as the MSA and Late Nubian complex of the Sodmein Cave sequence, Egypt (Rots et al., 2011) and Hohle Fels, Germany (Rots et al., 2022). For sites closer in age to TD10.3 and TD10.4, the use of wooden thrusting spears is well documented at the Middle Pleistocene site of Schöningen, Germany (Conard et al., 2020). However, the possibility of stone tools bearing traces of impact motion or high pressure has also been suggested there (Rots et al, 2015), based on impact fractures similar to those reported in this study.

Although this issue deserves specific research, in both cases the tool broke transversally with both parts recovered inside the cave, which seems to support not only a spatial but a temporal relationship between them, and even the possible existence of stone tip spears.

The presence of 57 groups of refits and anthropic conjoins, 43 of which resulted from deliberate hominin activity, confirm the low disturbance of the deposits. Interestingly, the spatial distribution of the anthropic refits and conjoins (including accidental fractures, use and knapping) show that some pieces were moved to other areas of the cave, certainly to be used. The majority stayed within the natural fall radii for knapped pieces, in accordance with analogous evidence from experimental programs (Bargalló et al., 2018). In some cases, these radii may have been exceptionally large in the occupational surfaces of TD10.3, considering that the ground would have literally been covered by blocks of various sizes, which could make knapping products both bounce off of them and become wedged between them. Theoretically, the steep slope of the eastern half of the Dolina paleosurface would have facilitated the downward movement of these pieces. However, the density maps show that the slope did not actually influence the larger concentrations of faunal remains or lithics when considering both mass and size.

The total mass of the raw materials introduced into each deposit indicates sporadic and/or practically individual visits, or even more sporadic visits carried out by small groups. The results of the zooarchaeological and taxonomic studies point in the same direction, and suggests that the human occupations were spatially partial, possibly not covering the entire habitable surface.

Although hominin action on bones is scarce, the cutmarks documented in TD10.3 coincide with primary access to the carcasses, mainly of large ungulates. However, this access does not seem to have been intense inside the cave: human modifications are absent in TD10.4, but evidence of carnivores is present and diverse, which indicates the constant prowling of these animals within the cave. The spatial statistics on TD10.4 show clusters of faunal remains and lithics at distances exceeding 2 m, and at distances of about 70 cm in TD10.3-Inf and TD10.3-Sup. This surely means that the activities carried out in TD10.4 took up more space than those performed in TD10.3, where hominins might have worked in smaller areas, possibly more constrained by the high number of large blocks covering the ground.

All of this reinforces the idea of hominin occupational patches, likely individual, with sporadic and possibly short visits, leading to the alternating use of the cave by different predators. This model would explain (1) the remarkable variety of RMG, each with a reduced number of pieces, which might mean that a small amount of material was brought into the cave many times; (2) that only four of the 90 quartzite RMG were exploited in all three deposits; (3) that the large tools entered the cave already knapped, and, at most, only small reshapings were performed inside the site; and (4) that

some of the spatial relations among refits may result from the reuse of pieces abandoned in previous visits. Finally, the number of hammerstones, large tools and refits found among such a large, but scarcely modified faunal assemblage led us to explore the possibility that hominins were performing activities on perishable materials, actions for which we do not yet have a record.

TD10.3 and TD10.4 in Atapuerca

Comparative zooarchaeological and technological analyses support the assertion that the TD10.3-Sup, TD10.3-Inf, and TD10.4 assemblages were formed through the superimposition of multiple and independent events, similar to those identified in Upper TD10.1 (Saladié et al., 2018; de Lombera et al., 2020), the last archaeological deposit in Gran Dolina. They are consistent with short and sporadic occupations as part of a catchment territory that was probably exploited in an area larger than just the Sierra. The mixture of occupational events that do not involve the entire surface gave rise to spatial horizontal and vertical palimpsests, which are characteristic of Pleistocene sites in caves (Bailey, 2007; Bailey & Galanidou, 2009).

Several technological aspects haracterize the sequence from TD10.4 to TD10.3-Sup: (1) decreasing proportions of cores, percussive material and small tools; (2) decreasing knapping of large tools; (3) increasing centripetal knapping strategies; (4) sudden appearance of high proportions of fluvial materials in TD10.3-Inf, mainly in the form of hammerstones and manuports; (5) increasing number of flakes in TD10.3-Sup, at the expense of large tools; (6) absence of choppers and chopping tools in TD10.3-Sup; and (7) exclusive use of both Neogene and Cretaceous chert for knapping production in TD10.3-Sup, and twice the proportion of Cretaceous chert within that deposit, mainly invested in simple flakes and small tools.

Each of these aspects may be related to occupational/functional variables of each deposit. For example, the decrease in the number and shaping of large tools in TD10.3-Sup may mean that they were not needed as much at the end of the sequence, or that they were transported outside the occupation. Other aspects are interrelated, such as the sudden appearance of high proportions of hammerstones and manuports in TD10.3-Inf, which in turn seems to be linked to the functionality of the occupations, whatever they were. Also, the exclusive use of chert for knapping production in TD10.3-Sup may be related to the increase in centripetal knapping strategies and the decrease in longitudinal unipolar methods, which were preferentially applied to fluvial materials in the lower deposits.

However, the key question here is how likely is it that all these aspects occurred together, particularly in TD10.3-Sup? In response, another hypothesis arises: perhaps these actions resulted from a change in technology, particularly considering this upper part of Gran Dolina and the Galería site.

In our view, the Acheulean that entered Gran Dolina for the first time in TD10.4 was fully developed and it apparently changed slightly over the course of the sequence. The maintenance of or decrease in the number and intensity of knapping of large tools occurred alongside an increase in flakes. This trend generally occurs from the bottom to the top of unit TD10. Thus, it is possible that TD10.3-Sup marks a change of trend from the full Acheulean to a later form. This is the same deposit that evidences the exclusive use of chert for the production of flakes and small tools, a trend that would intensify in the overlying unit: TD10.2.

Subunit TD10.2 and the overlying subunit TD10.1 contain at least two episodes of intense hominin occupations: the kill-butchering Bison bone-bed of TD10.2 and the residential Bone-bed level of Lower TD10.1 (de Lombera-Hermida et al., 2020; Ollé et al., 2016a, 2016b; Rodríguez-Hidalgo et al., 2015, 2017). So, considering the 3 m of stratigraphic sequence that make up unit TD10, the same pattern is present in TD10.4 and TD10.3 as well as in Upper-TD10.1, the last archaeological deposit in Gran Dolina. Upper-TD10.1 is characterized by small and mobile hominin occupations with low percentages of artifacts, temporal and spatial fragmentation of reduction sequences of large tools and maybe some flakes, which means they were not produced there. In addition, the raw materials became more diverse, and most of the fluvial materials were acquired from the fluvial terraces of Arlanzón River and its tributaries, instead of the higher quality Utrillas facies in the northwest Sierra.

Another technical characteristic is the change from the classical "tear-drop" (oval) shapes in TD10.4 and TD10.3-Inf, to wider shapes increasing their variability in TD10.3-Sup. The instruments present a tendency to lose their shape, something that was documented up in the sequence in TD10.1 sublevel (García-Medrano et al., 2015). This variability is represented in the reduction of the bilateral and the bifacial symmetries, which in turn occurred due to the scarce shaping of these tools in TD10.3-Sup. Interestingly, this same trend also occurs in Lower TD10.1.

The numbers of small tools tend to increase in short, sporadic, and mobile hominin occupations, especially in those in which there is not much meat to process (Mosquera, 1998, 2004; Terradillos and Díez, 2012). In fact, this is evidenced by the huge number of simple flakes that usually comprise the assemblages of residential and/or campsites, and it is the case of Gran Dolina unit TD10, where the percentages of small tools compared to the whole assemblages are high in TD10.4 (9.7%), TD10.3-Inf (8.8%), TD10.3-Sup (5.8%), and Upper TD10.1-A (6.2%), while percentages in intense occupations are lower: Bison-Bone bed (3.34%) and Lower TD10.1 (3.2%).

However, other aspects do not seem to be related to the type of occupation, such as the knapping strategies documented. In general, the orthogonal and centripetal strategies of TD10.3 and TD10.4 also dominated in the other Middle Pleistocene assemblages of Atapuerca (i.e., TD10.1, Galería and Sima del Elefante-TE18-19, whose dates are *c.* 520 ka for TE18 and c. 250 ka for TE19 (Demuro et al., 2022). Nevertheless, bifacial centripetal strategies with core surface hierarchization—virtually absent at TD10.4 and TD10.3—are present in TD10.2, and very common at TD10.1 and the upper levels of Galería.

In addition, aspects such as the high proportion of large tools and percussive material in TD10.4 and TD10.3 (particularly, TD10.3-Inf) are extremely similar to units GII (lowermost) and GIIIb (uppermost) of Galería, with a similar archaeological record in terms of both the faunal taxa and the lithic industry. Moreover, Galería is located just 50 m from Gran Dolina, which allows for the inference that both caves were used simultaneously during these chronologies.

At a technological level, Galería is characterized by great homogeneity and repetitive lithic patterns (García-Medrano et al., 2014, 2015; Ollé et al., 2016a, 2016b), although some technological changes have been identified along the sequence. These characteristics and diachronic trends are the following:

a. The proportions of large tools in Galería are very high (more than 3% of the assemblage) in all subunits, and their representation decreases along the sequence (from 6.1 to 3%). In TD10, their proportions are not as high but higher than in any other Atapuerca record. They also decrease along the sequence (from c. 4.5% in TD10.4 and TD10.3-Inf to 1.6% in TD10.3-Sup).
b. Cobbles/blocks were shaped to produce about 70% of the large tools at the bottom (GIIa) of Galería. This percentage reversed along the sequence, through GIIb (c. 50%) to GIIIa and finally GIIIb (30%). In contrast, in Gran Dolina the majority of the large tools were made from the beginning on flake, starting in TD10.4 (66.7%), then in TD10.3-Inf (75%) and in TD10.3-Sup (77.7%), like the increase in this type of blank along the sequence in Galería.
c. The percussive material (manuports and hammerstones) is very high in both caves, exceeding any other record excavated up to now at any of the Atapuerca sites. They range between 11.5 and 26.6% in the Galería units and 9 and 10% in TD10.3 and TD10.4. The difference is that while percussive material in Galería reach the highest proportions in the last half of the sequence, in Dolina they reach their highest in TD10.4 and, especially in TD10.3-Inf.
d. Subunit GIIIa of Galería contained a wider diversity of raw materials and more chert and sandstone. The increase in chert also occurs in the Gran Dolina TD10.3-Sup deposit.
e. In unit GIII of Galería the size and knapping intensity of large tools decrease. This also occurs from TD10.4 to TD10.3-Sup.
f. Along the sequence of both caves more complex knapping schemes were progressively introduced, notably bifacial discoid strategies with core surface hierarchization. However, this type of strategy in Dolina is not present in TD10.3 and TD10.4, but it is present in TD10.2. In Galería it appears in the uppermost subunit GIIIb.
g. Obviously, some of these characteristics, especially proportions, may be due to functional strategies, occupational strategies or any number of circumstances. However, taken together, they may also point to particular correlations between the two sites. We might suggest that subunit GIIb of Galería broadly correlates with subunits TD10.4 and TD10.3-Inf, while subunit GIIIa of Galería may correlate with TD10.3-Sup of Gran Dolina. Putting aside subunit TD10.2 for the moment, with its particular lithic and faunal characteristics, subunit TD10.1, the latest of Gran Dolina, may as well correlate with subunit GIIIb, the latest of Galería.

It is not now possible to correlate the two sites at the geochronological level (Ollé et al., 2016a, 2016b): firstly, because current dates for TD10.4 (*c.* 400 ka) are younger than those for the overlying subunit TD10.3 (458 ± 39 ka and 455 ± 47 ka); and second, because of the great inconsistencies inside the Galería sequence (ESR/US: for the lower layers (GIIa) 363–350 ka and 220 ka for the uppermost layer (GIIIb) (Falgueres et al., 2013), but TT-OSL and pIR-IR methods: 313 ± 14 ka for the lowermost subunit GIIa, and a range of 260 to 220 ka for GIII (Demuro et al., 2014)).

Aside from the geochronological inconsistencies, the Acheulean of TD10.4 and TD10.3 could be the same as the Acheulean of Galería GIIb and GIIIa, with a sort of similar hominin occupational pattern. Although the faunal remains of Galería exhibit more intense marks of hominin modification than those of TD10.3 and TD10.4, they do not exceed 3%. In addition, hammerstones from Galería show marks and fractures resulting from percussion activities (García-Medrano et al., 2014: 176) in higher proportions than in TD10.3 and TD10.4. However, the production of flakes and shaped tools in Galería is as low as in Dolina. Therefore, the question about the relation between fauna and lithics in TD10.4 and TD10.3 still remains unsolved.

The impressive number of hammerstones and manuports in both caves—particularly relevant in Gran Dolina, where faunal remains were scarcely modified—needs to be explained. Different hypotheses can be proposed: one hypothesis already mentioned is that hominins were

performing activities yet unidentified, which did not leave marks of use, or if they did, we do not know how to recognize them. Another hypothesis is that the hominins occupying the cave repeatedly left manuports and hammerstones there in order to use them in future visits (García-Medrano et al., 2014, 2015, 2017; Mosquera, 1995). This hypothesis has also been proposed in relation to the hammerstones, tested cores and large tools from the upper levels of Sima del Elefante (de Lombera-Hermida et al., 2015). Another common-sense hypothesis is that many of these manuports may have been transported into the caves to use in self-defense against the predators that actually used these caves, as these spaces tend to be dark and having a cobble ready to throw could have made the difference between life and death. However, this hypothesis cannot explain why they carried so many manuports if the entrance to the cave and its surroundings had numerous blocks. It is also possible that hominins used to carry some cobbles in their daily life as a preventive means.

The hypothesis of using cobbles as weapons for self-defense or attack has been proposed for much older sites, such as Dmanisi (Georgia) (Coil et al., 2020) and Fuente Nueva 3 (Spain), where at least one-third of the manuports show no traces of use (Palmqvist et al., 2023), as is the case in TD10.3 and TD10.4. Actually, these authors suggest that the pieces may have been used to drive away carnivores in order to steal their prey from them. Although it is extremely difficult to archaeologically prove this hypothesis, some experimental studies focused on natural "spheroids" from the archaeological site of the Cave of Hearths (South Africa) point to their use as thrown missiles (Wilson et al., 2016). In addition, ethnographic studies have documented examples of current hunter-gatherer communities that hunt small and medium-sized prey using this method. Likewise, written documentation recording historical cases of human confrontations is quite sparse, although there are some eloquent examples of the skill, strength and precision with which certain tribes and communities used stones in confrontations with much better armed intruding settlers, causing serious casualties among the troops and even their withdrawal (Isaac, 1987).

All of these scenarios suggest anticipatory behavior extended to at least two caves (the upper levels of Sima del Elefante are not fully excavated), during the second half of the Middle Pleistocene. Because it has not been documented before or repeated later in the Gran Dolina and Galería records, it might be assumed either that this behavior responded to a strategy that subsequently disappeared or that the needs these pieces were intended for were met by different means. Clearly, none of these caves were a camp or residential site at that time. If these hominins had one, it was in another cave no longer known to us.

TD10.3 and TD10.4 in the western European Context

The composition of the archaeological assemblages of TD10.3 and TD10.4 are intriguing, in our view, because it comprises many manuports and hammerstones, as well as numerous handaxes and cleavers associated to a large faunal assemblage with so few remains with anthropic modifications.

Comparison with other similar archaeological assemblages is difficult because of the nature of the search and the characteristics of each site. For example, no comparison can be made with sites where the sediments do not preserve faunal remains (i.e., most British and western Iberian sites), nor with sites located on fluvial or marine terraces where natural cobbles and pebbles are part of the sediments (e.g., Terra Amata, in France). In this case, only hammerstones can be identified, not possible manuports.

On the other hand, some western European archaeological sites may have a technological composition including large cutting tools, but they display very few percussive material (e.g., Cueva del Ángel, Spain), or the lithic assemblages are associated with faunal remains moderately to highly modified by hominins (e.g., level 6 of Orgnac 3, France). These is also the case of the similar aged Portuguese site of Aroeira (Almonda), whose level X yielded a hominin cranium, associated with a faunal assemblage highly modified by humans and a lithic assemblage (Daura et al., 2017, 2018), interestingly resembling that of TD10.3 and TD10.4. Layer X of the karstic cave of Aroeira was a residential occupation dated to 436-389 ka, where the lithic assemblage was mostly made in quartzite and quartz. It includes hammerstones, manuports, handaxes, centripetal cores, flakes, and retouched flakes. Some handaxes, flakes and one core showed traces of woodworking and butchering. Among the faunal remains identified cervids and equids dominate, although rhino and bear are also documented (Daura et al., 2018). All technological characteristics of Aroeira layer X resemble that of TD10.3 and TD10.4, including a big percentage (c. 22%) of percussive material (at least $n = 85$) among the total of lithic items ($n = 393$) in the Portuguese site. The only noticeable difference so far is the presence of five cleavers on flake in TD10.3 and TD10.4.

Another archaeological site that achieves even a larger percentage of percussive material (c. 25% of the total) and contains large tools on flake is the lithic assemblage from the entrance breccias of the Spanish cave of Santa Ana (Cáceres) (García-Vadillo et al., 2022). Here too bones show rare hominin modifications (Rodríguez-Hidalgo, 2008), but in fact faunal remains are scarce. The type of occupation of this site has been interpreted as occupational episodes of low impact and short duration. Different stalagmitic floors on the cave have yielded radiometric ages between

183 + 14/ − 12 and 117 + 17/ − 14 ka (Peña, 2008), but it is also more than possible that the analyzed assemblage was of an older age, given two significant technological features: the absence of Levallois technique and the presence of several spheroids, only present in western Europe at the 1.3 Ma site of Barranco León (Granada, Spain) (Titton et al., 2020). Unfortunately, the Santa Ana lithic assemblage studied in García-Vadillo and colleagues (2022) is derived from 7 m thick Pleistocene breccias and blocks of breccias that have undergone severe postdepositional alteration, making it difficult to discern whether the archaeological material comes from a unitary assemblage.

Other western European Middle Pleistocene sites, both open-air and cave/shelter occupations, do not fulfil the features that characterize TD10.3 and TD10.4. Such is the case, for example, of the karstic cave of Arago (Tautavel, France), with a huge stratigraphy entailing from 690 to 400 ka. Unit III of Arago has been quartz dated by ESR 430 ± 85 ka, so it may roughly correspond to TD10.3 and TD10.4 chronologies. This Unit III (Barsky, 2013) shows the highest proportion of percussive material (12.2%) of the whole deposit of Arago, whose importance has already been highlighted (Guibert, 2022). However, handaxes and cleavers are very scarce, and most of them located at the bottom of the whole stratigraphic sequence (Level P), where percussive material drastically decreases (1.3%). Unit III entails hominin occupations corresponding with seasonal stays (levels D, E and F), bivacs (level FG) and long-term stays (level G), but all of them with the numerous signals of hominin modification in bones.

Also in France, the cave of Vallonnet is an interesting case, with faunal remains hardly modified by hominins and a high percentage of percussive material. However, the lithic assemblage is very small ($n = 104$) and recent dating places the archaeological levels between 1.2 and 1.1 Ma. The assemblage therefore lacks large cutting tools (Cauche, 2022).

The US2 unit of the Bois-de-Riquet site also fulfils the characteristics of both TD10.3 and TD10.4. It is a well-preserved sedimentary unit with a high proportion of basalt pebbles and cobbles and a faunal assemblage with little evidence of hominin modification, both cut-marks and breakage. However, the Bois-de-Riquet unit US2 is dated between 1.07 and 0.99 Ma. As in the case of Vallonnet, the Bois-de-Riquet lithic assemblage is not Acheulean (i.e., it lacks LCT), and consists of small-sized flakes, cores, and blanks on basalt (Bourguignon et al., 2016, 2021).

On the contrary, US4 from the same site is dated to the beginning of the Middle Pleistocene, around 780 ka to 680 ka. It is an Acheulean containing large flakes on giant cores, handaxes, cleavers, and polyhedrons (Bourguignon et al., 2016). However, manuports and hammerstones only reach 4%. In addition, it seems to contain very few faunal remains, the zooarchaeological analyses of which have not yet been published.

Conclusions

The Acheulean that was brought into TD10.4 was fully developed and seems to have changed slightly through the sequence from TD10.3 and from there upwards. After subunit GIIa of Galería, the TD10.4 and TD10.3 records have the second highest proportions of large tools in all of the excavated sites at Atapuerca. In both caves, these implements were usually brought in already shaped. Together with manuports and hammerstones (in some cases intensely used, and in others without any clear sign of use) they are possibly the most characteristic tools in the records of these two sites. In addition, compared to camp-sites and butchery sites, signs of hominin intervention on faunal remains are scarce and the signs of knapping resulting from the production of tools are equally low, both in TD10.3 and TD10.4 and in Galería.

Nevertheless, the association of hammerstones, large tools, small tools and simple flakes with the faunal remains is undeniable, as evidenced by spatial, zooarchaeological and, particularly, use-wear analyses, which have revealed traces of butchering, hide-working and also thrusting evidence in some pieces. Therefore, the hominins who visited Gran Dolina seem to have been engaged in hunting-related activities.

Thus, we conclude that TD10.4 and TD10.3 responded to occupational stages of sporadic visits by small hominin groups, or even isolated individuals, which would explain both the low mass of the raw materials and the diversity of raw material varieties. These small groups possibly never occupied the entire surface of the cave and they reused some of the lithics abandoned in previous visits.

Technical analyses suggest that the occupations of TD10.3-Inf are technologically closer to TD10.4 than to TD10.3-Sup, where cores are only in chert, choppers and chopping tools are absent, and the shaping of large tools is much scarcer. The presence of the latest *Homotherium latidens* in TD10.4 and TD10.3-Inf may mean that this technological proximity may also be chronological. The relative slowdown in the block falls around the middle of TD10.3, which separates TD10.3-Inf from TD10.3-Sup, may indicate an environmental change that would support this hypothesis.

The presence of numerous refits and conjoins of anthropic origin and the relative scarcity of postdepositional fractures pays testament to the good preservation of both deposits, despite the markedly dynamic character of Gran Dolina cave at that time: the most intense opening of a cave that we have recorded so far in the Sierra de Atapuerca sites. This good preservation is also confirmed by the use-wear analyses, which confirmed that the unweathered materials had fresh surfaces and thus provided evidence of limited postdepositional alterations.

The Acheulean of TD10.4 and TD10.3 is likely the same technology as that documented in Galería. And both caves were likely used as regular venues for the processing of meat (and possibly other material) by small groups of hominins. In this sense, it is possible to broadly correlate TD10.4 and TD10.3-Inf with Galería subunit GIIb, and TD10.3-Sup with Galería subunit GIIIa. The possible use of Gran Dolina, Galería and other Middle Pleistocene caves of Atapuerca simultaneously must not be excluded. These regular visits were characterized by short occupations by a few hominins that reused some of the material left behind during earlier visits. They may have deliberately left the manuports for future visits or they may have carried them with them as weapons for self-defense. This would explain why so much percussive material was found at the site in the presence of so little evidence of faunal modification. In many instances, they may have taken advantage of some of the meat of the animals possibly hunted by other predators. However, singular events of hunting likely occurred. These hominins were not opportunistic, since they did this with large tools that were shaped before entering the caves. So, the explanation for why so many of these tools were documented at the site remains unclear. In fact, the preliminary use-wear results point to a wider variety of activities than initially thought, which, in addition to butchery, includes a variety of percussive actions, intensive resharpening and reuse, and the presence of thrusting elements.

As far as we know, only the Spanish site of Santa Ana is comparable to TD10.3 and TD10.4 (i.e., Middle Pleistocene assemblages containing many manuports and hammerstones, and also handaxes and cleavers associated with few hominin-modified faunal remains), although the correlation between the Santa Ana deposits needs to be refined and excavation and analysis are still ongoing.

Finally, it is worth noting that neither Galería nor Gran Dolina-TD10.3 and TD10.4 were residential sites during the Acheulean period. If these hominins did use a residential site in a cave in the Sierra de Atapuerca, it was not in these caves.

Supplementary Information The online version contains supplementary material available at https://doi.org/10.1007/s41982-024-00171-5.

Acknowledgements We thank Arturo Cueva-Temprana and Xose Pedro Rodríguez-Álvarez for their help in identifying lithic connections, and Maria D. Guillén for the professional photography of the lithics. We also thank the Atapuerca Research Team that excavated subunits TD10.3 and TD10.4. Finally, we would like to thank the reviewers for their interesting comments and suggestions, which have undoubtedly improved our study.

Author Contribution M.M.: conceptualization, methodology, validation, formal analysis, investigation, resources, data curation, writing-original draft, writing—review and editing, visualization, supervision, project administration, funding acquisition. A.O.: methodology, validation, formal analysis, investigation, resources, data curation, writing-original draft, writing—review and editing, visualization. P.S.: methodology, validation, formal analysis, investigation, resources, data curation, writing-original draft, writing—review and editing, visualization. A.Arr.: methodology, validation, formal analysis, investigation, resources, writing—original draft. L.A.: methodology, validation, formal analysis, investigation, resources, writing—original draft. A.B.: methodology, validation, formal analysis, investigation, resources, writing—original draft. A.dL-H.: methodology, validation, formal analysis, investigation, resources, writing—original draft. JL.F-M.: methodology, validation, formal analysis, investigation, resources, writing—original draft. P.G-M.: methodology, validation, formal analysis, investigation, resources, writing—original draft. D.L.: methodology, validation, formal analysis, investigation, resources, writing—original draft. A.R-H: methodology, validation, formal analysis, investigation, resources, writing—original draft. M.S.: methodology, validation, formal analysis, investigation, resources, writing—original draft. J.V: methodology, validation, formal analysis, investigation, resources, writing—original draft. A.Art.: formal analysis, investigation, resources. J.V.: formal analysis, investigation. GC.Y.: formal analysis, investigation. E.C.: project administration, funding acquisition.

Funding Open Access funding provided thanks to the CRUE-CSIC agreement with Springer Nature. Fieldwork at Atapuerca is supported by Junta de Castilla y Leon and Fundación Atapuerca. This work has been possible thanks to PGC2018-093925-B-C32 and PID2021-122355NB-C32 funded by MCIN/AEI/https://doi.org/10.13039/501100011033, by "ERDF A way of making Europe" to the Agency for Management of University and Research Grants of Generalitat de Catalunya SGR2021-01239 and SGR2021-01237), and to Universitat Rovira i Virgili (2022PFR-URV-64). Fieldwork and research were also funded by the Institut Català de Paleoecologia Humana i Evolució Social (IPHES-CERCA), which has received financial support from the Spanish Ministry of Science and Innovation through the "María de Maeztu" program for Units of Excellence (CEX2019-000945-M). This research is part of the ERC101052653 project. The contribution of L. Asryan is supported by a MSCA Individual Fellowship (MSCA-IF-2020–101028232 BaTEx). The contribution of A. Bargalló is supported by a Juan de la Cierva Incorporación. The contribution of J.L. Fernández-Marchena is supported by a contract APOSTD (CIAPOS/2022/022), funded by Generalitat Valenciana-FSE. The contribution of P. Garcia-Medrano is supported by a Beatriu de Pinós MSCA-COFUND (AGAUR). The contribution of A. de Lombera-Hermida is supported by the Spanish Ministry of Universities and Next-Generation EU (Margarita Salas Program). The contribution of A. Arroyo, A. Rodríguez-Hidalgo, and G.C. Yeşilova is supported by the Spanish Ministry of Science and Innovation through the "María de Maeztu" (CEX2019-000945-M).

Data Availability All the materials studied here are deposited at Centro Nacional de Investigación sobre la Evolución Humana (CENIEH, Burgos, Spain), and Institut de Paleoecologia Humana i Evolució Social (IPHES, Tarragona, Spain).

Declarations

Ethics Approval Not applicable.

Competing Interests The authors declare no competing interests.

References

Álvarez-Posada, C., Parés, J. M., Cuenca-Bescós, G., Van der Made, J., Rosell, J., Bermúdez de Castro, J. M., & Carbonell, E. (2018). A post-Jaramillo age for the artefact-bearing layer TD4 (Gran Dolina, Atapuerca): New paleomagnetic evidence. *Quaternary Geochronology., 45*, 1–8. https://doi.org/10.1016/j.quageo.2018.01.003

Andrefsky, W. J. (1998). *Lithics: Macroscopic approaches to analysis. Cambridge manuals in archaeology*. Cambridge University Press.

Antón, M., Galobart, A., & Turner, A. (2005). Co-existence of scimitar-toothed cats, lions and hominins in the European Pleistocene. Implications of the post-cranial anatomy of *Homotherium latidens* (Owen) for comparative palaeoecology. *Quaternary Science Reviews., 24*, 1287–1301. https://doi.org/10.1016/j.quascirev.2004.09.008

Arteaga-Brieba, A., Courtenay, L. A., Cobo-Sánchez, L., Rodríguez-Hidalgo, A., Saladié, P., Ollé, A., & Mosquera, M. (2023). An archaeostratigraphic consideration of the Gran Dolina TD10.2 cultural sequence from a quantitative approach. *Quaternary Science Reviews, 309*, 108033. https://doi.org/10.1016/j.quascirev.2023.108033

Asryan, L., & Ollé, A. (2021). Experimental and multi-technique approach with Cretaceous chert, in *Rock and Roll: 13th International Symposium on Knappable Materials. Multi-scalar characterization of raw materials.* B. Gómez de Soler, M. Soto, M. G. Chacón, & M. Soares (Eds.), (Tarragona), *162*.

Baddeley, A. J., Møller, J., & Waagepetersen, R. (2000). Non- and semi-parametric estimation of interaction in inhomogeneous point patterns. *Statistica Neerlandica, 54*, 329–350. https://doi.org/10.1111/1467-9574.00144

Baddeley, A., Rubak, E., & Turner, R. (2015). Spatial point patterns: Methodology and applications with R. *Chapman and Hall/CRC Press, New Tork*. https://doi.org/10.1007/s11004-016-9670-x

Bailey, G. (2007). Time perspectives, palimpsests and the archaeology of time. *Journal of Anthropological Archaeology, 26*(2), 198–223. https://doi.org/10.1016/j.jaa.2006.08.002

Bailey, G., & Galanidou, N. (2009). Caves, palimpsests and dwelling spaces: Examples from the Upper Palaeolithic of south-east Europe. *World Archaeology, 41*(2), 215–241. https://doi.org/10.1080/00438240902843733

Bargalló, A., Mosquera, M., & Lorenzo, C. (2018). Identifying handedness at knapping; an analysis of the scatter pattern of lithic remains. *Archaeological and Anthropological Sciences, 10*(3), 587–598. https://doi.org/10.1007/s12520-016-0378-0

Barsky, D. (2013). The Caune de l'Arago stone industries in their stratigraphical context. *Comptes Rendus - Palevol, 12*(5), 305–325. https://doi.org/10.1016/j.crpv.2013.05.007

Berger, G. W., Pérez-González, A., Carbonell, E., Arsuaga, J. L., Bermúdez de Castro, J.-M., & Ku, T.-L. (2008a). Luminescence chronology of cave sediments at the Atapuerca paleoanthropological site, Spain. *Journal of Human Evolution, 55*(2), 300–311. https://doi.org/10.1016/j.jhevol.2008.02.012

Berger, G. W. W., Pérez-González, A., Carbonell, E., Arsuaga, J. L. L., de Castro, J.-M.B., Ku, T.-L.L., Bermúdez de Castro, J.-M.M., & Ku, T.-L.L. (2008b). Luminescence chronology of cave sediments at the Atapuerca paleoanthropological site, Spain. *Journal of Human Evolution, 55*(2), 300–311. https://doi.org/10.1016/j.jhevol.2008.02.012

Bertran, P., Klaric, L., Lenoble, A., Masson, B., & Vallin, L. (2010). The impact of periglacial processes on Palaeolithic sites: The case of sorted patterned grounds. *Quaternary International, 214*(1), 17–29. https://doi.org/10.1016/j.quaint.2009.10.021

Besag, J. (1977). Contribution to the discussion on Dr Ripley's paper. *Journal of the Royal Statistical Society, 39*, 193–195. https://doi.org/10.4236/wjns.2016.62020

Binford, L. R. (1981). *Bones: Ancient men and modern myths*. Academic Press.

Blain, H.-A.A.H.-A., Bailon, S., & Cuenca-Bescós, G. (2008). The Early-Middle Pleistocene palaeoenvironmental change based on the squamate reptile and amphibian proxies at the Gran Dolina site, Atapuerca, Spain. *Palaeogeography, Palaeoclimatology, Palaeoecology, 261*(1), 177–192. https://doi.org/10.1016/j.palaeo.2008.01.015

Blain, H.-A., López-García, J. M., & Cuenca-Bescós, G. (2011). A very diverse amphibian and reptile assemblage from the late Middle Pleistocene of the Sierra de Atapuerca (Sima del Elefante Burgos Northwestern Spain). *Geobios, 44*(2–3), 157–172. https://doi.org/10.1016/j.geobios.2010.08.003

Blair, T., & McPherson, J. G. (1999). Grain-size and textural classification of coarse sedimentary particules. *Journal of Sedimentary Research, 69*(1), 6–19. https://doi.org/10.2110/jsr.69.6

Blumenschine, R. J., & Selvaggio, M. M. (1988). Percussion marks on bone surfaces as a new diagnostic of hominid behaviour. *Nature, 333*, 763–765. https://doi.org/10.1038/332141a0

Blumenschine, R. J., Marean, C. W., & Capaldo, S. D. (1996). Blind tests of inter-analyst correspondence and accuracy in the identification of cut marks, percussion marks, and carnivore tooth marks on bone surfaces. *Journal of Archaeological Science, 23*, 493–507. https://doi.org/10.1006/jasc.1996.0047

Bourguignon, L., Barsky, D., Ivorra, J., de Weyer, L., Cuartero, F., Capdevila, R., Cavallina, C., Oms, O., Bruxelles, L., Crochet, J. Y., & Garaizar, J. R. (2016). The stone tools from stratigraphical unit 4 of the Bois-de-Riquet site (Lézignan-la-Cèbe, Hérault, France): A new milestone in the diversity of the European Acheulian. *Quaternary International, 411*, 160–181. https://doi.org/10.1016/j.quaint.2016.01.065

Bourguignon, L., Ivorra, J., de Weyer, L., Cuartero, F., Barsky, D., Capdevila, R., & Ivorra, M.-H. (2021). Les nodules sphériques de basalte de l'unité archéologique US2 du site de « Bois-de-Riquet », France: Origine et caractérisation d'une sélection. *L'anthropologie, 125*(1), 102847. https://doi.org/10.1016/j.anthro.2021.102847

Brain, C. K. (1981). *The hunters or the hunted? An introduction to African cave taphonomy.* The University of Chicago Press. https://doi.org/10.1017/S0016756800025103

Byrne, L., Ollé, A., & Vergès, J. M. (2006). Under the hammer: Residues resulting from production and microwear on experimental stone tools. *Archaeometry, 48*(4), 549–564. https://doi.org/10.1111/j.1475-4754.2006.00272.x

Campaña, I., Benito-Calvo, A., Pérez-González, A., Ortega, A. I., Bermúdez de Castro, J. M., & Carbonell, E. (2017). Pleistocene sedimentary facies of the Gran Dolina archaeo-paleoanthropological site (Sierra de Atapuerca, Burgos, Spain). *Quaternary*

International, 433, 68–84. https://doi.org/10.1016/j.quaint.2015.04.023

Campy, M., Bintz, P., Evin, J., Laville, H., & Chaline, J. (1994). Sedimentary record in French karstic infillings during the last climatic cycle. *Quaternaire, 5*(3–4), 157–163.

Carbonell, E., Guilbaud, M., & Mora, R. (1983). Utilización de la Lógica Analítica para el estudio de los tecnocomplejos a cantos tallados. *Cahier Noir, 1*, 3–64.

Carbonell, E., Mosquera, M., Ollé, A., Rodríguez-Álvarez, X. P., Sala, R., Vaquero, M., & Vergès, J. M. (1992). New elements of the logical analytical system. First international meeting on technical systems to configure lithic objects of scarce elaboration. *Cahier Noir, 6*, 3–61.

Cauche, D. (2022). The Vallonnet cave on the northern Mediterranean border: A record of one of the oldest human presences in Europe. *L'Anthropologie (France), 126*(1). https://doi.org/10.1016/j.anthro.2021.102974

Coil, R., Tappen, M., Ferring, R., Bukhsianidze, M., Nioradze, M., & Lordkipanidze, D. (2020). Spatial patterning of the archaeological and paleontological assemblage at Dmanisi, Georgia: An analysis of site formation and carnivore-hominin interaction in Block 2. *Journal of Human Evolution*, *143*. https://doi.org/10.1016/j.jhevol.2020.102773

Conard, N.J., Serangeli, J., Bigga, G., & Rots, V. (2020). A 300,000-year-old throwing stick from Schöningen, northern Germany, documents the evolution of human hunting. *Nature Ecology & Evolution,* 1–4. https://doi.org/10.1038/s41559-020-1139-0

Coppe, J., Lepers, C., & Rots, V. (2022). Projectiles under a new angle: A ballistic analysis provides an important building block to grasp Paleolithic weapon technology. *Journal of Archaeological Method and Theory., 29*, 1131–1157. https://doi.org/10.1007/s10816-022-09551-z

Costa, A. G. A. (2010). A Geometric Morphometric assessment of plan shape in bone and stone Acheulean bifaces from the Middle Pleistocene site of Castel di Guido, Latium, Italy. In S. L. Lycett, & P. R. E. Chauhan (Eds.), *New perspectives on old stones: Analytical approaches to paleolithic technologies* (pp. 23–41). Springer. https://doi.org/10.1007/978-1-4419-6861-6_2

Cuenca-Bescós, G., Melero-Rubio, M., Rofes, J., Martínez, I., Arsuaga, J. L., Blain, H.-A., López-García, J. M., Carbonell, E., & Bermúdez de Castro, J. M. (2011). The Early-Middle Pleistocene environmental and climatic change and the human expansion in Western Europe: A case study with small vertebrates (Gran Dolina, Atapuerca, Spain). *Journal of Human Evolution, 60*(4), 481–491. https://doi.org/10.1016/j.jhevol.2010.04.002

Daura, J., Sanz, M., Arsuaga, J. L., Hoffmann, D. L., Quam, R. M., Ortega, M. C., Santos, E., Gómez, S., Rubio, A., Villaescusa, L., Trinkaus, E., Zilhão, J., Souto, P., Mauricio, J., Rodrigues, F., Ferreira, A., Godinho, P., Trinkaus, E., & Zilhão, J. (2017). New Middle Pleistocene hominin cranium from Gruta da Aroeira (Portugal). *Proceedings of the National Academy of Sciences, 114*(13), 3397–3402. https://doi.org/10.1073/pnas.1619040114

Daura, J., Sanz, M., Deschamps, M., Matias, H., Igreja, M., Villaescusa, L., Gómez, S., Rubio, A., Souto, P., Rodrigues, F., & Zilhão, J. (2018). A 400,000-year-old Acheulean assemblage associated with the Aroeira-3 human cranium (Gruta da Aroeira, Almonda karst system, Portugal). *Comptes Rendus - Palevol, 17*(8), 594–615. https://doi.org/10.1016/j.crpv.2018.03.003

de Lombera-Hermida, A. (2009). The scar identification of lithic quartz industries. In F. Sternke, L. Eigeland & L. Costa (Eds.), *Non-flint raw material use in prehistory. Old prejudices and new direction. XV UISPP Meeting, 4th-9th September 2006, Lisbon, Portugal* (pp. 193–202). British Archaeological Report. International Series.

de Lombera-Hermida, A. (2020). Gestión de materiales silíceos macrocristalinos en el Pleistoceno de Europa occidental. Evolución de las estrategias de adaptación a los condicionantes litológicos [Universidade de Santiago de Compostela]. http://hdl.handle.net/10347/24003

de Lombera-Hermida, A., Bargalló, A., Terradillos-Bernal, M., Huguet, R., Vallverdú, J., García-Antón, M.-D., Mosquera, M., Ollé, A., Sala, R., Carbonell, E., & Rodríguez-Álvarez, X.-P. (2015). The lithic industry of Sima del Elefante (Atapuerca, Burgos, Spain) in the context of Early and Middle Pleistocene technology in Europe. *Journal of Human Evolution, 82*, 95–106. https://doi.org/10.1016/j.jhevol.2015.03.002

de Lombera-Hermida, A., Rodríguez-Álvarez, X. P., Mosquera, M., Ollé, A., García-Medrano, P., Pedergnana, A., Terradillos-Bernal, M., López-Ortega, E., Bargalló, A., Rodríguez-Hidalgo, A., Saladié, P., Bermúdez de Castro, J. M., & Carbonell, E. (2020). The dawn of the Middle Paleolithic in Atapuerca: The lithic assemblage of TD10.1 from Gran Dolina. *Journal of Human Evolution, 145*, 102812. https://doi.org/10.1016/j.jhevol.2020.102812

Demuro, M., Arnold, L. J., Parés, J. M., Pérez-González, A., Ortega, A. I., Arsuaga, J. L., Bermúdez De Castro, J. M., & Carbonell, E. (2014). New luminescence ages for the Galería Complex archaeological site: Resolving chronological uncertainties on the Acheulean record of the Sierra de Atapuerca, Northern Spain. *PLoS ONE*, *9*(10). https://doi.org/10.1371/journal.pone.0110169

Demuro, M., Arnold, L. J., Parés, J. M., Aranburu, A., Huguet, R., Vallverdú, J., Arsuaga, J. L., Bermúdez de Castro, J. M., & Carbonell, E. (2022). Extended-range luminescence chronologies for the Middle Pleistocene units at the Sima del Elefante archaeological site (Sierra de Atapuerca, Burgos, Spain). *Quaternary Geochronology*, 101318. https://doi.org/10.1016/j.quaint.2014.08.035

Dibble, H. L. (1995). Biache Saint-Vaast, Level IIA: A comparison of analytical approaches. In H. L. Dibble & O. Bar-Yosef (Eds.), *The definition and interpretation of Levallois Technology. Monographs in World Archaeology* (Vol. 23, pp. 93–116). Prehistory Press.

Duval, M., Falguères, C., & Bahain, J.-J. (2012). Age of the oldest hominin settlements in Spain: Contribution of the combined U-series/ESR dating method applied to fossil teeth. *Quaternary Geochronology, 10*, 412–417. https://doi.org/10.1016/j.quageo.2012.02.025

Duval, M., Arnold, L. J., Demuro, M., Parés, J. M., Campaña, I., Carbonell, E., & Bermúdez de Castro, J. M. (2022). New chronological constraints for the lowermost stratigraphic unit of Atapuerca Gran Dolina (Burgos, N Spain). *Quaternary Geochronology*, *71*, 101292. https://doi.org/10.1016/j.quageo.2022.101292

Falguères, C., Bahain, J.-J., Yokoyama, Y., Arsuaga, J. L., Bermúdez de Castro, J. M., Carbonell, E., Bischoff, J. L., & Dolo, J.-M. (1999). Earliest humans in Europe: the age of TD6 Gran Dolina, Atapuerca, Spain. *Journal of Human Evolution, 37*(3), 343–352. https://doi.org/10.1006/jhev.1999.0326

Falguères, C., Bahain, J.-J., Bischoff, J. L., Pérez-González, A., Ortega, A. I., Ollé, A., Quiles, A., Ghaleb, B., Moreno, D., Dolo, J.-M., Shao, Q., Vallverdú, J., Carbonell, E., Bermúdez de Castro, J. M., & Arsuaga, J. L. (2013). Combined ESR/U-series chronology of Acheulian hominid-bearing layers at Trinchera Galería site, Atapuerca, Spain. *Journal of Human Evolution, 65*(2), 168–184. https://doi.org/10.1016/j.jhevol.2013.05.005

Fernández-Marchena, J. L., & Ollé, A. (2016). Microscopic analysis of technical and functional traces as a method for the use-wear analysis of rock crystal tools. *Quaternary International, 424*, 171–190. https://doi.org/10.1016/j.quaint.2015.10.064

Fernández-Marchena, J. L., Rabuñal, J. R., Mateo-Lomba, P., Lombao, D., Hernando, R., Cueva-Temprana, A., & Cazalla, I. (2020). Rainbow in the dark. The identification of diagnostic projectile

impact features on rock crystal. *Journal of Archaeological Science: Reports, 31*, 102315. https://doi.org/10.1016/j.jasrep.2020.102315

Fischer, A., Hansen, P. V., & Rasmussen, P. (1984). Macro and micro wear traces on lithic projectile points. Experimental results and prehistoric examples. *Journal of Danish Archaeology., 3*, 19–46.

Font, B., López-Polín, L., & Ollé, A. (2010). Description and characterization of the natural alteration of chert artefacts from Atapuerca (Burgos, Spain), Cansaladeta (Tarragona, Spain) and Orgnac 3 (Ardèche, France). *Annali Dell'università Di Ferrara Museologia Scientifica e Naturalistica., 6*, 103–110.

García, N., (2003). Osos y otros carnívoros de la Sierra de Atapuerca. Fundación Oso de Asturias, Oviedo. *ISBN,* 10: 8493086975

García-Antón, M. (2016). La captación, selección y gestión de recursos líticos en la Prehistoria: Una visión diacrónica del uso del territorio y sus recursos en el entorno de la Sierra de Atapuerca (Burgos) durante el Pleistoceno Inferior y Medio. En Departamento de Historia e Historia del Arte: Vol. PhD Thesis. Universitat Rovira i Virgili.

García-Antón, M. D., Mosquera-Martínez, M., Moncel, M. H., Moigne, A. M., Arzarello, M., & Peretto, C. (2007). Preliminary data on areas of supply and first lithic material selection in Middle Pleistocene occupations on level TD10-1. *Raw Material Supply Areas and Food Supply Areas: Integrated Approach of the Behaviours, 1725*, 171–185.

García-Medrano, P., Ollé, A., Mosquera, M., Cáceres, I., Díez, C., & Carbonell, E. (2014). The earliest Acheulean technology at Atapuerca (Burgos, Spain): Oldest levels of the Galería site (GII Unit). *Quaternary International, 353*, 170–194. https://doi.org/10.1016/j.quaint.2014.03.053

García-Medrano, P., Ollé, A., Mosquera, M., Cáceres, I., & Carbonell, E. (2015). The nature of technological changes: The Middle Pleistocene stone tool assemblages from Galería and Gran Dolina-subunit TD10.1 (Atapuerca, Spain). *Quaternary International, 368*, 92–111. https://doi.org/10.1016/j.quaint.2015.03.006

García-Medrano, P., Cáceres, I., Ollé, A., & Carbonell, E. (2017). The occupational pattern of the Galería site (Atapuerca, Spain): A technological perspective. *Quaternary International, 433*, 363–378. https://doi.org/10.1016/j.quaint.2015.11.013

García-Vadillo, F. J., Canals-Salomó, A., Rodríguez-Álvarez, X. P., & Carbonell-Roura, E. (2022). The large flake Acheulean with spheroids from Santa Ana Cave (Cáceres, Spain). *Journal of Archaeological Science: Reports*, *41*. https://doi.org/10.1016/j.jasrep.2021.103265

Guibert, J. (2022). L'outillage sur galet au Paléolithique ancien en Europe de l'Ouest. Étude technicofonctionnelle de l'UA G de la Caune de l'Arago (Tautavel, France). *Bulletin de la Sociéte Préhistorique Francaise, 119*(1), 7–35.

Guilbaud, M. (1995). Introduction sommaire au concept de champ opératoire. *Cah. Noir, 7*, 121–133.

Herzlinger, G., & Goren-Inbar, N. (2020). Beyond a cutting edge: A morpho-technological analysis of Acheulian handaxes and cleavers from Gesher Benot Ya'aqov, Israel. *J Paleo Arch, 3*, 33–58.

Herzlinger, G., & Grosman, L. (2018). AGMT3-D: A software for 3-D landmarks-based geometric morphometric shape analysis of archaeological artifacts. *PLoSOne, 13*(11), e0207890.

Herzlinger, G., Goren-Inbar, N., & Grosman, L. (2017). A new method for 3D geometric morphometric shape analysis: The case study of handaxe knapping skill. *Journal of Archaeological Science: Reports, 14*, 163–173. https://doi.org/10.1016/j.jasrep.2017.05.013

Hoyos, M., & Aguirre, E. (1995). El registro paleoclimático pleistocénico en la evolución del karst de Atapuerca (Burgos): El corte de Gran Dolina. *Trabajos De Prehistoria, 52*(2), 31–45.

Inizan, M. L., Reduron-Ballinger, M., Roche, H. & Tixier, J. (1999). *Technology and Terminology of Knapped Stone. Cercle de Recherches et d'Etudes Préhistoriques*. Maison de l'Archéologie et de l'Ethnologie.

Iovita, R., & Sano, K. (Eds.) (2016). *Multidisciplinary approaches to the study of Stone Age weaponry*. Vertebrate Paleobiology and Paleoanthropology Series. Springer. https://doi.org/10.1007/978-94-017-7602-8

Isaac, B. (1987). Throwing and human evolution. *The African Archaeological Review, 5*, 5–17.

Isaac, G. (1977). *Olorgesailie: Archaeological studies of a Middle Pleistocene lake basin in Kenya* (272 pp., 73 figs., 23 plates. 61 plates). University of Chicago Press.

Laplace, G. (1968). Recherches de typologie analytique. *Origini*, 1968, II, 7–64, 26 figs.

Laplace, G. (1974) La typologie analytique et structurale: base rationnelle d'étude des industries lithiques et osseuses, dans *Banques de données archéologiques* (Colloques nationaux du CNRS), *1974*, 91–143.

Lombao, D., (2021). Reducción y gestión volumétrica: aproximación a la variabilidad y evolución de las dinámicas de explotación durante el Pleistoceno inferior y medio europeo, a través de los conjuntos de Gran Dolina y Galería (Sierra de Atapuerca, Burgos) y de El Barranc de la Boella (La Canonja, Tarragona). Tesis Doctoral. Universitat Rovira i Virgili, Tarragona.

Lombao, D., Rabuñal, J. R., Morales, J. I., Ollé, A., Carbonell, E., & Mosquera, M. (2023). The technological behaviours of *Homo antecessor*: Core management and reduction intensity at Gran Dolina-TD6.2 (Atapuerca, Spain). *Journal of Archaeological Methods and Theory*, *30*(3), 964–1001. https://doi.org/10.1007/s10816-022-09579-1

López-Ortega, E., Rodríguez, X. P., & Vaquero, M. (2011). Lithic refitting and movement connections: The NW area of level TD10-1 at the Gran Dolina site (Sierra de Atapuerca, Burgos, north-western Spain). *Journal of Archaeological Science, 38*, 3112–3121. https://doi.org/10.1016/j.jas.2011.07.011

López-Ortega, E., Bargalló, A., de Lombera-Hermida, A., Mosquera, M., Ollé, A., & Rodríguez-Álvarez, X. P. (2017). Quartz and quartzite refits at Gran Dolina (Sierra de Atapuerca, Burgos): Connecting lithic artefacts in the Middle Pleistocene unit of TD10.1. *Quaternary International, 433*, 85–108. https://doi.org/10.1016/j.quaint.2015.09.026

López-Ortega, E., Rodríguez-Álvarez, X. P., Ollé, A., & Lozano, S. (2019). Lithic refits as a tool to reinforce postdepositional analysis. *Archaeological and Anthropological Sciences, 11*, 4555–4568. https://doi.org/10.1007/s12520-019-00808-5

Machado, J., Hernández, C. M., & Galván, B. (2011). Contribución teórico-metodológica al análisis histórico de palimpsestos arqueológicos a partir de la producción lítica. Un ejemplo de aplicación para el Paleolítico medio en el yacimiento de El Salt (Alcoy, Alicante). *Recerques Del Museu D'alcoi, 20*, 33–46.

Mallol, C., & Carbonel ilRoura, E. (2008). The collapse of Gran Dolina cave, Sierra de Atapuerca, Spain: Site formation processes of layer TD10-1. *Geoarchaeology, 23*(1), 13–41. https://doi.org/10.1002/gea.20206

Martín-Viveros, J. I., & Ollé, A. (2020). Use-wear and residue mapping on experimental chert tools. A multi-scalar approach combining digital 3D, optical, and scanning electron microscopy. *Journal of Archaeological Science: Reports., 30*, 102236. https://doi.org/10.1016/j.jasrep.2020.102236

Moncel, M. H., García-Medrano, P., Despriée, J., Arnaud, J., Voinchet, P., & Bahain, J. J. (2021). Tracking behavioral persistence and innovations during the Middle Pleistocene in Western Europe. Shift in occupations between 700 and 450 ka at la Noira site (Centre, France). *Journal of Human Evolution*, *156*. https://doi.org/10.1016/j.jhevol.2021.103009

Moreno, D., Falguères, C., Pérez-González, A., Duval, M., Voinchet, P., Benito-Calvo, A., Ortega, A. I., Bahain, J. J., Sala,

R., Carbonell, E., Bermúdez de Castro, J. M., & Arsuaga, J. L. (2012). ESR chronology of alluvial deposits in the Arlanzón valley (Atapuerca, Spain): Contemporaneity with Atapuerca Gran Dolina site. *Quaternary Geochronology, 10*, 418–423. https://doi.org/10.1016/j.quageo.2012.04.018

Moreno, D., Falguères, C., Pérez-González, A., Voinchet, P., Ghaleb, B., Despriée, J., Bahain, J. J., Sala, R., Carbonell, E., Bermúdez de Castro, J. M., & Arsuaga, J. L. (2015). New radiometric dates on the lowest stratigraphical section (TD1 to TD6) of Gran Dolina site (Atapuerca, Spain). *Quaternary Geochronology, 30*, 535–540. https://doi.org/10.1016/j.quageo.2015.05.007

Mosquera, M. (1995). Differential use of the space and raw materials at the Sierra de Atapuerca sites (Burgos, Spain): An approach to some economical and ecological inferences. *Non-Flint Raw Materials and the Palaeolithic Occupation of the Iberian Peninsula. Tempus Separatum. British Archaeological Research, International Series, 649*, 81–87.

Mosquera, M. (1998). Differential raw material use in the Middle Pleistocene of Spain: Evidence from Sierra de Atapuerca, Torralba. *Ambrona and Aridos. Cambridge Archaeological Journal, 8*(1), 15–28. https://doi.org/10.1017/S0959774300001281

Mosquera, M. (2004). Middle Pleistocene human occupations - Similarities and differences of Atapuerca, Aridos, Torralba, Ambrona, Bilzingsleben, Schönin, Lehringen and Ehringsdorf. In M. Burdukiewicz, L. Fiedler, W. Heinrich, A. Justus, & E. Brühl (Eds.), *Halle, Veröffentlichungen des Landesamt für Archäologie Sachsen-Anhalt, 2003* (pp. 403–414).

Mosquera, M., Ollé, A., & Rodríguez, X. P. (2013). From Atapuerca to Europe: Tracing the earliest peopling of Europe. *Quaternary International, 295*, 130–137. https://doi.org/10.1016/j.quaint.2012.01.031

Ollé, A. (2003). Variabilitat i patrons funcionals en els sistemes tècnics de Mode 2. Anàlisi de les deformacions d'ús en els conjunts lítics del Riparo Esterno de Grotta Paglicci (Rignano Garganico, Foggia), Áridos (Arganda, Madrid) i Galería-TN (Sierra de Atapuerca, Burgos). Dept. d'Història i Geografia. Universitat Rovira i Virgili, Tarragona. Ph.D. Thesis. http://tdx.cat/handle/10803/8603

Ollé, A., & Vergès, J. M. (2014). The use of sequential experiments and SEM in documenting stone tool microwear. *Journal of Archaeological Science, 48*, 60–72. https://doi.org/10.1016/j.jas.2013.10.028

Ollé, A., Cáceres, I., & Vergès, J. M. (2005). Human occupations at Galería site (Sierra de Atapuerca, Burgos, Spain) after the technological and taphonomical data. In N. Molines, M.-H. Moncel, & J.-L. Monnier (Eds.), *Les Premiers Peuplements En Europe. Colloque International: Données Récentes Sur Les Modalités de Peuplement et Sur Le Cadre Chronostratigraphique, Géologique et Paléogéographique Des Industries Du Paléolithique Ancien et Moyen En Europe (Rennes, 22–25 September 2023)* (pp. 269–280). BAR International Series. S1364 John and Erika Hedges Ltd.

Ollé, A., Mosquera, M., Rodríguez, X. P., de Lombera-Hermida, A., García-Antón, M. D., García-Medrano, P., Peña, L., Menéndez, L., Navazo, M., Terradillos, M., Sala, R., & Carbonell, E. (2013). The Early and Middle Pleistocene technological record from Sierra de Atapuerca (Burgos, Spain). *Quaternary International, 295*, 138–167. https://doi.org/10.1016/j.quaint.2011.11.009

Ollé, A., Mosquera, M., Rodríguez-Álvarez, X. P., García-Medrano, P., Barsky, D., de Lombera-Hermida, A., & Carbonell, E. (2016a). The Acheulean from Atapuerca: Three steps forward, one step back. *Quaternary International, 411*, 316–328. https://doi.org/10.1016/j.quaint.2016.01.042

Ollé, A., Pedergnana, A., Fernández-Marchena, J. L., Martin, S., Borel, A., & Aranda, V. (2016b). Microwear features on vein quartz, rock crystal and quartzite: A study combining Optical Light and Scanning Electron Microscopy. *Quaternary International., 424*, 154–170. https://doi.org/10.1016/j.quaint.2016.02.005

Ortega Martínez, A. I. (2009). *La evolución geomorfológica de la sierra de Atapuerca (Burgos) y su relación con los yacimientos pleistocenos que contiene*. Universidad de Burgos.

Pales, L., & Lambert, P. (1971). *Atlas ostéologique des mammifères*. C.N.R.S.

Palmqvist, P., Rodríguez-Gómez, G., Martínez-Navarro, B., Espigares, M. P., Figueirido, B., Ros-Montoya, S., Guerra-Merchán, A., Granados, A., García-Aguilar, J. M., & Pérez-Claros, J. A. (2023). Déjà vu: on the use of meat resources by sabretooth cats, hominins, and hyaenas in the Early Pleistocene site of Fuente Nueva 3 (Guadix-Baza Depression, SE Spain). *Archaeological and Anthropological Sciences*, *15*(17). https://doi.org/10.1007/s12520-022-01712

Parés, J. M., Álvarez-Posada, C., Sier, M. J., Moreno, D., Duval, M., Woodhead, J., Ortega, A. I., Campaña, I., Rosell, J., Bermúdez de Castro, J. M., & Carbonell, E. (2018). Chronology of the cave interior sediments at Gran Dolina archaeological site, Atapuerca (Spain). *Quaternary Science Reviews., 186*, 1–16. https://doi.org/10.1016/j.quascirev.2018.02.004

Pedergnana, A., & Ollé, A. (2017). Monitoring and interpreting the use-wear formation processes on quartzite flakes through sequential experiments. *Quaternary International., 427*, 35–65. https://doi.org/10.1016/j.quaint.2016.01.053

Pedergnana, A., & Ollé, A. (2018). Building an experimental comparative reference collection for lithic micro-residue analysis based on a multi-analytical approach. *Journal of Archaeological Method and Theory, 25*, 117–154. https://doi.org/10.1007/s10816-017-9337-z

Pedergnana, A., & Ollé, A. (2020). Use-wear analysis of the late Middle Pleistocene quartzite assemblage from the Gran Dolina site, TD10.1 subunit (Sierra de Atapuerca, Spain). *Quaternary International, 569–570*, 181–211. https://doi.org/10.1016/j.quaint.2019.11.015

Pedergnana, A., Asryan, L., Fernández-Marchena, J. L., & Ollé, A. (2016). Modern contaminants affecting microscopic residue analysis on stone tools: A word of caution. *Micron, 86C*, 1–21. https://doi.org/10.1016/j.micron.2016.04.0030968-4328

Pedergnana, A., García-Antón, M. D., & Ollé, A. (2017). Structural study of two quartzite varieties from the Utrillas facies formation (Olmos de Atapuerca, Burgos, Spain): From a petrographic characterisation to a functional analysis design. *Quaternary International, 433*, 163–178. https://doi.org/10.1016/j.quaint.2015.06.031

Peña, L., Biy, D., Canals, A., de Lumley, H., Mosquera, M., & Tárraco, I. (2008). Morpho-technological study of the Lower and Middle Palaeolithic lithic assemblages from Maltravieso and Santa Ana cave (Cáceres, Extremadura). Comparison of two lithic assemblages knapped in milky quartz: Maltravieso cave-Sala de los Huesos-and level C of L'Arago cave (Tautavel, France). *Annali dell'Università degli Studi di Ferrara. Museologia Scientifica e Naturalistica.* ISSN 1824–2707, volume speciale 2008: 145–150.

Pérez-González, A., Parés, J. M., Carbonell, E., Aleixandre, T., Ortega, A. I., Benito, A., Merino, M. Á. M., Martín Merino, M. Á., & Merino, M. Á. M. (2001). Géologie de la Sierra de Atapuerca et stratigraphie des remplissages karstiques de Galería et Dolina (Burgos, Espagne). *L'Anthropologie, 105*(1), 27–43. https://doi.org/10.1016/S0003-5521(01)80004-2

Prieto, A., Yusta, I., & Arrizabalaga, A. (2020). From petrographic analysis to stereomicroscopic characterisation: A geoarchaeological approach to identify quartzite artefacts in the Cantabrian Region. *Archaeological and Anthropological Sciences, 12*(1), 32. https://doi.org/10.1007/s12520-019-00981-7

Ripley, B. D. (1979). Tests of 'randomness' for spatial point patterns. *Journal of the Royal Statistical Society.* Series B, Statistical

methodology. https://doi.org/10.1111/j.2517-6161.1979.tb01091.x

Rodríguez, J., Burjachs, F., Cuenca-Bescós, G., García, N., van der Made, J., Pérez González, A., Blain, H.-A., Expósito, I., López-García, J. M., García Antón, M., Allué, E., Cáceres, I., Huguet, R., Mosquera, M., Ollé, A., Rosell, J., Parés, J. M., Rodríguez, X. P. , Díez, C., … & Carbonell, E. (2011). One million years of cultural evolution in a stable environment at Atapuerca (Burgos, Spain). *Quaternary Science Reviews*, *30*(11), 1396–1412. https://doi.org/10.1016/j.quascirev.2010.02.021

Rodríguez-Álvarez, X. P. (2004). Technical systems of lithic production in the Lower and Middle Pleistocene of the Iberian Peninsula: Technological variability between north-eastern sites and Sierra de Atapuerca sites. *BAR International Series*. https://doi.org/10.30861/9781841713922

Rodríguez-Hidalgo, A. J. (2008). *Zooarqueología de los yacimientos kársticos del Complejo Cacereño (Cueva de Santa Ana y la Cueva de Maltravieso).* Master thesis. Universidad Rovira i Virgili. 349 pp.

Rodríguez-Hidalgo, A. (2016). Subsistence dynamics during the lower paleolithic in Gran Dolina Cave (Atapuerca, Spain). *Mitteilungen Der Gesellschaft Für Urgeschichte, 25*, 11–47. https://doi.org/10.1111/j.1467-8330.1974.tb00606.x

Rodríguez-Hidalgo, A., Saladié, P., Ollé, A., & Carbonell, E. (2015). Hominin subsistence and site function of TD10.1 bone bed level at Gran Dolina site (Atapuerca) during the late Acheulean. *Journal of Quaternary Science, 30*(7), 679–701. https://doi.org/10.1002/jqs.2815

Rodríguez-Hidalgo, A., Saladié, P., Ollé, A., Arsuaga, J. L., Bermúdez de Castro, J. M., & Carbonell, E. (2017). Human predatory behavior and the social implications of communal hunting based on evidence from the TD10.2 bison bone bed at Gran Dolina (Atapuerca, Spain). *Journal of Human Evolution, 105*, 89–122. https://doi.org/10.1016/j.jhevol.2017.01.007

Rots, V. (2013). Insights into early Middle Palaeolithic tool use and hafting in Western Europe. The functional analysis of level IIa of the early Middle Palaeolithic site of Biache-Saint-Vaast (France). *Journal of Archaeological Science., 40*, 497–506. https://doi.org/10.1016/j.jas.2012.06.042

Rots, V., & Plisson, H. (2014). Projectiles and the abuse of the use-wear method in a search for impact. *Journal of Archaeological Science., 48*, 154–165. https://doi.org/10.1016/j.jas.2013.10.027

Rots, V., Van Peer, P., & Vermeersch, P. M. (2011). Aspects of tool production, use and hafting in Palaeolithic assemblages from Northeast Africa. *Journal of Human Evolution., 60*, 637–664. https://doi.org/10.1016/j.jhevol.2011.01.001

Rots, V., Hardy, B. L., Serangeli, J., & Conard, N. J. (2015). Residue and microwear analyses of the stone artifacts from Schöningen. *Journal of Human Evolution., 89*, 298–308. https://doi.org/10.1016/j.jhevol.2015.07.005

Rots, V., Coppe, J., & Conard, N. J. (2022). A leaf point documents hunting with spears in the Middle Paleolithic at Hohle Fels, Germany. *Mitteilungen der Gesellschaft für Urgeschichte*, *30*, 67–94. https://doi.org/10.51315/mgfu.2021.30004

Saladié, P., Rodríguez-Hidalgo, A., Marín, J., & Vallverdú i Poch, J., & Carbonell, E. (2018). The top of the Gran Dolina (Atapuerca, Spain) sequence: A zooarchaeological and occupational perspective. *Quaternary Science Reviews, 195*, 48–71. https://doi.org/10.1016/j.quascirev.2018.07.010

Sano, K. (2009). Hunting evidence from stone artefacts from the Magdalenian cave site Bois Laiterie, Belgium: a fracture analysis. *Quartär, 56*, 67–86. https://doi.org/10.7485/QU56_03

Shipman, P., & Rose, J. (1983). Evidence of butchery and hominid activities at Torralba and Ambrona; an evaluation using microscopic techniques. *Journal of Archaeological Science, 10*, 465–474. https://doi.org/10.1016/0305-4403(83)90061-4

Sisk, M. L., & Shea, J. J. (2008). Intrasite spatial variation of the Omo Kibish Middle Stone Age assemblages: Artifact refitting and distribution patterns. *Journal of Human Evolution, 55*, 486–500. https://doi.org/10.1016/j.jhevol.2008.05.016

Terradillos-Bernal, M., & Díez-Fernández-Lomana, J.-C. (2012). La transition entre les Modes 2 et 3 en Europe: Le rapport sur les gisements du Plateau Nord (Péninsule Ibérique). *L'anthropologie, 116*(3), 348–363. https://doi.org/10.1016/j.anthro.2012.06.001

Titton, S., Barsky, D., Bargalló, A., Serrano-Ramos, A., Vergès, J. M., Toro-Moyano, I., Sala-Ramos, R., Solano, J. G., & Jiménez Arenas, J. M. (2020). Subspheroids in the lithic assemblage of Barranco León (Spain): Recognizing the late Oldowan in Europe. In *Plos One* (Vol. 15, Issue 1). https://doi.org/10.1371/journal.pone.0228290

Vaquero, M. (1999). Variabilidad de las estrategias de talla y cambio tecnológico en el Paleolítico Medio del Abric Romaní (Capellades, Barcelona). *Trabajos De Prehistoria, 56*, 37–58. https://doi.org/10.3989/tp.1999.v56.i2.275

Vaquero, M. (2011). Una cuestión de método... o tal vez no. La variabilidad de la talla discoidal en el Paleolítico Medio del Abric Romaní. *Mainake, 33*, 233–250.

Vergès, J. M., & Ollé, A. (2011). Technical microwear and residues in identifying bipolar knapping on an anvil: Experimental data. *Journal of Archaeological Science., 38*, 1016–1025. https://doi.org/10.1016/j.jas.2010.11.016

Wilson, A. D., Zhu, Q., Barham, L., Stanistreet, I., & Bingham, G. P. (2016). A dynamical analysis of the suitability of prehistoric spheroids from the Cave of Hearths as thrown projectiles. *Scientific Reports*, *6*. https://doi.org/10.1038/srep30614

Zornoza-Indart, A., López-Arce, P., & López-Polín, L. (2017). Durability of traditional and new nanoparticle based consolidating products for the treatment of archaeological stone tools: Chert artifacts from Atapuerca sites (Burgos, Spain). *Journal of Cultural Heritage, 24*, 9–21. https://doi.org/10.1016/j.culher.2016.10.019

Zornoza-Indart, A., López-Arce, P., & López-Polín, L. (2021). Archaeological chert artifacts from Atapuerca sites (Burgos, Spain): Characterization, causes of decay and selection of compatible consolidating products. *Conservar Patrimonio*, *36*, 20–35. https://doi.org/10.14568/cp2019037

Authors and Affiliations

Marina Mosquera[1,2] · Andreu Ollé[1,2] · Palmira Saladié[1,2,3] · Adrián Arroyo[1,2] · Lena Asryan[2,4] · Amèlia Bargalló[1,2] · Arturo de Lombera-Hermida[2,5,6] · Juan Luis Fernández-Marchena[2,7] · Paula García-Medrano[1,2,8,9] · Diego Lombao[2,10] · Antonio Rodríguez-Hidalgo[2,11] · María Soto[2,12] · Josep Vallverdú[1,2,3] · Andion Arteaga-Brieba[1,2] · Javier Villalobos[1,2] · Görkem-Cenk Yeşilova[1,2] · Eudald Carbonell[1,2]

✉ Marina Mosquera
marina.mosquera@urv.cat

[1] Departament d'Història i Història de l'Art, Universitat Rovira I Virgili, Avinguda de Catalunya 35, 43002 Tarragona, Spain

[2] Present Address: Institut Català de Paleoecologia Humana i Evolució Social (IPHES-CERCA), Zona Educacional 4, Campus Sescelades URV (Edifici W3), 43007 Tarragona, Spain

[3] Unit Associated With CSIC, Departamento de Paleobiología, Museo Nacional de Ciencias Naturales (CSIC), Calle José Gutiérrez Abascal, 2, 28006 Madrid, Spain

[4] Present Address: Faculté de Philosophie & Lettres, Université de Liége, Bâtiment A1, Place du 20-Août 7, 4000 Liége, Belgique

[5] Present Address: Dpto. Historia. Fac. Filosofía y Letras, Universidad de Oviedo, C/ Amparo Pedergal s/n, Asturias, 33011 Oviedo, Spain

[6] Universidade de Santiago de Compostela, Edificio Fontán, Santiago de Compostela, 15702 A Coruña, Spain

[7] Present Address: Dept. Prehistòria, d' Arqueologia i d'Història Antiga, Universitat de València, Avda. Blasco Ibáñez 28, 46010 Valencia, Spain

[8] UMR 7194 HNHP (MNHN-CNRS-UPVD), Département Homme et Environnement, Muséum National d'Histoire Naturelle, Paris, France

[9] Department Britain, Europe and Prehistory, British Museum, London, UK

[10] Present Address: GEPN-AAT. Departamento de Historia, Facultade de Xeografía e Historia, Universidade de Santiago de Compostela, Praza da Universidade 1, 15782 Santiago de Compostela, Spain

[11] Present Address: Departamento de Prehistoria y Arqueología - Facultad de Geografía e Historia, Universidad de Sevilla, María de Padilla s/n, 41004 Sevilla, Spain

[12] Present Address: MIAS, Departamento de Prehistoria y Arqueología, Universidad Autónoma de Madrid, C/ Francisco Tomás y Valiente 1, Campus de Cantoblanco, 28049 Madrid, Spain